NASA-CR-191323

NASA   NAS7-963
NASA CR-
PSI-1001/TR-871

NOVEL OXYGEN ATOM SOURCE FOR
MATERIAL DEGRADATION STUDIES

FINAL REPORT

Prepared by:

R.H. Krech and G.E. Caledonia
Physical Sciences Inc.
Research Park, P.O. Box 3100
Andover, MA   01810

Prepared for:

NASA Resident Office - JPL
4800 Oak Grove Drive
Pasadena, CA   91109
Attnention: Mr. Peter Tackney

October 1988

NASA NAS7-963
NASA CR-
PSI-1001/TR-871

NOVEL OXYGEN ATOM SOURCE FOR
MATERIAL DEGRADATION STUDIES

FINAL REPORT

Prepared by:

R.H. Krech and G.E. Caledonia
Physical Sciences Inc.

Prepared for:

NASA Resident Office - JPL
4800 Oak Grove Drive
Pasadena, CA 91109
Attnention: Mr. Peter Tackney

October 1988

REPORT DOCUMENTATION PAGE

1a. REPORT SECURITY CLASSIFICATION UNCLASSIFIED	1b. RESTRICTIVE MARKINGS
2a. SECURITY CLASSIFICATION AUTHORITY	3. DISTRIBUTION / AVAILABILITY OF REPORT
2b. DECLASSIFICATION / DOWNGRADING SCHEDULE	

4. PERFORMING ORGANIZATION REPORT NUMBER(S) PSI-1001/TR-871	5. MONITORING ORGANIZATION REPORT NUMBER(S) NAS7-963

6a. NAME OF PERFORMING ORGANIZATION Physical Sciences Inc.	6b. OFFICE SYMBOL (If applicable)	7a. NAME OF MONITORING ORGANIZATION NASA
6c. ADDRESS (City, State, and ZIP Code) Research Park, P.O. Box 3100 Andover, MA 01810		7b. ADDRESS (City, State, and ZIP Code) NASA Resident Office – JPL 4800 Oak Drive, Pasadena, CA 91109

8a. NAME OF FUNDING / SPONSORING ORGANIZATION NASA	8b. OFFICE SYMBOL (If applicable)	9. PROCUREMENT INSTRUMENT IDENTIFICATION NUMBER NAS7-963

8c. ADDRESS (City, State, and ZIP Code) NASA Resident Office – JPL 4800 Oak Drive, Pasadena, CA 91109	10. SOURCE OF FUNDING NUMBERS

PROGRAM ELEMENT NO.	PROJECT NO.	TASK NO.	WORK UNIT ACCESSION NO.

11. TITLE (Include Security Classification)
NOVEL OXYGEN ATOM SOURCE FOR MATERIAL DEGRADATION STUDIES

12. PERSONAL AUTHOR(S)   R.H. Krech and G.E. Caledonia

13a. TYPE OF REPORT FINAL	13b. TIME COVERED FROM 3/1/86 TO 9/1/88	14. DATE OF REPORT (Year, Month, Day) October 1988	15. PAGE COUNT 110

16. SUPPLEMENTARY NOTATION

17. COSATI CODES			18. SUBJECT TERMS (Continue on reverse if necessary and identify by block number)
FIELD	GROUP	SUB-GROUP	O-Atom, Plasma, Material Testing

19. ABSTRACT (Continue on reverse if necessary and identify by block number)

Physical Sciences Inc. (PSI) has developed a high flux pulsed source of energetic (8 km/s) atomic oxygen to bombard specimens in experiments on the aging and degradation of materials in a low earth orbit environment. The proof-of-concept of the PSI approach was demonstrated in a Phase I effort. In Phase II a large O-atom testing device (FAST-2) has been developed and characterized. Quantitative erosion testing of materials, components, and even small assemblies (such as solar cell arrays) can be performed with this source to determine which materials and/or components are most vulnerable to atomic oxygen degradation. The source is conservatively rated to irradiate a 100 cm^2 area sample at $>10^{17}$ atoms/s at a 10 Hz pulse rate. Samples can be exposed to an atomic oxygen fluence equivalent to the on-orbit ram direction exposure levels incident on Shuttle surfaces at 250 km during a week-long mission in a few hours.

20. DISTRIBUTION / AVAILABILITY OF ABSTRACT ☐ UNCLASSIFIED/UNLIMITED ☐ SAME AS RPT. ☐ DTIC USERS	21. ABSTRACT SECURITY CLASSIFICATION
22a. NAME OF RESPONSIBLE INDIVIDUAL Mr. Peter Tackney	22b. TELEPHONE (Include Area Code) (818) 354-4909	22c. OFFICE SYMBOL M/S 1800-805

DD FORM 1473, 84 MAR   83 APR edition may be used until exhausted.
All other editions are obsolete.   UNCLASSIFIED

CONTENTS

FIGURES

vi

PROJECT SUMMARY

Physical Sciences Inc. (PSI) has developed a high flux pulsed source of energetic (8 km/s) atomic oxygen to bombard specimens in experiments on the aging and degradation of materials in a low earth orbit environment. The proof-of-concept of the PSI approach was demonstrated in a Phase I effort. In Phase II a large O-atom testing device (FAST-2) has been developed and characterized. Quantitative erosion testing of materials, components, and even small assemblies (such as solar cell arrays) can be performed with this source to determine which materials and/or components are most vulnerable to atomic oxygen degradation. The source is conservatively rated to irradiate a 100 cm^2 area sample at $>10^{17}$ atoms/s at a 10 Hz pulse rate. Samples can be exposed to an atomic oxygen fluence equivalent to the on-orbit ram direction exposure levels incident on Shuttle surfaces at 250 km during a week-long mission in a few hours.

2

1. INTRODUCTION

Satellites in low earth orbit sweep at velocities of 8 km/s through a rarefied atmosphere which consists primarily of atomic oxygen. Experimental pallets flown on the early Space Shuttle missions clearly demonstrated a dependence of material degradation and mass loss on ram direction atomic oxygen exposure. These experiments clearly indicate that virtually all hydrocarbons and active metals are highly reactive, and suggest that materials containing silicones, fluorides, oxides, and noble metals are moderately inert or less reactive. The severity of this effect is emphasized for Kapton, an important aerospace polymer, where it is observed that approximately one in ten oxygen atoms chemically react with the surface resulting in mass loss.

The need for continued materials development and degradation studies has been emphasized over the past few years because of the severe impact that atomic oxygen induced material degradation will have on the performance and longevity of large space structures such as Space Station. In light of these observations, the international aerospace community is actively pursuing the development of various hardening techniques to make materials more resistant to the effects of energetic atomic oxygen interactions.

The difficulty and expense of conducting on-orbit materials testing has fostered the world-wide development of ground based energetic atomic oxygen sources and test facilities. In the United States alone over twenty five different sources are currently under development. Most of these sources are neutralized ion beams. The inherent drawback of an ion beam source is that the electrical space charge limits the intensity within the beam to less than 10^{14} atoms/cm$^2 \cdot$s^1 which is not suitable for accelerated testing. The only demonstrated techniques that can generate 8 km/s atomic oxygen beams with intensities in excess of the 10^{15} atoms/cm$^2 \cdot$s^1 low earth orbit flux utilize laser induced breakdown and heating combined with supersonic expansion of the recombining plasma.

Physical Sciences Inc. (PSI) of Andover, Massachusetts, USA, has developed and has patents pending on a high flux pulsed source of energetic atomic oxygen to bombard specimens in experiments on the aging and degradation of materials in a low earth orbit environment. The proof-of-concept of the PSI approach was demonstrated in a Phase I effort. In Phase II a large 0-atom testing device (FAST-2) has been developed and characterized. Quantitative erosion testing of materials, components, and even small assemblies (such as solar cell arrays) can be performed with this source to determine which materials and/or components are most vulnerable to atomic oxygen degradation. The source is conservatively rated to irradiate a 100 cm^2 area sample at $>10^{17}$ atoms/s at a 10 Hz pulse rate. Samples can be exposed to an atomic oxygen fluence equivalent to the on-orbit ram direction exposure levels incident on Shuttle surfaces at 250 km during a week-long mission, in a few hours.

The design details, operating principles and operating characteristics of the FAST-2 device are presented in Section 2. Device calibration techniques and a review of our present understanding of the beam properties are reviewed

3

in Section 3, and the results of typical material erosion studies are provided in Section 4. The program results are summarized in Section 5.

A number of papers concerning the source and its applications were written during the program period of performance. These are included as an appendix.

2. DESCRIPTION OF THE PSI ATOMIC OXYGEN EXPOSURE FACILITY

In the Phase I SBIR program, PSI built a small prototype device to demonstrate the laser supported detonation wave technique to produce high velocity pulsed beams of atomic oxygen. During the first year of the Phase 2 program, the prototype was incorporated as the source chamber for a much larger exposure facility, commonly known as FAST-2 (Fast Atom Sample Tester). In this section of the report we will review the principles of operation of the source, and describe in some detail the existing facility.

2.1 Principles of Operation

Generation of the atomic oxygen beam in the PSI source starts by introducing molecular oxygen at several atmospheres pressure through a pulsed molecular beam valve into an evacuated conical nozzle mounted inside a high vacuum test chamber. When the nozzle is partially filled with gas, the output of a pulsed CO_2 TEA laser is focused by a lens into the nozzle to increase the enthalpy of the flow. A general schematic of the source is shown in Figure 1. Rapid absorption of the laser energy occurs during the 200 ns gain-switched laser spike via inverse Bremsstrahlung inducing a breakdown at the throat, and the resulting plasma absorbs a large part of the remaining energy in the tail of the 2 μs laser pulse. The breakdown generates a blast wave at temperatures in excess of 20,000 K which causes complete dissociation and partial ionization of the gas. This process is illustrated in Figure 2.
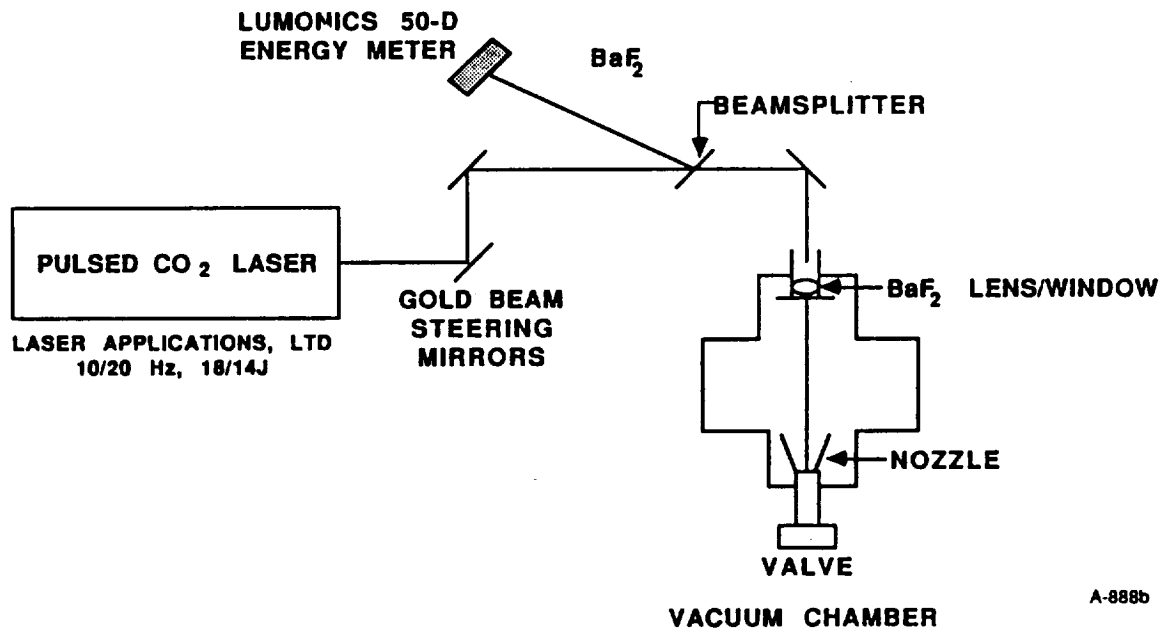
Figure 1. - General source schematic.

5

- INITIAL PULSED NOZZLE FILL

- BREAKDOWN
- RAPID LSD WAVE HEATING

- LASER ENERGY ABSORBED
- BLAST WAVE PROCESSES NOZZLE FILL

A-2060 a
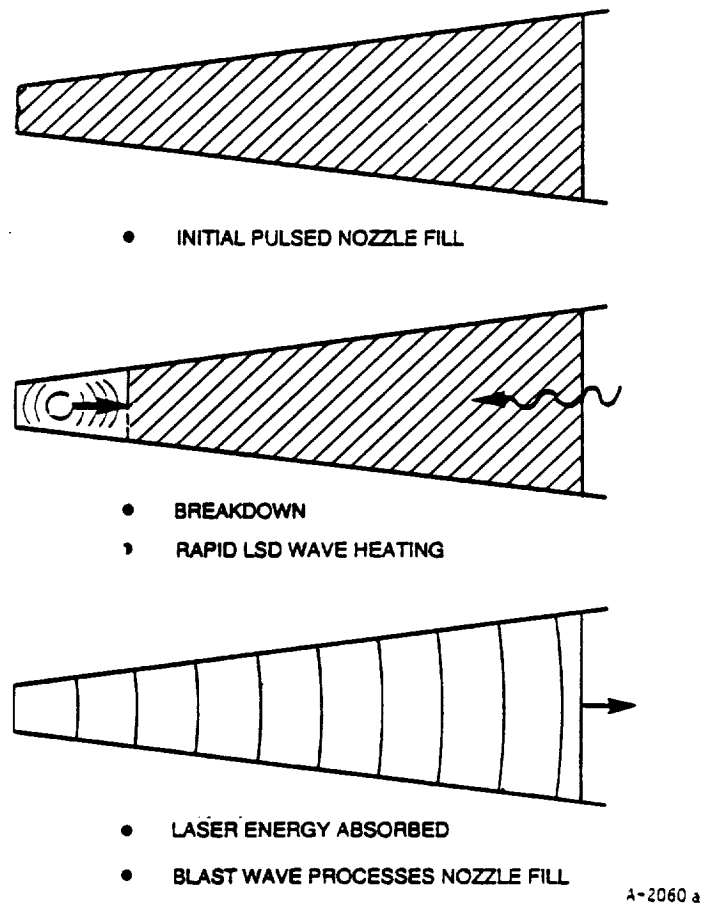
Figure 2. - Simplified gas dynamic model.

Within the confines of the nozzle, the expanding high density plasma undergoes rapid electron-ion recombination into atomic oxygen, but the high random translational temperature inhibits atomic recombinations. As the expansion continues, the gas temperature (random kinetic energy) and density decrease as the directed kinetic energy increases. Thus as the stagnation energy of the plasma is converted into directed kinetic energy, a cold (low spread in random velocity), high energy beam of oxygen atoms flows out of the nozzle. The average velocity of the atomic oxygen beam can be adjusted between 5 and 13 km/s simply by varying the ratio of the laser energy to the mass of oxygen in the nozzle. At higher velocities the ionic content of the beam is observed to increase. At 8 km/s the ionic content is believed to be less than 1 percent.

2.2 Description of the FAST-2 Atomic Oxygen Exposure Facility

The FAST-2 Facility (see Figure 3) consists of a 20 cm o.d. stainless steel 6-way cross source chamber (the Phase I prototype chamber) close coupled to a 40 cm o.d. stainless steel 6-way cross exposure chamber.

6
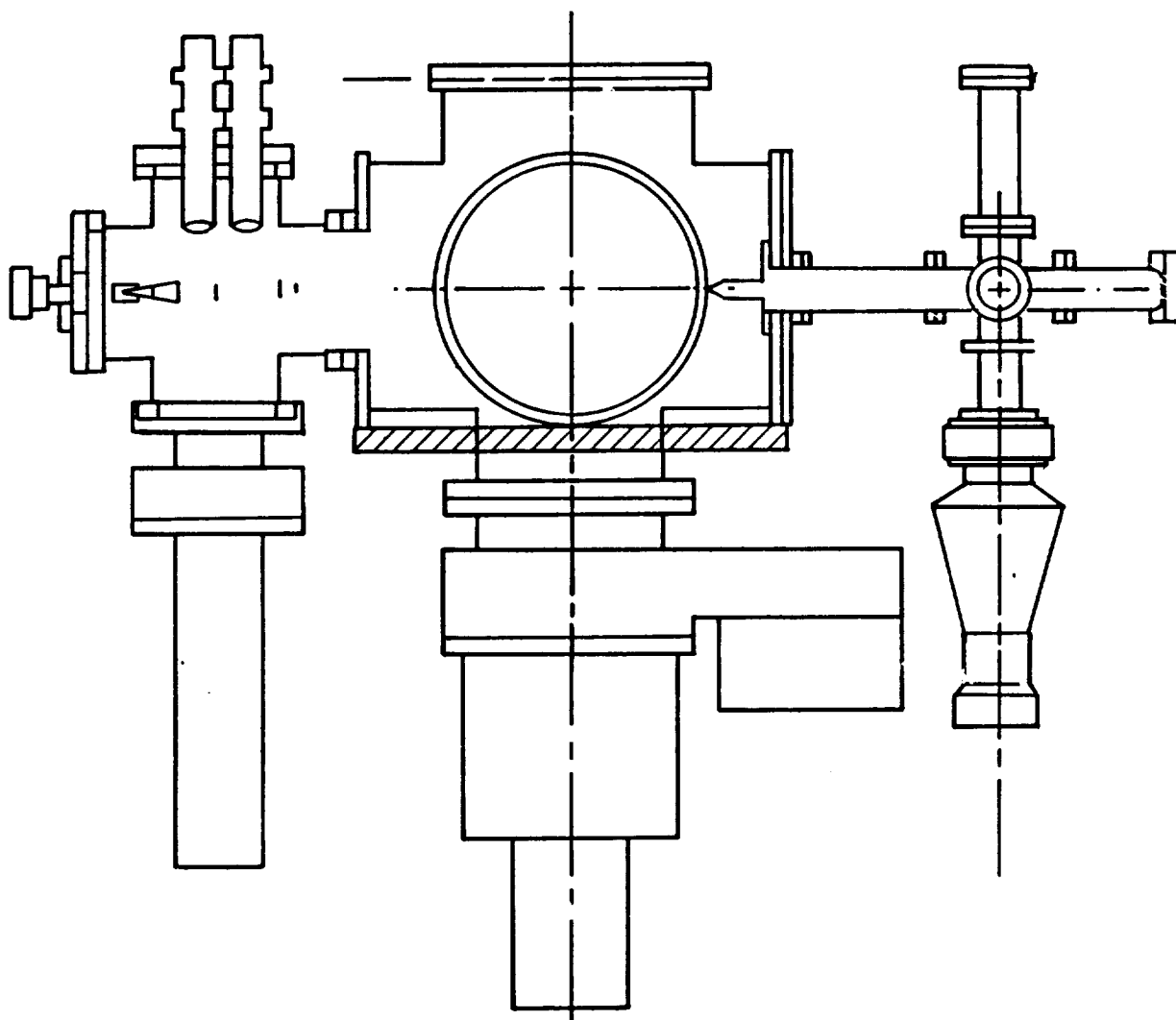
A-7410

Figure 3. - Basic experimental layout of the FAST-2 atomic oxygen exposure
test facility. Laser beam is directed from laser using three gold-coated
mirrors through an attenuator and a 100 cm focal length BaF_2 lens.
Molecular oxygen feed gas enters the nozzle through a pulsed molecular
beam valve in the source chamber. Beam velocity is monitored using two
overhead 777.3 nm radiometers. The exposure chamber is a 6-way 40 cm
o.d. stainless steel cross with a 3000 l/s cryopump. A differentially
pumped quadrupole mass spectrometer monitors the O-atom beam.

The source chamber has two glass view ports, and three (3) modified 10 in. o.d. CF flanges for o-ring feed through couplers for the pulsed valve, the laser beam focusing telescope, optical radiometers, and BNC and motion feedthroughs. The source pumping system contains a 1200 l/s Varian M4 oil diffusion pump stack with Fomblin 25/9 Fluorocarbon oil, a 750 l/m two stage Alcatel roughing pump with hydrocarbon oil, ionization and thermocouple pressure gauging, pneumatic valving and Kurt J. Lesker Micromaze molecular sieve foreline trap.

The pulsed beam valve/supersonic nozzle assembly (Figure 4) is mounted on a 10 in. o.d. CF Flange which is attached to one of the horizontal faces of the cross. This flange has one central 1.25 in. i.d. o-ring vacuum coupling in the center for the beam valve and 12 2.54 cm i.d. ports on a 15 cm circle to allow the insertion of cooling water, and electrical and motion feedthroughs.

A 10 in. o.d. CF flange with two 50 mm i.d. o-ring couplers mounted on top of the chamber holds the optical radiometers. Each radiometer consist of R406 Hamamatsu photomultiplier tube in an EMI shielded housing attached to a filter holder containing 50 mm square, 780 nm, 10 nm band pass interference filters attached to a 250 mm long x 50 mm o.d. aluminum telescope tube. A 50 mm diameter, 50 mm focal length quartz lens is epoxied to the other end of the tube to collect the radiation. The radiometer is set up to image a 4 mm wide x 20 mm long mask placed on the filter to a 1 x 5 mm spot on beam centerline. The photomultiplier is typically set to 720V, and the output from the radiometers sent through 50Ω terminating resistors to monitor the beam.

A PCB Model 112 (20, 40 or 100 mV/PSI) piezoelectric pressure transducer can be located down stream from the throat to measure the dynamic pressure of the cold or hot flow.
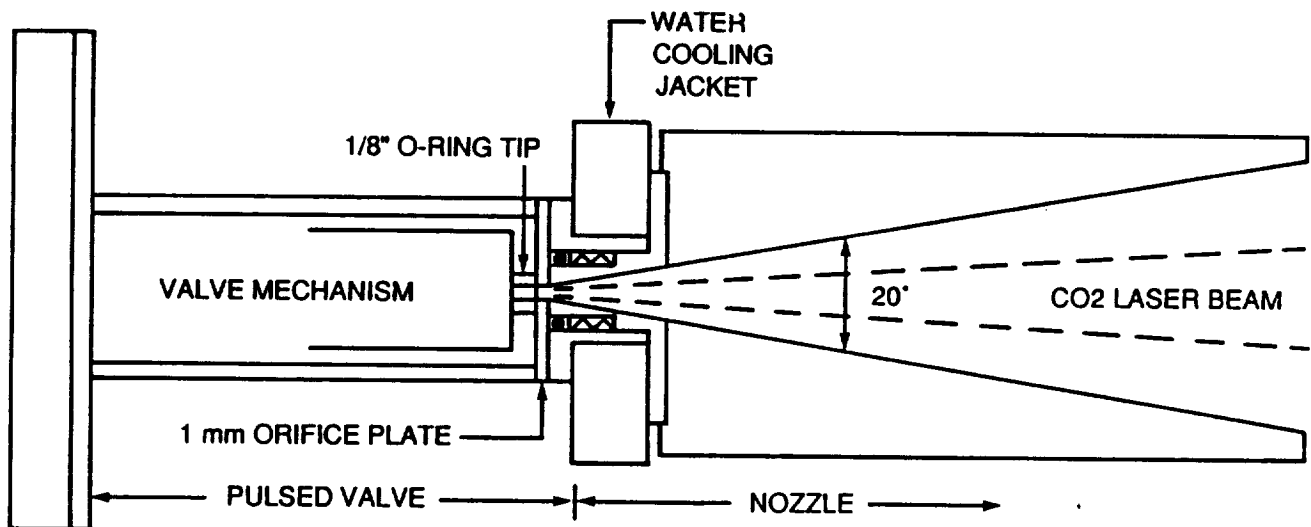
A-890c

Figure 4. – 0-Atom source pulsed valve/nozzle assembly.

The test chamber is made from a standard 40 cm o.d. six-way stainless steel cross with ISO 400 o-ring flanging to allow for convenient sample access, and is close coupled to the source chamber with an adapter flange. FAST-2 is equipped with mass spectrometer probes for beam and target product analysis. Provisions allow for target irradiation by a UV solar simulator, and observation with several radiometers and spectrometers as optical emission diagnostics. A 3000 l/s Varian Cryostack 12 cryopump maintains an oil free vacuum below 10^{-4} torr during testing, and an ultimate vacuum of 10^{-7} torr.

Samples can be located from 20 to 100 cm from the nozzle throat. The center of the test chamber is located about 75 cm the throat and the beam radius for 50 percent of the centerline flux is about 16 cm and the area is approximately 750 cm^2. The laser beam may be directed into the nozzle either on-axis or off-axis as required. One single sample or structure as large as 20 x 20 cm can receive a relatively uniform exposure. It is also possible to expose up to six circular samples 12 to 14 cm in diameter at once.

FAST-2 generator in excess of 10^{18} atoms/pulse at rats to 10 Hz. We estimate that we can expose one batch of samples to an atomic oxygen flux of 2 x 10^{20} atoms/cm^2 at 75 cm or 10^{21} atoms/cm^2 at 30 cm per 8 hr shift at 5 Hz, and 10^{22} atoms/cm^2 in a little over 2 weeks of continuous running (400 hr) at 75 cm or a little over 3 days (80 hr) at 30 cm without pushing the limits of the system. We estimate that the o-ring in the beam valve will have to be replaced every 16 hr of operation under these conditions.

10

3. CALIBRATION STUDIES

The atomic oxygen source has been characterized for velocity and beam composition by a number of techniques. The source has demonstrated the ability to produce beams with average velocities from 5 to 13 km/s by changing the nozzle mass loading and laser beam energy (the oxygen atom content will vary monotonically with velocity). Laser induced fluorescence has been used to demonstrate the dominance of ground electronic state atomic oxygen at 8 km/s. Mass spectrometer studies of the dissociation and ionic content of the beam have been conducted, and, finally, spatial beam profiles within the test chamber as a function of distance from the nozzle throat and distance off beam centerline have been conducted. The results of these studies are summarized in the following sections.

3.1 Velocity Variations as a Function of Gas Loading and Laser Timing

The velocity of the atomic oxygen beam is determined by monitoring the time histories of the 777.3 nm atomic oxygen emission line with band pass optical radiometers located at two different positions on the top flange of the source chamber. Typical traces are shown in Figure 5. Average velocities from 5 to 13 km/s can be observed by varying the laser energy deposited per unit mass of feed gas.

For a fixed set of driver settings at a stagnation pressure of 6.3 atmospheres oxygen, 5J of laser energy was required to generate an atomic oxygen beam with a mean velocity of 9 km/s as determined by the optical radiometers (see traces in Figure 5a). The energy per molecule was then increased by reducing the stagnation pressure to 3 atmospheres. The velocity of the beam should increase roughly by square root 2 for a doubling of the energy per unit mass and the velocity of 13 km/s as indicated in Figure 5b confirms this hypothesis. Likewise a reduction of energy per unit mass will reduce the beam velocity. A reduction of the energy from 5 to 3J into the same mass of oxygen reduces the velocity from 9 to 5.2 km/s as indicated in Figure 5c.

The cold flow dynamic pressure profile is recorded on a digital storage scope by positioning a piezoelectric pressure transducer 7.5 cm from the throat inside the nozzle. The expansion pressure ratio is so large, (8 atmospheres into 4×10^{-5} torr) that the gas velocity quickly approaches limiting velocity (for a 300 K stagnation temperature) and therefore the dynamic pressure is proportional to the instantaneous mass flow rate. See Figures 6 and 7 for typical dynamic pressure traces and transducer location. The integral under the dynamic pressure trace represents the total mass flow during the pulse. The mass per pulse is determined by measuring the average mass flow rate through the nozzle with a mass flow meter located in the inlet gas line, and measuring the repetition rate with a counter. Division of the the average mass flow rate by the pulse rate yields the mass per pulse.

The average beam velocity and the number of oxygen atoms are determined by the mass of gas processed by the laser pulse. If the laser is fired early in the flow profile, a relatively small fraction of the oxygen is processed,

11
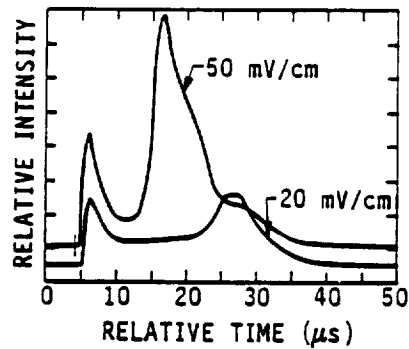
(a) E_L = 5 J, $P_{stagnation}$ = 6-1/3 atm
    V_1 = 10 km/s, V_2 = 9 km/s, the lower
    gain trace corresponds to the down-
    stream radiator.
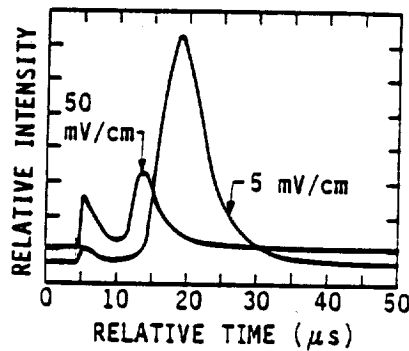
(b) E_L = 5 J, $P_{stagnation}$ = 3 atm
    V_1 = V_2 = 13 km/s, the lower
    gain trace corresponds to the
    downstream radiator.
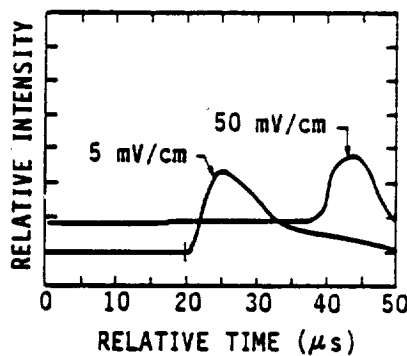
(c) E_L = 3.1 J, $P_{stagnation}$ = 7-1/3 atm
    V_1 = 5.2 km/s, the lower gain trace
    corresponds to the downstream radiator.

Figure 5. - Radiometer traces.

12
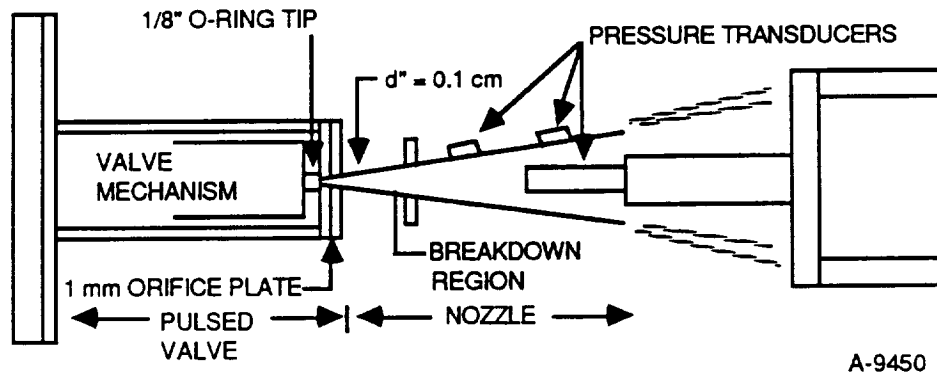
Figure 6. – Positioning of piezoelectric pressure transducer in nozzle for cold flow dynamic pressure measurements.
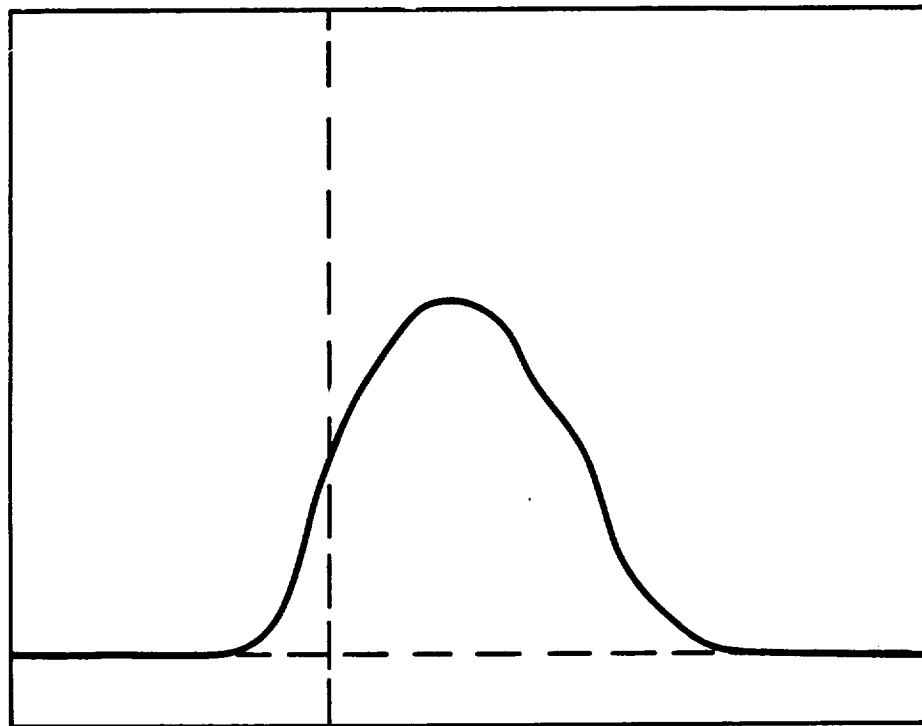
Figure 7. – Dynamic pressure profile of flow in Nozzle at 7.5 cm distance from throat. Amplitude of curve is directly proportional to instantaneous flow rate. Area to left of vertical dashed line represent amount of mass processed by laser. Horizontal scale width = 2.0 x 10^{-3}s. Percent processed = 7%; mass 3.3 x 10^{-5}g.

13

and the resulting atomic flow has higher velocity than if the same energy were deposited at a later time into a larger mass of gas. To establish a desired velocity, the dynamic pressure transducer is removed and the laser timing adjusted to obtain the necessary time differential in the peaks of the two radiometer signals. (Each radiometer images a 1 by 5 mm strip along the beam centerline onto the filtered photomultiplier.) The cold flow profile at the throat is offset by 1.0×10^{-4}s when the dynamic pressure is recorded at 7.5 cm from the throat. After correcting for the offset the mass fraction of the gas processed by the laser is determined as the fractional portion of the flow profile intercepted by the laser beam. Figure 6 shows a typical trace. The processed mass fractions generally are 5 to 25% for velocities 13^{-6} km/s, respectively.

3.2 Overview of the Laser Induced Fluorescence Measurements

Laser induced fluorescence has been used to obtain the ground state number density of atomic oxygen in flow tubes.[1-3] We have performed similar measurements in our pulsed O-atom source to determine the number density of atomic oxygen produced by the laser supported detonation wave within the hypersonic expansion nozzle. In this technique the output of a frequency doubled YAG pumped dye laser is focused into the flow field. Laser output was fixed around 226 nm to excite ground state atomic oxygen ($O2p^3P_2$) to an upper state ($O3p^3P_{2,1,0}$) via a two photon pumping process. This upper level then will radiate promptly at 845 nm to a metastable state ($O3s^3S$). An energy level diagram of the process is shown in Figure 8. Since the two photon cross-section and radiative transfer rates are known and theoretically understood, the ground state number density can be determined if the temporal and spatial laser beam profiles and optical collection efficiencies are precisely measured. Due to the limited availability of the laser system we were unable to perform all the necessary calibrations to obtain an unambiguous absolute quantitative number density, so these measurements are more semi-quantitative in nature and accurate to factors of two to three. They do however clearly demonstrate the presence of a significant quantity of oxygen atoms in the PSI expanded plasma pulse.

The major difficulty encountered during these measurements was in synchronizing the Quantel YAG laser with the O-atom facility because the YAG can not be fired at any arbitrary rate. The Quantel system is rather unique in that the flash lamps must be fired at a 10 Hz rate, whether or not
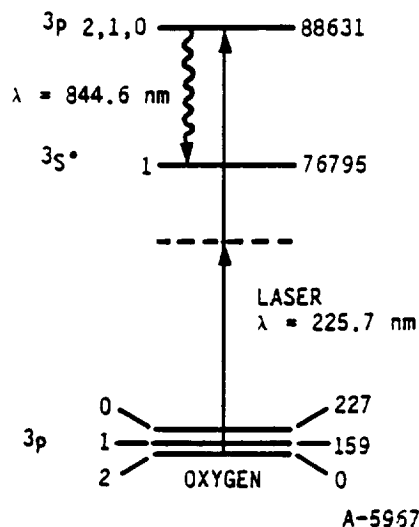

Figure 8. - Energy levels involved in two photon LIF detection of ground state atomic oxygen.

laser output is desired, for purposes of thermal control. Laser output cannot be obtained for about 5s after startup and should the lamps fail to fire after a period of 1/8s, the entire firing system is automatically and unavoidably shut down. Then a complete restart of the firing sequence is required.) To circumvent this a Candella three phase laser trigger generator was tied to a master 10 Hz system clock. Two of the three clock outputs can be delayed from the master reference. A circuit was built to invert and stretch the +15V 1 μs outputs from the Candella trigger unit to deal with the inverted (i.e., switch closure) logic required by the Quantel. To complicate matters more, three fire commands, each in the right sequence, are required to fire the YAG. First, a command to charge the capacitor banks, followed by a command to fire the bank into the flash lamps after confirmation of completion of the charge cycle, and lastly a command to fire the Q-switch to obtain laser output. This sequence required further circuits consisting of 556 CMOS to run the laser. Since the small O-atom device can not run at 10 Hz, a ÷N circuit controlled the firing of the O-atom system at 2.5 Hz. In addition, the laser harmonic tracking system would often fail to keep the output up and the system required frequent retuning. About 6 of the 8 hr in a normal day were used to align and tune up the laser output.

A separate flow system was set up on an auxiliary optical table to produce a CW source of ground state O-atoms that was used to calibrate the laser output for the desired LIF transition. The above two tasks consumed about 60 percent of the laser time allocated to this measurement series. Figure 9 shows a typical calibration scan through the LIF of the ground state O-atom
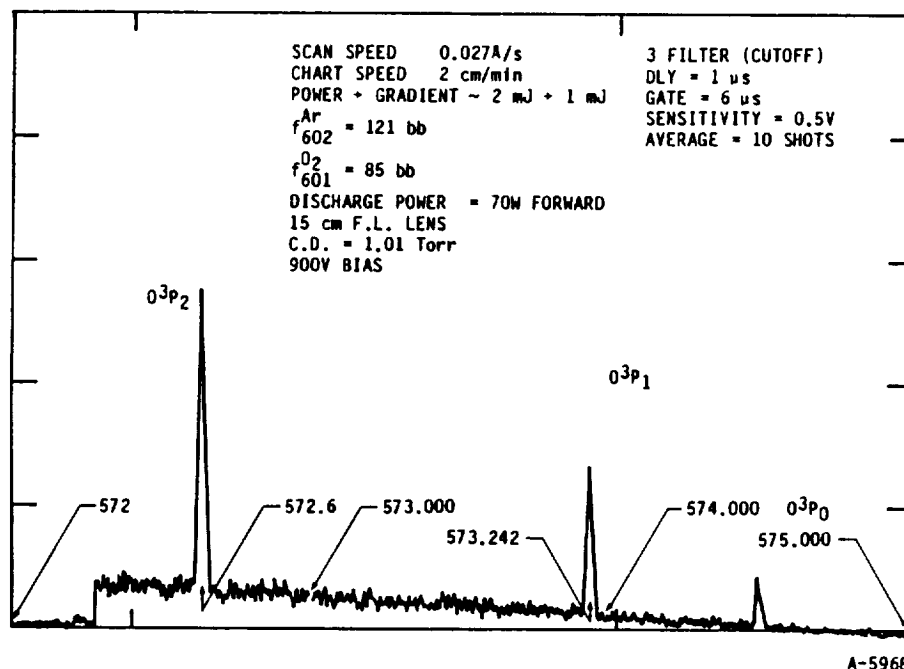

A-5968

Figure 9. - Typical LIF spectrum of O^3P generated in discharge flow tube.
Laser tune to center of O^3P_2 for beam diagnostic tests.

transitions. After adjusting the laser output of the center of the strongest
transition, we then unsuccessfully attempted to record the LIF signal. It
turned out that the computer controlled laser grating, which has no mechanical
position indicator, would for no apparent reason shift its position
occasionally, and was in fact 3.5 nm off of line center. Thus for the
remainder of the measurements we had to continuously monitor the fluorescence
in the flow tube and the O-atom chamber to insure that the laser had not
drifted away from the desired wavelength.

The final obstacle which was not overcome during the allocated laser time
was the timing jitter between the two laser systems and the data acquisition
system. The best jitter obtainable was ± 150 ns. Since the radiative lifetime
is less than 35 ns the LIF signals tend to be smeared out when averaged to
obtain statistics and thus peak heights obtained with a box car or averaging
Camac system proved worthless. The only clean data was obtained on a LeCroy
digital scope, but unfortunately we had no hard copy software written for it
during the measurements so only visual observations were able to be recorded
when the scope was operated in a single shot mode. In spite of these diffi-
culties we were able to obtain useful information on the ground state number
density, but we were not able to conduct the measurements to determine the O^1D
and O^1S number densities as we had planned.

The configuration of the apparatus for the LIF measurements is shown in
Figure 10. The Quantel YAG pumped dye laser system produced more than 1 mJ
pulse at 226 nm. The beam was directed from the laser to the center of the
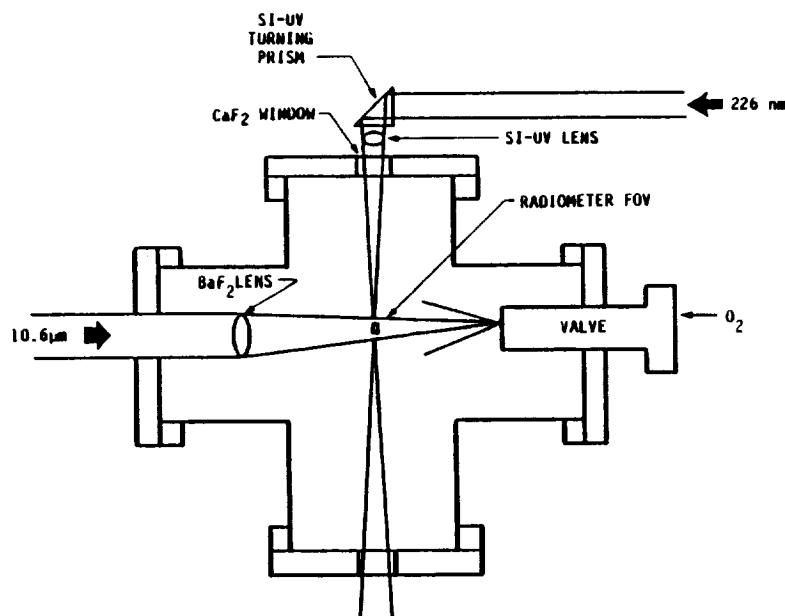
A- 889c

Figure 10. - LIF experiment setup.

16

cell by a periscope consisting of three 20 x 20 mm S1 UV grade quartz turning prisms and focused through a calcium fluoride window into the center of the cell with a 300 mm focal length S1 UV grade quartz lens. Approximately 1 mJ of energy was focused into a 1 mm diameter spot located 15 cm from the throat of the nozzle on the flow centerline. The pulse length is approximately 10 ns. The fluorescence is collected perpendicular to both the beam and flow by a bandpass filtered radiometer with a collection efficiency of f/# = 2 and focused on centerline to an area of 1 x 5 mm. The interference filter (Corion S25-850-S) had a 25 nm bandpass centered at 850 nm, and extra rejection of scattered laser light was insured by a colored filter (Corion LG-595-S) which blocked all radiation below 600 nm. The dominant radiation in the bandpass has been shown to arise from atomic oxygen excited during the initial break-down. This is readily observed in emission and has a width of about 10 μs corresponding to the transit time of the atom beam across the field of view of the radiometer. The LIF signal is readily distinguishable from the background emission since the radiative lifetime of the transition is 34.6 ns, and occurs promptly as a spike in the emission profile after the laser pulse. The filtered radiation is detected with a Hamamatsu R955 photomultiplier tube, and was recorded on a LeCroy digital oscilloscope and terminated into a 50 ohm load resistor. The overall optical transmission efficiency of the photo-multiplier is about 0.01 and it was operated at 450V which corresponds with a gain of about 5000.

The number density in the ground state, N_g, then can be readily estimated through the following relationship:

$$N_g = \frac{\{[\pi D(f/\#)]^2\} \, t_p h\nu V}{Yl\alpha E^2 GQTK_r CR}$$

where:

D = 0.1 cm, the diameter of the beam
$f/\#$ = 2, the collection efficiency of the optics
t_p = 10^{-8}s, the laser pulse duration
h = 6.6.6262 x 10^{-34} J-s, the frequency of the transition
ν = 1.327 x 10^{15} s^{-1}, the frequency of the transition
V = peak voltage output of the detector
Y = 0.4, the estimated fluorescence quantum yield for a peak beam
    pressure of 1.5 torr
l = 0.5 cm, the path length of the radiometer system
α = 5.5 x 10^{-28} cm^4-W^{-1}, measured absorption cross-section
E = 0.001J, energy of the laser pulse
G = 5000, gain of the photomultiplier
Q = 0.01, quantum efficiency of PMT at 845 nm
T = 0.25, transmission efficiency of optical system
K_r = 2.89 x 10^7 s^{-1}, spontaneous emission rate
C = 1.6 x 10^{-19} coul/amp
R = 50 ohms, the value of the load resistor
    = 1.1 x 10^{16}V atoms-cm^{-3}-v^{-1}.

The total number of oxygen atoms produced in a single breakdown is simply the number density times the volume. The cross-sectional beam area at the radio-meter is A, $cm^2 = \pi(15\ cm\ tan\ 12)^2 = 32\ cm^2$. With a velocity of about 8 km/s and an actual pulse width of about $5 \times 10^{-6}s$, the beam length is about 6 cm long, therefore the volume is about 200 cm^3. Using this crude analysis. The total number of atoms generated is approximately 2×10^{18} atoms/V of fluor-escence signal. The voltage obtained for a variety of conditions range from 0.1 to 1.5V, and depended on the energy per molecule deposited into the gas flow. The largest signals were obtained by lowering the laser energy deposited into the flow somewhat, and reducing the amount of gas processed. It may well be that collisional quenching of the upper state, which is pres-sure dependent, is coming into play when more gas is processed. Unfortun-ately, we were not able to investigate this further, nor perform more detailed calibrations because the dye laser failed and could not be repaired in our allocated use period.

In summary, we have measured the ground state atomic oxygen density directly via two photon LIF techniques. The ground state number density was found to vary from 10^{15} to 1.5×10^{16} cm^{-3} depending on the energy deposition. Estimates of the total number of atoms produced in a pulse were obtained and range from 2×10^{17} to 3×10^{18} depending on the exact energy deposition rates. These values are in order of magnitude agreement with our known mass flow rates. It appears that the LIF technique as applied to our system can only provide a qualitative estimate of the 0-atom concentration.

3.3 Mass Spectrometer Studies

A mass spectrometer was also employed to characterize the beam atomic oxygen. At PSI we have used a Balzers Model 311 quadrupole mass spectrometer controller coupled to a Model 150 head with a cross beam ionizer and Ithaco high speed current to voltage converter to investigate the atomic beam (The stock Balzers electrometer does not have the rise time required to follow the pulse and cannot be used).

The main obstacles to overcome in conducting these measurements are: maintaining a line of sight flight path from the nozzle through the ionizer (no surface contact); minimizing the electrical noise pickup from the laser on the nanoammeter; amplifying the ion current to counter the low ionization efficiency of the electron impact ionizer; and interpretation of the mass spectrometer signals clouded by oxygen background level due to low pumping speeds in the mass spectrometer chamber.

The mass spectrometer is housed in its own chamber, and coupled to the test chamber through a small, conical beam skimmer with a 1 mm aperture. The ionizer is located as closely behind this skimmer as possible to ensure that the greatest possible fraction of the beam will pass through the ionizer volume. The pressure in the mass spectrometer chamber is as low as possible to prevent background gas signals (i.e., 0^+ from O_2) from clouding the measurements, however with a 300 l/s pump, this is marginal for the measurements.

18

The pressure in the mass spectrometer chamber typically runs in the low to middle 10^{-6} torr range during operation. In FAST-2 the plume from the nozzle is a reddish-pink during normal operation. The mass spectrometer indicates that the ionic content of this beam is low, somewhere between 1 PPM and 1 PPT when compared to the atomic oxygen content using literature values for ionization efficiency and collection geometry. The initial mass spectrometer scans indicate that the beam consists primarily of atomic oxygen with perhaps as much as 50 percent O_2, although the source of O_2 is not certain and is probably due to wall recombination in the mass spectrometer skimmer sampling system, since the O_2 peak signal is detected about 25 microseconds after the peak of the O signal. If the recombination occurred in the gas phase, the velocities of the two components should be the same; however, if the recombination occurred on the walls, then conservation of momentum dictates a slower O_2 beam. In any case, the source of the O_2 content in the beam is presently being investigated.

Non-optimum operating conditions, however, can substantially alter the composition of the beam. If the gas load is reduced enough to give rise to a blue plume, then the beam is found to contain substantial amounts of fast ions, predominantly O^+. In addition, when the gas flow is not large enough to absorb the radiation, species such as F, F^+, Na, Na^+, K, K^+, and CF_3, and CF_3^+ can be observed as ablation products from the nozzle components. These species can have velocities from 15 to 25 km/s depending on exact nozzle conditions. If the valve occasionally misfires and does not fill the nozzle sufficiently before the laser fires, then these species could impinge upon the samples being tested for atomic oxygen exposure. The fluorine content as determined by ESCA on some samples recently exposed for JPL might be explained by this observation, since the valve can occasionally misfire.

Figures 11 to 13 represent typical m/e = 16 spectrum for optical velocity measurements of 13.6, 10.0, and 6.5 km/s as recorded on a LeCroy 9400 digital oscilloscope, transferred to a PC, and plotted by Lotus. The data is characterized by a noise spike at 80 µs indicative of the initial laser breakdown in the nozzle throat, a positive spike approximately 100 µs later due primarily to fast ions followed by a gradual rise to a peak whose time peak depends upon the beam velocity. The data must be corrected for the transit time through the quadrupole before a velocity can be obtained. Figure 14 shows how long it takes ions with different m/e ratios to go from the ionizer to the electron multiplier. As expected it is proportional to the square root of the mass of the ion. For O^+ (m/e = 16) it is 26.8 µs, for O_2^+ (m/e = 32) the delay is 38.0 µs. Thus the ion spike corresponds to a velocity of about 20 km/s which is about the expected LSD wave velocity, and is seen only in Figures 11 and 12 which correspond to rather fast velocities. This ion signal probably occurs in the faster velocity beams when the LSD wave runs out of mass within the nozzle and the hot wave front runs unattenuated through the evacuated chamber. It should be noted that it is not visible in Figure 13 where there is more mass in the nozzle than can be processed while the laser is on.

Three major corrections must be applied to the data before velocity distributions can be extracted from such data. First, the mass spectrometer does

O-ATOM SIGNAL-13.6km/S

A-8113
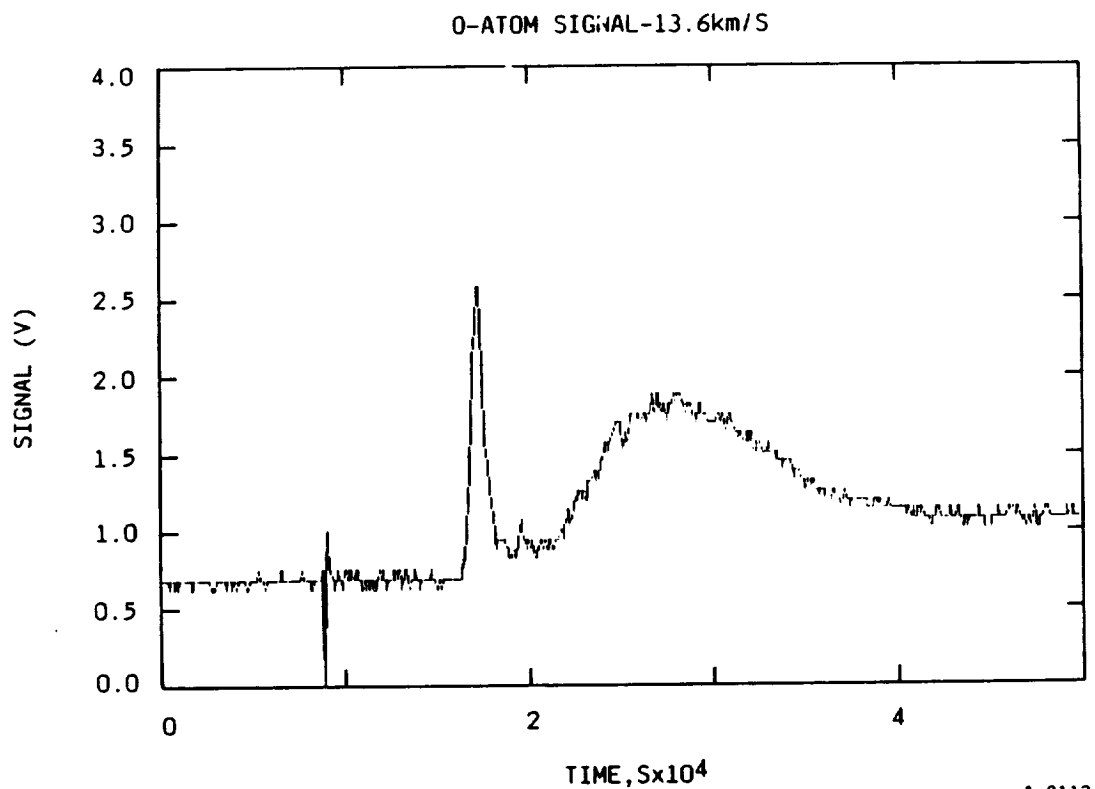
Figure 11. - O-Atom signal versus time for 13.6 km/s beam

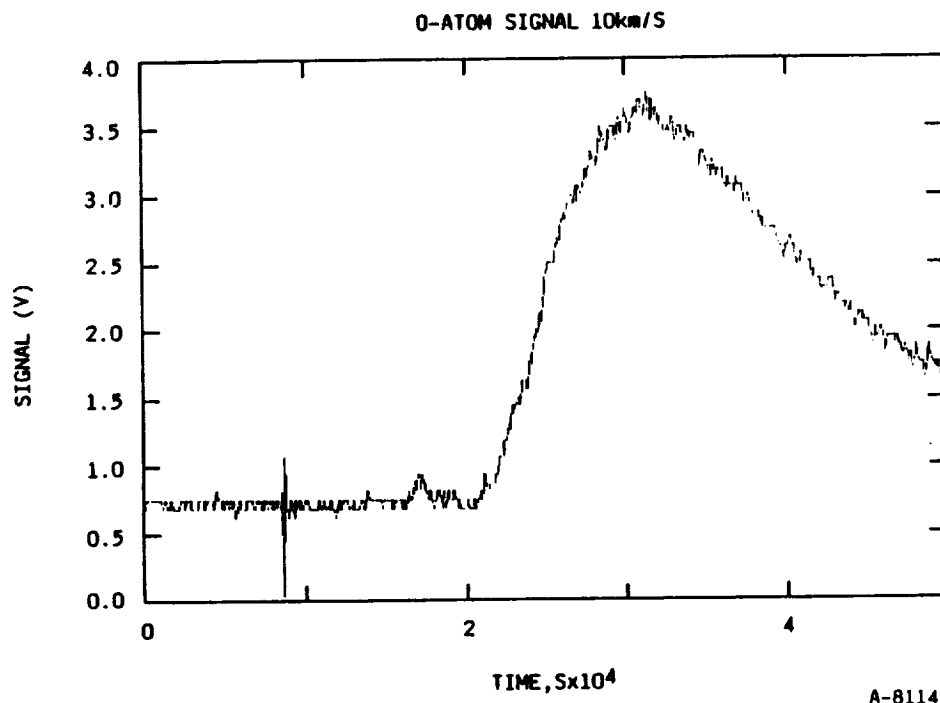O-ATOM SIGNAL 10km/S

A-8114

Figure 12. - O-Atom signal versus time for 10.0 km/s beam.
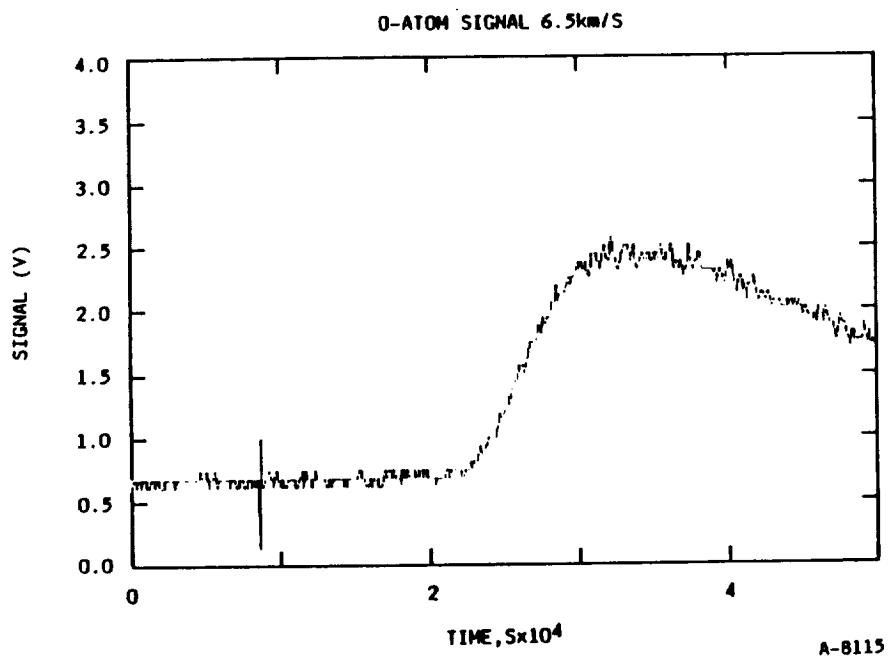
20

O-ATOM SIGNAL 6.5km/S

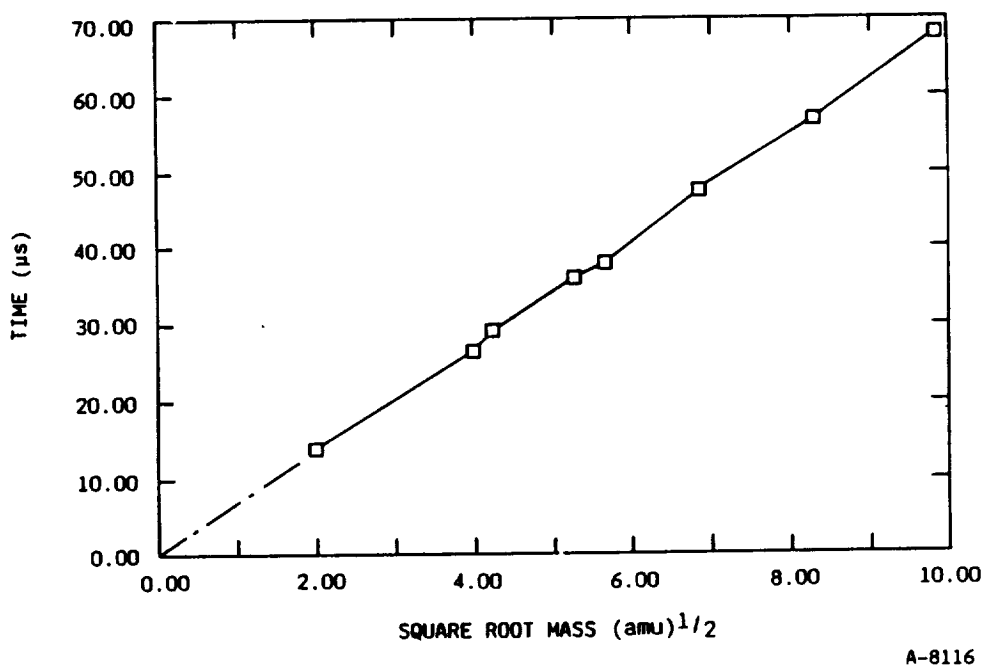Figure 13. - O-Atom signal versus time for 6.5 km/s beam.

Figure 14. - Transit time of ions through quadrupole mass spec versus m/e.

21

not have uniform sensitivity for atoms of differing velocities. The same number of atoms transiting through the ionizer at 10 km/s give only 1/2 the signal of 5 km/s atoms and therefore a correction must be made for the velocity. Second, any O_2 present will generate O^+ fragments with about a 10 percent probability. Third, the velocity of the O_2 is not known, it might be present in the beam or it might arise from wall recombination in the mass spectrometer chamber; these yield two different extremes in the analysis procedures. In addition the rate at which gas can come into the mass spectrometer chamber from the beam at high velocity is initially higher than the pump out speed, so that a transient buildup of species might occur.

Figures 15 and 16 show how the same data can be corrected for a beam with an optical velocity of 8.7 km/s. Figure 15 shows an expanded trace similar to those above (a) corrected for transit time through the quadrupole, (b) corrected by 1/time for the velocity of the O-atom beam, and (c) subtracting out the contribution of O^+ from O_2 which is assumed to be thermal. The beam appears to be virtually all O-atoms with a gradual buildup of O_2 due to recombination as time goes on. Figure 16 utilizes the same corrections but assumes that the O_2 comes from the beam and corrects the O_2 response as 1/time. In this case there is much more O_2 present at later times. We believe that the first procedure is the correct interpretation.
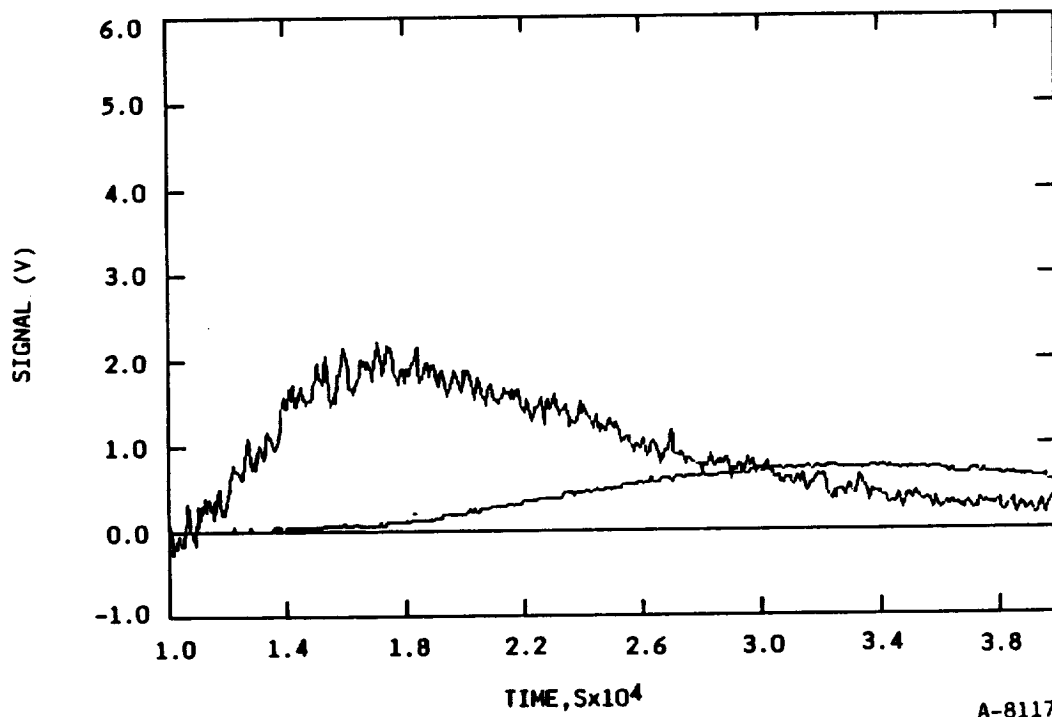

A-8117

Figure 15. - O + O_2 signal Corrected for Response Where O comes from fast beam and O_2 thermal.
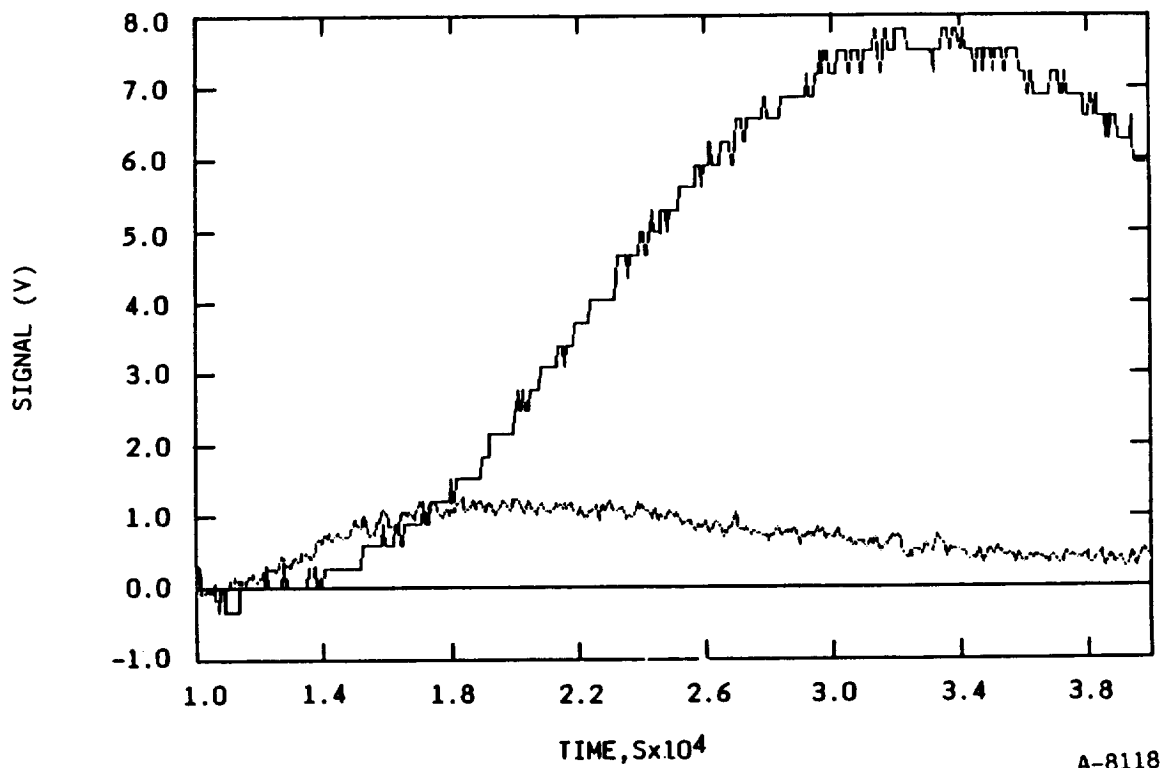
22

Figure 16. 0 + O_2 signals corrected for response where both 0 and O_2 originate in fast beam.

3.4 Erosion Measurements for Beam Shape Determination

We have determine the beam shape evolution as it expands through the chamber. This is particularly important when target materials are placed far downstream of the beam origin so that large areas of material can be irradiated.

In order to assess the beam growth we have placed kapton targets at different distances from beam center and measured relative mass loss which should be directly proportional to intercepted fluence. Two such measurements, corresponding to targets positioned at 30 cm and 40 cm, respectively, from the throat, are shown in Figures 17 and 18.

Focusing first on Figure 17, we note that there are no measurements around beam origin. This is because the laser pulse is focused along beam center and target materials cannot be positioned so as to block the beam. The curve shown on the figure is the result of a fourth degree polynomial fit of the data and the beam may actually be flatter on center. The observed beam is several centimeters wider than we had expected. The beam growth is further exemplified in Figure 18 where measurements taken at 40 cm exhibit a significantly flatter beam shape.
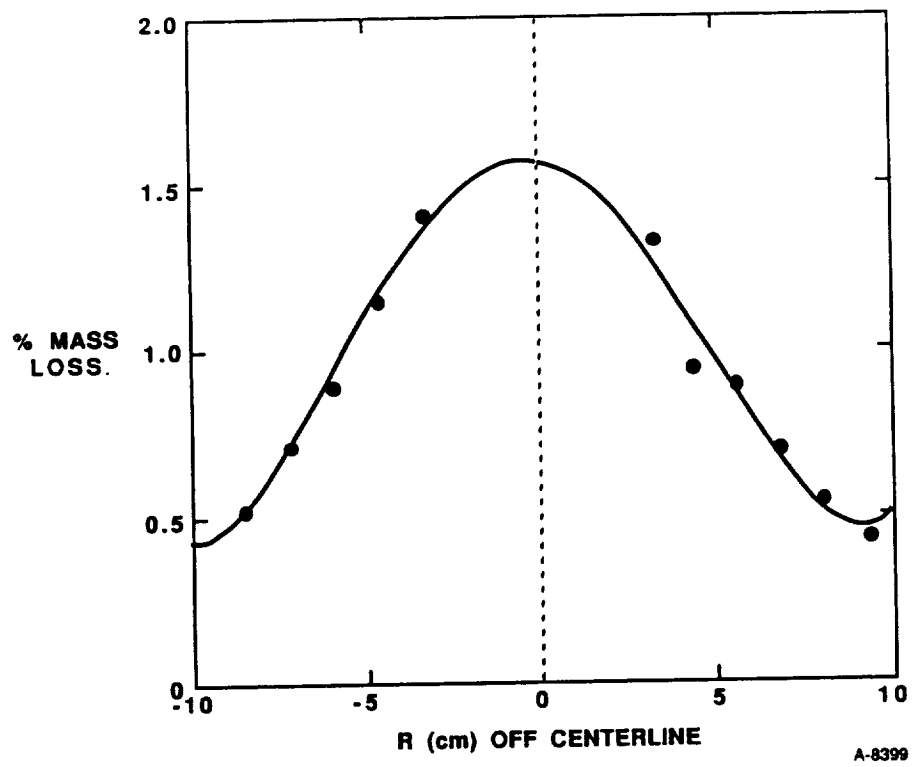
23

Figure 17. – Kapton 500 HN erosion profile in FAST-1. Sample plane 30 cm from nozzle throat.
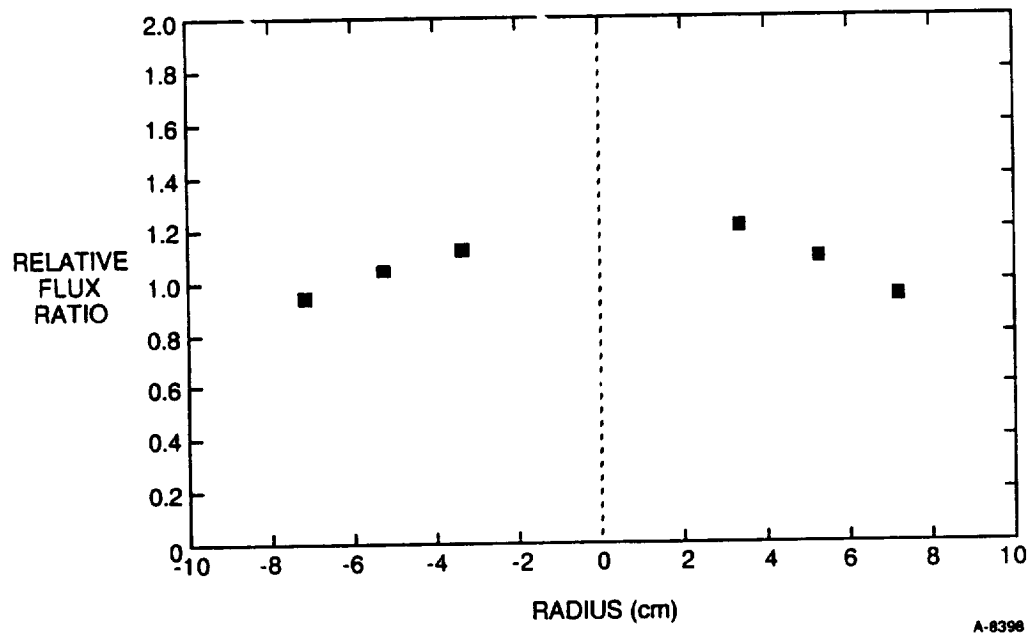

Figure 18. – Beam shape from kapton erosion data at distance of 40 cm from throat.

24

Kapton tends to be somewhat hygroscopic and thus it can be difficult to measure more than a half dozen samples on a humid day before water uptake becomes serious. To overcome this problem we also performed further erosion profiling with polyethylene. We duplicated the Kapton measurements at 40 cm with the polyethylene and then did another radial measurement at 75 cm. The results are shown in Figures 19 and 20. From an inspection of the data obtained simultaneously at 40 and 75 cm with polyethylene it is apparent that the beam follows the expected r^{-2} intensity dependence on centerline as a function of distance from the nozzle throat. The beam is seen to be quite flat at 75 cm, providing for relative uniform areal irradiation. The approximate off axis position at which the beam intensity drops to 50 percent of the centerline value is described by the following relationship:

$$R_{50,x} \sim 12.5 \ x \ \tan 10 + (x-12.5) \ x \ \tan 12$$

where x is the distance from the nozzle throat, 12.5 cm is the length of the nozzle, and 10 degrees is the half angle of the nozzle.

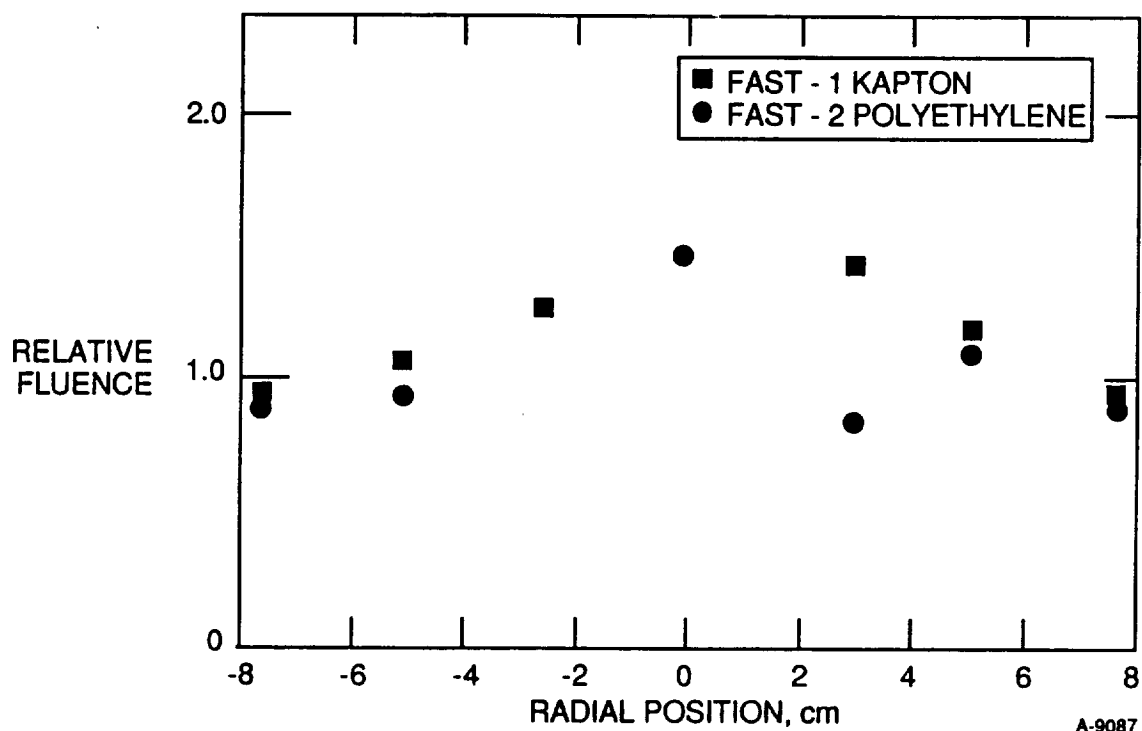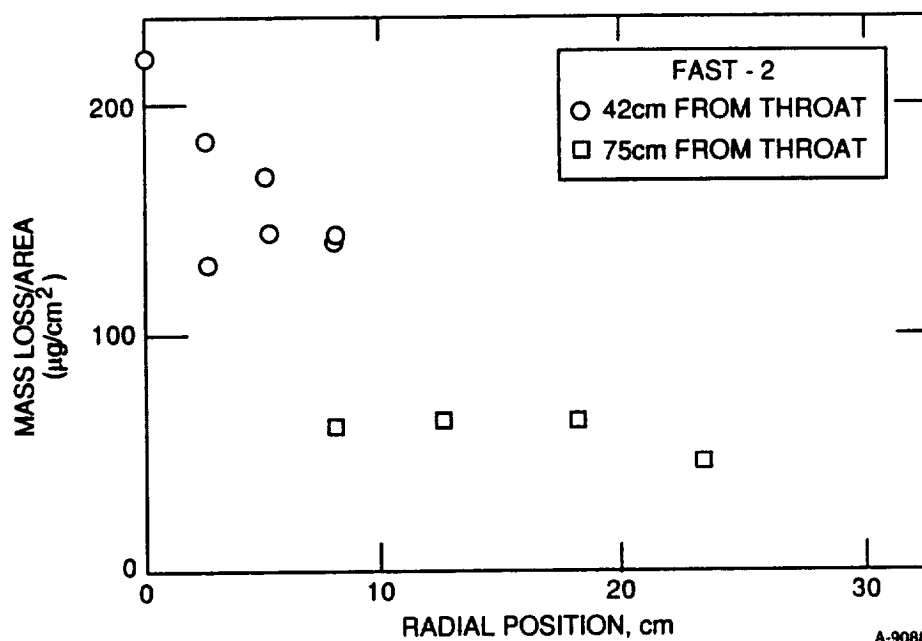Figure 19. - Radial profile from mass erosion data.

25

Figure 20. – Relative beam shape at two different beam positions from polyethylene mass loss measurements.

4. TYPICAL MEASUREMENT PROCEDURES

4.1 Source Startup

Proper operation of the source requires careful synchronization of the gas pulse with the laser firing. The standard procedure is as follows:

1. Evacuate the chamber to a base pressure in the 10^{-9} range for no-flow operation.

2. Set the oxygen regulator to 4 to 8 absolute, turn on the beam valve to 100 pulses per minute, and adjust settings to obtain a 10 to 20 sccm flow indication.

3. Insert the piezoelectric transducer into the nozzle 7.5 cm from the throat and record the dynamic pressure trace. (At this distance the real flow history is offset by +100 μs due to the time of arrival of the gas from the throat to the transducer.), adjust driver timing settings to get a pulse between 200 and 300 μs wide, store this trace in the digital scope, then retract the dynamic pressure probe from the nozzle.

4. Set the time delay on the laser delay generator to correspond to the delay time to the peak in the dynamic pressure profile minus the 100 μs flow delay and minus any delay in the laser triggering circuitry.

5. Connect the output cables of the radiometers into 50Ω terminators on the oscilloscope, turn on the laser and observe the two radiometer traces, then adjust the laser delay timing to obtain a time delay between the peaks of the two radiometers corresponding to the desired velocity. The plume within the chamber should be pink or orange.

6. Recall the cold flow trace on the digital scope and observe where the laser noise spike falls on the trace.

   The ratio of the area under the curve up until the laser fires to the entire area under the curve represents the fraction of the oxygen processed.

   This coupled to the mass per pulse obtained from the mass flow meter yields the quantity of atomic oxygen generated per pulse.

7. The system is now ready for testing.

4.2 Sample Handling Procedures

The cleanliness of the surface of the samples can greatly impact the outcome of exposure testing, and in particular the surface morphology. The best way to prepare a clean surface is to repeatedly wash the samples in a freon bath to remove any organic contaminants. Once this is done, then the samples should be stored in a desiccator or under vacuum prior to weighing

before exposure. Samples should be weighed within 5 minutes of removal from the desiccant or chamber to ensure minimum water pickup.

Samples can be positioned from 20 to 100 cm from the throat depending upon the size and number of the samples and the desired exposure uniformity. Holders can be affixed to any of the flanges as required for sample position-ing. At a distance of 75 cm from the throat the beam diameter to 50 percent of centerline value is 32 cm or an area of about 750 cm^2. Thus it is easy to expose a structure as large as 20 x 20 cm uniformity, or as many as six 15 cm diameter samples at once.

4.3 Material Studies

We have examined a number of materials including many polymers such as polyethylene, kapton and teflon. Our observed surface morphologies are similar to those of samples exposed on Space Shuttle experiments. One such example, an SEM of carbon fiber reinforced plastic is shown in Figure 21. The irradiation level for this case was approximately 3 x 10^{20} O-atoms/cm^2. The top left scan contrasts the virgin and irradiated materials and the following scans show magnifications of the irradiated materials clearly delineating the different erosion structures in the fiber and filled regions of the material. A shag-rug like morphology is observed for kapton irradiated in our source (Figure 22).

Absolute radiometric measurements coupled with mass spectrometric evolutions can be invaluable in analyzing reaction mechanisms for different materials. For example, in one experiment a series of polyethylene samples were irradiated to different fluence levels and then ESCA was used to evaluate the surface oxygen atom content. It was found that the oxide concentration initially increased rapidly with fluence and then asymptoted to a constant value at a fluence level of several x 10^{17} atoms/cm^2. A radiometric measure-ment of the time history of the erosion products exhibited identical behavior, clearly coupling the erosion rate to the surface oxide content (Figure 23).

We have recently completed relative mass loss measurements for several standard materials provided by Banks[4]. Here we irradiated several 1 x 1 in. samples of three different materials simultaneously in two different entries. The irradiation level was ~1.7 x 10^{20} O-atoms/cm^2 for each entry. The results are tabulated in Table 1 and as can be seen the data scatter was quite small. Absolute volume removal cross sections are listed under the assumptions that the beam is either 80 or 50 percent oxygen atoms. Since our fluence monitor is total mass flow the difference between these two assumptions is a factor of two. We plan to remove this uncertainty in the near future.

In terms of the relative cross sections, it is clear that our teflon mass removal efficiency is much larger than the observed in Shuttle experiments.[5] One possible cause of this difference could be the UV loading produced by our source. The high temperature plasma produced in our initial breakdown may produce UV radiation with a significantly different spectral content than that of the sun. One advantage of a pulsed device is that there is a sufficient

FIBER   **MATRIX**
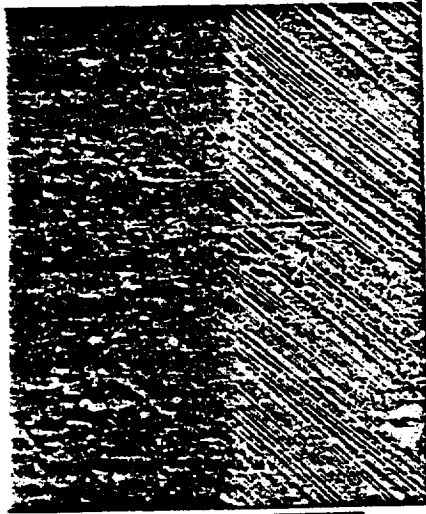
80092 20KV 500U

890098 20KV 5U

80092 20KV 500U

80099 20kV 0.5U

80098 20KV 5U

80000 20KV 0.5U

Figure 21. – Scanning electron micrograph analysis of carbon fiber reinforced plastic irradiated by ~3 x $10^{20}/cm^2$ 5 eV oxygen atoms. Top left contrasts virgin and irradiated materials. Remaining views emphasize erosion patterns at increased magnification as shown.

29
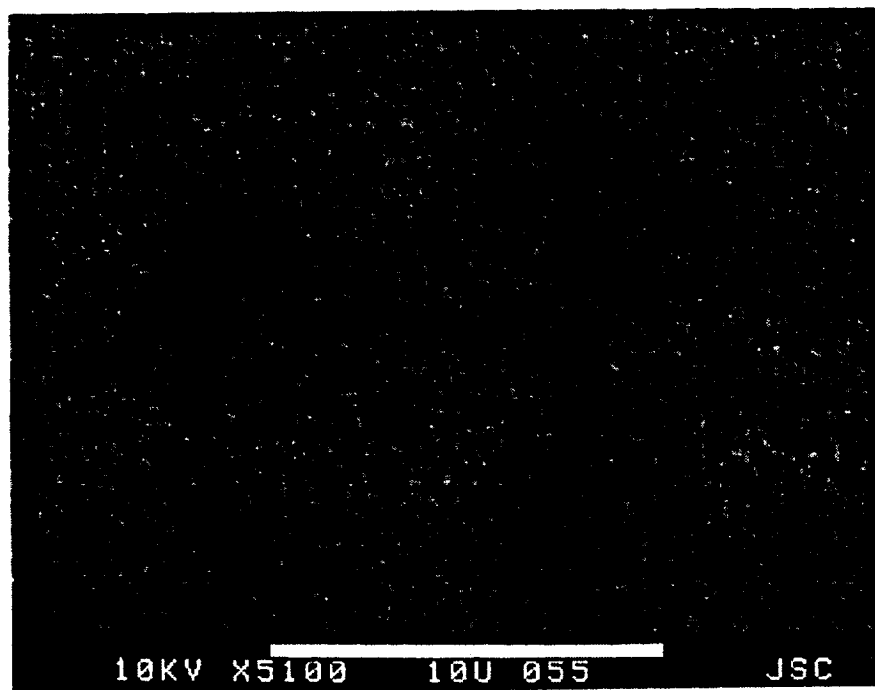
Figure 22. – Kapton after 10^{20} cm^{-2} exposure.
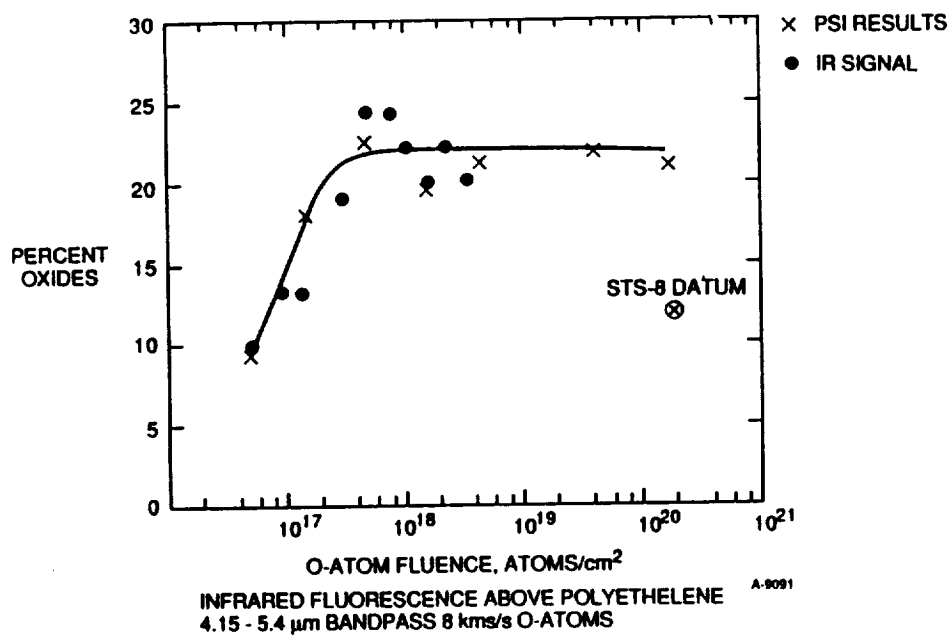
Figure 23. – Polyethylene oxides formed as a function of oxygen atom fluence.

time lag between plasma decay and 0-beam arrival so that plasma produced radiation can be shutter-screened from the sample. This should be investigated. Potential temperature dependent erosion effects should also be reviewed.

TABLE 1. FAST-1 EROSION STUDIES (FLUENCE 1.7 x 10^{20}/cm^2)

Material (# Samples)	Relative σ	$\sigma(20\% \ O_2)$ x 10^{24} cm^3/Atom	$\sigma(50\% \ O_2)$ x 10^{24} cm^3/Atom
Kapton HN(5)	1($\pm$ 20%)	1.3	2.6
Polyethylene (6)	0.9($\pm$ 7%)	1.1	2.2
FEP Teflon (6)	0.6($\pm$ 11%)	0.8	1.6

32

5. CONCLUSIONS

We have developed a high flux, large area pulsed source of 8 km/s oxygen atoms which can be used for materials testing for purposes of low earth orbit survivability assessment. The device operates reproducibly with high fidelity and has been operated continuously for as long as 24 hours without failure.

The oxygen atoms beam shape, composition and fluence has been characterized. At present both beam fluence and O/O_2 ratio are uncertain to a factor of two.

ACKNOWLEDGMENTS

36

REFERENCES

1. Beschel, W.K., Perry, B.E., Crosley, D.R., "Detection of Fluorescence from O- and N-Atoms Induced by Two-Photon Absorption," Appl. Opt. 21, 1419 (1982.)

2. DiMauro, L.F., Gottscho, R.A., and Miller, T.A., "Two-Photon Laser-Induced Fluorescence Monitoring of O-Atoms in a Plasma Etching Environment," J. Appl. Phys., 56, (7), 1 October 1984, p. 2007-11.

3. Bamford, D.A., Jusinski, L.E., and Bischel, W.K., "Absolute Two-Photon Absorption and Three Photon Ionization Cross Sections for Atomic Oxygen," Phys. Rev. A. 34, (1), July 1986, p. 185-98.

4. Banks, B., Private communication.

5. Visentine, J.T., Leger, L.J., Kuminecz, J.F., and Spiker, I.K., "STS-8 Atomic Oxygen Effects Experiment," AIAA-85-0415, presented at AIAA 23rd Aerospace Sciences Meeting, January 14-17, 1985 Reno, Nevada.

PRECEDING PAGE BLANK NOT FILMED

A High Flux Source of Energetic Oxygen Atoms for Material Degradation Studies

G. E. Caledonia, R. H. Krech, B. D. Green

A High Flux Source of Energetic Oxygen Atoms for Material Degradation Studies

George E. Caledonia,* Robert H. Krech,† and Byron D. Green‡
Physical Sciences Inc., Andover, Massachusetts

A novel technique for generation of a high flux of energetic (nominal ~5 eV) oxygen atoms has been demonstrated in the laboratory. The generation technique involves a laser-induced breakdown of molecular oxygen followed by a rapid expansion of the recombining plasma, resulting in the production of a flux of nearly monoenergetic oxygen atoms. We have developed consistently high velocity streams of oxygen atoms in an evacuated hypersonic nozzle. The oxygen flow is introduced into the nozzle through the mediation of a fast (~100 μs) pulsing valve and broken down with a CO_2 laser. We have measured average oxygen atom velocities of ~5 to 13 km/s with an estimated total production of 10^{18} atoms per pulse over pulse durations of several μs. Although these were single pulse measurements, scaling to a repetitively pulsed device appears straightforward. The O-atom source was used to irradiate sample targets, including Al, Fe, and polyethylene, and target-material-specific radiation was observed above the target surfaces, indicating energetic O-atom induced mass removal.

Introduction

ONE of the most significant observations during the early missions of the Space Shuttle was the degradation and mass loss of certain materials upon exposure to the low Earth orbit environment. For example, Kapton suffered a loss of transparency, paint lost gloss, carbon was removed from surfaces, and silver underwent oxidation.[1-4] As the Shuttle sweeps through its orbit at velocities of 8 km/s, the Earth's natural atmospheric species energetically impact on the Shuttle's ram direction surfaces. At low Earth-orbit Shuttle mission altitudes (230-310 km), the natural atmosphere is dominantly O-atoms. Although the atmosphere is quite variable at these altitudes, a surface at normal incidence to the orbital velocity vector is subjected to O-atom fluxes in the range of 4×10^{14}-2×10^{15} cm^{-2} s^{-1} (Refs. 1-3). These atoms are chemically reactive and are strongly suspected to be the major source of the observed material degradation. Experimental pallets flown on STS-5 and -8 clearly demonstrated the dependence of the degradation on ram atom flux exposure and began to quantify mass losses and changes in various material properties (tensile strength, optical quality) for a host of materials of aerospace interest over a range of material thickness, coatings, temperatures, and reactive fluxes (and exposure times) while on orbit.[2] The STS-8 pallet was exposed to an integrated O-atom flux of 3.5×10^{20} cm^{-2} and the observations revealed that material ranged from quite reactive (e.g., polymeric hydrocarbons, epoxies, urethanes, graphites, osmium, and silver) to relatively inert (e.g., silicons, silicates, fluorides, fluorinated hydrocarbons, oxide pigments, and noble metals). For the most reactive compounds such as Kapton, 10% of surface/O-atom collisions led to mass loss, most probably through chemical reaction.[2,3]

The observations from STS-5 and -8 have laid the groundwork for more detailed measurements planned for a later Shuttle flight—the EOIM-3 measurement program, where mechanisms and O-atom combustion reaction products will be investigated using sophisticated detection techniques. The need for such measurements has been emphasized recently in a study by Leger et al.[5] where it was demonstrated that O-atom material degradation also could have a severe impact on the performance of the Space Station. These observations have led NASA to pursue the development of various material hardening techniques directed to make materials more impervious to the effects of energetic oxygen atoms.

These observations and program directions stress the need for a laboratory facility that can be used to measure/study material degradation due to energetic O-atoms. While the Space Shuttle provides a valuable testbed for such investigations, both the large number of materials/flight conditions to be studied and flight scheduling constraints mandate that the major portion of such studies be performed in a ground facility. For example, important parameters include material composition, material temperature, solar UV exposure, sample stress loading, impact angle of reactive flux, etc.[6,7] Furthermore, issues such as flux dependencies and variations in degradation rates with exposure time[8] also require investigation.

We have conceived and successfully implemented a new approach for the production of large fluxes of energetic oxygen atoms, which draws on years of research in the area of pulsed laser propulsion.[9,10] In this concept, an incoming laser beam is focused into the throat of a nozzle to yield a breakdown in the ejected gas. The resulting high-pressure plasma is characteristic of a detonation wave initiated by a high-power laser-induced breakdown. With a short duration laser pulse, the detonation wave quickly becomes a blast wave, which propagates to the nozzle exit plane, converting all of the high pressure of the gas behind it into a propelling force. The stagnation energy of the laser-produced plasma is converted effectively to velocity of the exhaust gases.

In the experiments described below, we introduce ~10^{-4} g of pure O_2 into an evacuated expansion nozzle using a fast (~100 μs) pulsed molecular valve. The fast switching allows the gas to remain localized within the nozzle while the 10.6 μm CO_2 laser having pulse energy of ~5 J and pulse length of 2.5 μs is focused into the nozzle so as to cause breakdown at the throat. The subsequent laser-initiated detonation wave heats the major portion of the gas within the nozzle during

the laser pulse time, creating a high temperature plasma. This plasma then expands through a nozzle, tailored to allow electron-ion recombination but not atomic recombination. As the gas expands its temperature and density drop, however, its directed velocity increases correspondingly. Thus a thermally "cold," high energy beam of oxygen atoms is available at the nozzle exit. For example, with 10^{-4} g of gas and 5 J laser pulse, we estimate formation of $\geq 10^{18}$ oxygen atoms with a characteristic energy of 5 eV. For comparison with other sources, if such a device could be pulsed at 1 Hz (easily achieved with available laser devices) and be expanded out of a nozzle with 100 cm^2 base, an average flux of 10^{16} O-atoms/cm^2-s could be maintained on a 100 cm^2 target. The details of our experimental apparatus and observations are provided below.

Experimental Apparatus

A schematic diagram of the apparatus is shown in Fig. 1. The laser is located in an electromagnetic interference (EMI) reducing enclosure approximately 3 m from the test chamber. Two radiometers for time-of-flight velocity measurements are located on the top flange of the vacuum chamber. An optical multichannel analyzer (OMA) spectrograph is positioned at the side of the vacuum chamber to diagnose the atomic oxygen beam.

A Lumonics K-103 TEA laser is used to generate up to 10 J pulses of 10.6 μ radiation. The laser pulse width is 2.5 μs, with approximately one-third of the energy delivered in the first 200 ns (the gain-switched spike). The radiation in the initial spike generates a laser induced breakdown in the high pressure oxygen at the nozzle throat, forming a plasma that continues to absorb the radiation as long as the laser is on.

The laser beam is directed to the test chamber by three gold turning mirrors. A sodium chloride flat between the second and third mirror reflects 8% of the beam to a Lumonics Model 50D calorimeter to monitor the laser energy. A 300 mm focal length barium fluoride lens (35 mm clear aperture), located in a focusing tube at the entrance window, is used to focus the laser beam approximately to a 1 mm diam spot size at the nozzle throat. Accounting for various losses, approximately one half of the laser energy typically is delivered to the focal spot. Peak spike intensity is about 2×10^9 W/cm^2, which is sufficient to cause a rapid breakdown in the gas.

The test chamber is a standard 20 cm diam six-way stainless steel high vacuum cross with Con-Flat flanges (MDC Inc.). The top flange of the chamber has two 5 cm i.d. quick connect O-ring vacuum couplers to allow the insertion of time-of-flight O-atom radiometers into the chamber. The end flange opposite the pulsed valve assembly has a 5 cm O-ring quick connect to allow for positional adjustment of the laser input lens, which is mounted inside a 5 cm o.d. focusing tube. Each side flange has two 5 cm diam quartz view ports for visual and spectroscopic observations. The bottom flange is connected to a 5 cm diffusion pump stack, which provides for an ultimate pressure in the chamber of 3×10^{-5} torr. In operation, the chamber pressure is kept below 1×10^{-4} torr to prevent beam interaction with the background gas.

The pulsed valve/nozzle assembly is shown schematically in Fig. 2. The valve is a Model BV-100V pulsed molecular beam valve from Newport Research Inc. This valve allows the generation of short duration pulses of gas at high flow rates. The valve is operated with a 1 mm i.d. orifice plate, and is bolted directly to a 100 mm long, 20-deg full angle aluminum expansion nozzle with a 1 mm i.d. throat. The nozzle has two flush-mounted pressure transducers with 1 μs response located 43 and 93 mm from the throat. The choked flow rate of the valve/nozzle assembly is 0.19 g of oxygen per s per atmosphere stagnation pressure. In principle, the valve/driver combination can produce gas pulses as short as 100 μs. The device was operated for several thousand pulses with no observable degradation of the aluminum nozzle.

Optical Measurements

Two kinds of optical measurements are conducted to probe the laser processed O-atom beam. The time history of the 777.3 nm atomic oxygen line emission is measured by two identical radiometers mounted on the top flange of the vacuum chamber to determine the beam velocity. The Hammamatsu R406 Photomultiplier tubes are coupled to a 50 mm focal length lens mounted on a 250 mm long by 50 mm diam telescope barrel passing through the flange plate in O-ring quick connect couplers. The field of view of each radiometer is restricted to a 1 x 10 mm rectangle perpendicular to and across the flow centerline, by positioning a 4 x 40 mm slit in the image plane of the lens. The radiometers are separated by 7.6 cm and are located 12 and 19.6 cm from the nozzle throat, respectively. They are filtered to observe only 777.3 nm O-atom emission.

Spectral Measurements

Spectral measurements of the laser processed O-atom beam (and target interactions) are obtained using a Princeton Instruments Optical Multichannel Analyzer (OMA) coupled to a 0.275 m Jarrel Ash Mark X spectrograph. The OMA head consists of a 1024 photodiode array with a gated S-20R intensifier. The spectrograph has a 600 line/mm grating blazed at 450 nm. With a 25 μ entrance slit, the measured
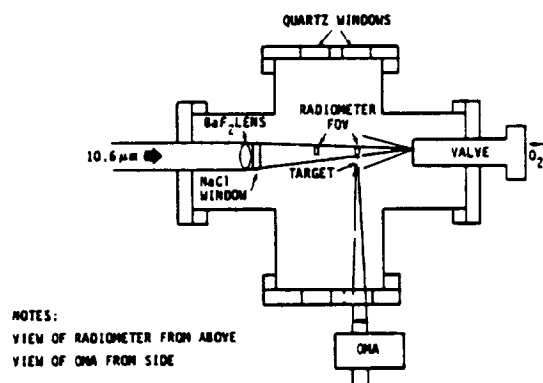
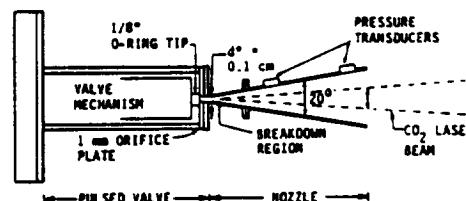

Fig. 1   O-atom experiment schematic.

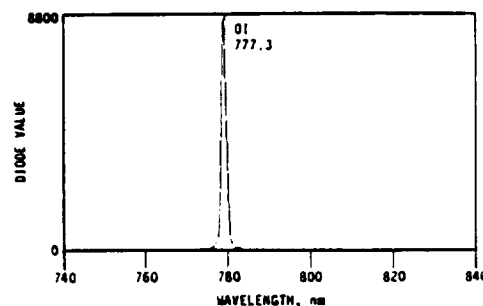**Fig. 2   Schematic of O-atom pulsed valve/nozzle assembly.**

Fig. 3   Red portion of the spectral survey of expanded oxygen plasma.

spectral resolution was 0.6 nm. The optical field of view in the chamber was restricted to a 0.090 by 0.90 cm rectangle centered 2 cm downstream of the nozzle exit by a collecting telescope matched to the f number of the spectrograph (f/4.2) attached to the entrance slit. Colored glass cut-on filters were used to prevent second and higher order spectra from being recorded. Spectra were recorded using the OMA in the gated mode.

O-Atom Source Characterization

Measurements typically were performed with a laser pulse energy of 5 J and an O_2 stagnation pressure of 6½ atmospheres. The laser was focused on an approximately 1 mm spot near the nozzle throat. Breakdown in pure O_2 was readily and consistently achieved under these conditions. It is anticipated that breakdown occurred slightly downstream of the nozzle throat, however this postion was not accurately measured.

It was found to be best to flow the O_2 gas for ~200 μs prior to applying the laser pulse. This ensured filling the nozzle without increasing the vacuum chamber pressure, which was held to ~10^{-4} torr. The nozzle pressure transducers were found to be ineffective due to a combination of electrical noise pick up and high frequency ringing, and thus the key diagnostics for monitoring the heated gas flow were the optical detectors. The OMA was triggered approximately 5 μs after the laser trigger in order to minimize the effect of scattered light from the initial high temperature plasma and was typically gated on for 100 μs.

A number of spectral scans of the radiation from the expanded oxygen plasma were performed over the wavelength range of 400–800 nm. Results were highly reproducible. Two main spectral subsets were observed. The first are the H_λ, H_β, and H_α lines. The impurity radiation later was found to arise from plasma-induced erosion of the hydrocarbon nozzle tip and can be eliminated by appropriate nozzle throat design. The second subset is a series of OI lines, strongly dominated by the transition at 777.3 nm, but also includes transitions at 615.7 and 436.8 nm, among others. These transitions have been identified through a cursory examination of standard tables.[11,12] There are a number of weaker spectral features also seen, many of which have been identified as due to atomic oxygen as seen in electron irradiated air studies.[13] Given that the spectral resolution of the data is 0.6 nm and that many transitions of species such as OII and A/II in addition to OI also fall in this spectral region, no attempt has been made to identify these transitions. Nonetheless, no strong transitions due to OII or A/ have been observed and it is clear that the dominant spectral features (with the exception of hydrogen impurity) are due to hot oxygen atoms with no evidence of significant radiation from the nozzle materials or their oxides. There are undoubtedly metastable oxygen atoms in the beam, although their radiation is too weak to be observed. We estimate that they will be present in equilibrium concentrations at the nozzle exhaust temperature.

A typical scan of the red portion of the spectrum is shown in Fig. 3. The only feature observed in this spectral region is the 777.3 nm line. This transition provides an excellent diagnostic for the presence of hot oxygen atoms and thus was used to monitor O-atom velocity. As described above, the two filtered radiometers were positioned to view 12 and 19.6 cm downstream from the nozzle throat. The observed onset of this emission corresponds to the time required for oxygen atoms to reach the monitored point. Thus measurements at different positions can be differentiated to evaluate velocity.
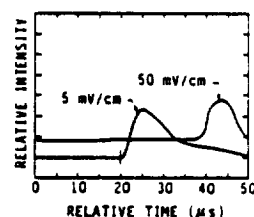
Typical radiometer traces are shown in Fig. 4. Two traces are shown on each oscillogram; the upper trace corresponds to the radiometer positioned at 12 cm and the lower to that positioned at 19.6 cm. Laser onset in each case is marked on the left-hand side of each trace by a small spike on the baseline. The trend is the same in all cases. Radiation is seen first
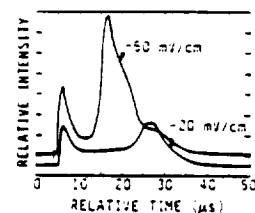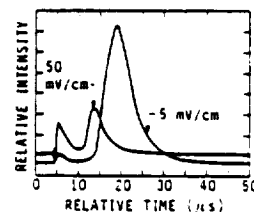
Fig. 4 777.3 nm radiometer histories (timescale is 5 μs per division).
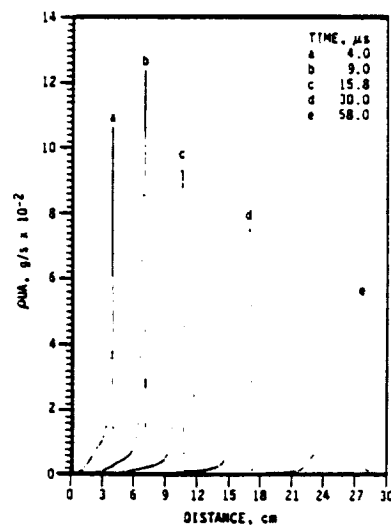
Fig. 5 Predicted profiles of mass flow (gas density * velocity × area) within the nozzle at different times. E_L = 5 J, $P_{stagnation}$ = 6½ atm.

within a few μs of the laser pulse. This radiation occurs much too soon to be from hot gases expanded through the nozzle. Rather it is anticipated that this is due perhaps to either photoexcitation of the ambient gases by the hard UV radiation produced by the oxygen plasma or scattered light from the plasma (recall that the laser pulse width is 2.5 μs). The second sharply rising peak is attributed to the passage of energetic oxygen atoms. This "spike" of radiation typically has a width of 10 μs and is delayed and slightly wider at the downstream location as anticipated.

The characteristic velocity of the oxygen atoms can be defined in several ways. We have chosen an average velocity as defined by the distance from the nozzle throat and the time to reach peak radiation after laser pulse initiation on both radiometers. The values of average velocity are listed in Fig. 4 with the subscripts 1 and 2 referring to the radiometers positioned 12 and 19.6 cm from the nozzle throat, respectively. The important quantity in determining O-atom velocity is the amount of energy deposited per unit mass of gas in the nozzle. The three cases shown in Fig. 4, were chosen to exemplify this variation. In these studies, we have not measured the total energy absorbed but only the total incident laser energy and thus the comparisons can only be qualitative. Nonetheless, the observed trends are as anticipated.

Figure 4a corresponds to ~5 J incident energy into a filled nozzle with a plenum pressure of $6\frac{1}{3}$ atm of O_2. Deduced velocities are found to be 9–10 km/s, slightly larger than Shuttle orbital velocities. Figure 4b corresponds to the same laser energy but a plenum pressure of 3 atm. As expected, the velocity is higher in this case, ~13 km/s. Figure 4c corresponds to a reduced laser energy of 3.1 J and a plenum pressure of $6\frac{1}{3}$ atm, i.e., the same as Fig. 4a except for a lower laser energy, and here the velocity is reduced to 5 km/s. We note that to first order we expect the velocity to scale as $V\alpha\sqrt{E/\Delta m}$, where E is the laser energy absorbed and Δm is the mass processed. The observations shown in Fig. 4, which are highly reproducible, are clearly in qualitative agreement with such scaling.

A theoretical prediction has been provided for comparison with the data using a validated code that can predict the unsteady expansion of the heated plasma.[14] The nozzle expansion is modeled by quasi-one-dimensional flow in a variable area nozzle. The physical phenomena included in the model are 1) conservation of mass, momentum, and energy; 2) chemical equilibrium of the flowing gas; and 3) heat addition by absorption of laser energy. The calculation was initiated by assuming one-third of the laser energy (the gain-switched spike) was absorbed instantaneously by the gas within the first cm from the nozzle throat. The remaining laser energy was then modeled as being absorbed through inverse Bremsstrahlung mechanisms occurring within the fluid dynamically active plasma. The area distribution specified, corresponded to that of the nozzle used in the experiments, except that the length was taken as 20 cm. The code thermodynamic data is sufficient to characterize accurately oxygen plasmas up to triply ionized states.

The calculation was performed for a CO_2 laser pulse energy of 5 J and a plenum pressure of $6\frac{1}{3}$ atm, corresponding to the case shown in Fig. 4a. The predicted fluid dynamical behavior is displayed in Fig. 5, which exhibits "snapshots" of the profile of mass flow rate in the nozzle as a function of distance at different flow times. What is depicted clearly is a narrow "slug" of gas moving rapidly down the nozzle. Predicted profiles of mass per unit length in the nozzle have very similar shapes, demonstrating that the major portion of the heated gas at any one time is moving at a characteristic velocity with very little spread, ideal for simulation studies of Shuttle material degradation.

Similar profiles of atom velocity vs distance at different flow times are shown in Fig. 6. These predictions are for the instantaneous local velocity distribution and are not to be confused with the average velocities deduced from the radiometer traces. The blips observed in the profiles are most probably a numerical artifact of the code and should be ignored. Note that the velocity profiles are quite broad. Nonetheless, from comparison with Fig. 5, it can be seen that the velocity variation over the axial range of the gas pulse is predicted to be very small, ideal for the present beam application. The predicted gas behavior is characteristic of that associated with a blast wave. Although the gas velocity scales inversely with distance from the source, most of the
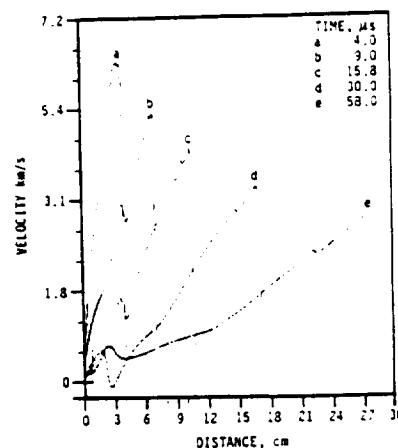

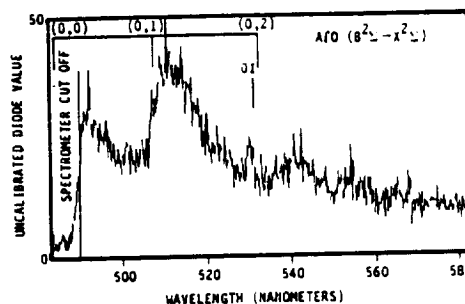Fig. 6   Predicted profiles of gas velocity for the conditions of Fig. 5.

Fig. 7   Observed emission over ALCLAD 7075 target (average of four shots) $(E_L \sim 5$ J, $P_{\text{plenum}} = 6\frac{1}{3}$ atm).

mass is at the wave front, and thus the resulting atomic beam is near monoenergetic.

The calculations can be compared only with the data out of the nozzle at 10 cm. This is because the code assumes that the flow continues to ingest gas at larger distances and thus slows down. In reality, the heated gases expand into near vacuum at the nozzle exhaust and should remain at near constant velocity beyond that point. Although the model predictions of gas flow are similar to the observations, the predicted velocities are approximately 30% lower than the measured values. It may be that the nozzle was not uniformly filled during the experiments. In the future, time-of-flight mass spectrometry will be used to characterize the beam velocity.

In summary, we have demonstrated the ability to produce high fluxes of approximately monoenergetic oxygen atoms at velocities comparable to those of interest to low Earth orbit. The actual O-atom flux has not been measured but is estimated from computer predictions to correspond to number densities of $\sim 10^{18}$ per pulse. Beam conditions appear readily scalable with nozzle pressure and laser energy, and extension to a repetitively pulsed device is straightforward. It is clear that the beam has only been crudely characterized to date and that an expanded system will require more sophisticated diagnostics.

Material Degradation Studies

Once the O-atom source had been characterized, a limited number of target irradiation observations were performed. The object of these was not to monitor mass loss or surface modification but merely to study the spectral signatures above irradiated surfaces in order to identify spectral

features peculiar to the O-atom/material interaction. To this end, small targets of aluminum and iron were introduced into the test chamber at a distance 17.1 cm downstream of the nozzle throat and irradiated with oxygen atoms generated under the $E_L = 5$ J, $P_{stagnation} = 6\frac{1}{3}$ atm conditions. The radiation above the surfaces of these targets was monitored with the OMA instrument in order to identify spectral features due to, for instance, metal oxides, which would provide evidence of oxygen atom induced material degradation. The OMA was positioned to look at the target at a ~ 10 deg grazing angle.

The first measurements were made above an aluminum target, ALCLAD 7075. The observed spectrum was compared directly to the measurement performed in the absence of the target and many of the spectral features previously observed were also seen above the aluminum target. The relative intensities are different, however, suggesting selective quenching/reaction on the surface. Several new spectral features appear, which remain to be identified.

The (0,0) bandhead of the AlO green band is unfortunately near coincident with the strong H_β transition. Radiation to the red of this latter transition was monitored and the results are shown in Fig. 7. Band head positions of the $(0, v')$ sequences are also designated[15] and, although the signal is quite noisy, it does appear that radiation from AlO has been observed. More careful and detailed measurements will be required to verify this.

Similar measurements were performed with a target of generic cold-rolled steel. Again the H_λ and H_β transitions are seen as well as the feature at 431 nm. Many of the other transitions observed over the aluminum target and in heated oxygen flow were not seen here however. A search was made for the FeO orange bands which fall between 530–680 nm[13]; although there was some evidence of banded structure in the spectra, the FeO bands could not be positively identified.

A polyethylene sample also was irradiated. The sample was supplied by the Jet Propulsion Lab and was from the same block of material as that flown on STS-8.[3] The polyethylene was irradiated with several hundred oxygen-atom pulses and then examined by Electron Spectroscopy for Chemical Analysis (ESCA). The measured oxygen surface enrichment of the polyethylene was very similar to that observed in post-flight analysis of the same flown on STS-8.[16] Portions of the sample within the test chamber, but not struck by the O-atom beam, showed no enhancement. The irradiation level was insufficient to measure mass loss.

Other polymeric targets were also examined briefly. Strong radiative features corresponding to electronic bands of CN and OH were observed. No quantitative evaluation of this data has been performed.

These target studies were necessarily quick surveys, however, it is clear that target interactions provide for significantly varying spectral signatures with some spectral features indicative of mass removal. It is clear that spectra averaged over many O-atom pulses should provide information on the kinetic mechanisms responsible for mass removal which could be used in conjunction with mass loss and surface modification observations for mechanistic interpretations of oxygen atom material interactions. Furthermore, there has been considerable discussion of observed glows over spacecraft surfaces.[4] It is clear that chemical reactions between ambient oxygen atoms and spacecraft surfaces can produce volatile species in excited states, thus introducing material specific radiation signatures. Such effects undoubtedly occur but have not yet been quantified in Space Shuttle observations. The present facility can be directly applied to study such signatures through the ultraviolet to the infrared.

References

[1]Leger, L. J., Spiker, I. K., Kuminecz, J. F., and Visentine, J. T., "STS Flight 5 LEO Effects Experiments—Background Description and Thin Film Results," AIAA Paper 83-2631, Oct. 1983.

[2]Leger, L. J., Visentine, J. T., and Kuminecz, J. F., "Low Earth Orbit Atomic Oxygen Effects on Surfaces," AIAA Paper 84-0548, Jan. 1984.

[3]Visentine, J. T., Leger, L. J., Kuminecz, J. F., and Spiker, I. K., "STS-8 Atomic Oxygen Effects Experiment," AIAA Paper 85-0415, Jan. 1985.

[4]Green, B. D., Caledonia, G. E., and Wilkerson, T. D., "The Shuttle Environment: Gases, Particulates and Glow," *Journal of Spacecraft and Rockets*, Vol. 22, Sept.–Oct. 1985, pp. 500–511.

[5]Leger, L. J., Visentine, J. T., and Schliesing, J. A., "A Consideration of Atomic Oxygen Interactions with Space Station," AIAA Paper 85-0476, Jan. 1985.

[6]Hall, D. F. and Steward, T. B., "Photo-Enhanced Spacecraft Contamination Deposition," AIAA Paper 85-0953, June 1985.

[7]Peterson, R. V., Hanna, W. D., and Mertz, L. O., "Results of Oxygen Atom Interaction with Kevlar and Fiberglass Fabrics on STS-8," AIAA Paper 85-0990, June 1985.

[8]Knopf, P. W., Martin, R. J., McCargo, M., and Dammann, R. E., "Correlation of Laboratory and Flight Data for the Effects of the Atomic Oxygen on Polymeric Materials," AIAA Paper 85-1066, June 1985.

[9]Simons, G. A. and Pirri, A. N., "The Fluid Mechanics of Pulsed Laser Propulsion," *AIAA Journal*, Vol. 15, June 1977, pp. 835–842.

[10]Rosen, D. I., Pirri, A. N., Weiss, R. F., and Kemp, N. H., "Repetitively Pulsed Laser Propulsion: Needed Research," *Progress in Astronautics and Aeronautics*, edited by L. H. Caveny, Vol. 89, 1984, pp. 95–108.

[11]Weise, W. L., Smith, M. W., and Glennon B. M., "Atomic Transition Probabilities, Vol. I, Hydrogen Through Neon," NSRDS-NBS 4, Washington, DC, 1966.

[12]Bashkin, S. and Stoner, J. O. Jr., "Atomic Energy-Level and Grotrian Diagrams, Vol. I, Hydrogen I—Phosphorous XV," North-Holland Publishing Co., Amsterdam, the Netherlands, 1978.

[13]Blumberg, W. A. M., Wolnik, S. J., Green, B. D., and Caledonia, G. E., "Formation and Relaxation of Highly Excited Atomic Oxygen," EOS 65, SA11–12, 1984.

[14]Kemp, N. H., "Computer Simulation of the Non-Steady Flow of a Real Gas with Laser Energy Absorption," AIAA Paper 84-1568, June 1984.

[15]Pearse, R. W. B. and Gaydon, A. G., *The Identification of Molecular Spectra*, Chapman and Hall Ltd., London, 1963, p. 63.

[16]Coulter, D., Jet Propulsion Laboratory, Pasadena, CA, private communication, 1985.

AIAA-87-0105
Energetic Oxygen Atom
Material Degradation Studies

G. E. Caledonia and R. H. Krech
Physical Sciences Inc., Andover, MA

AIAA 25th Aerospace Sciences Meeting
January 12-15, 1987/Reno, Nevada

Energetic Oxygen Atom Material Degradation Studies

George E. Caledonia and Robert H. Krech
Physical Sciences Inc.
Research Park, P.O. Box 3100
Andover, Massachusetts   01810

Abstract

Recent observations on Space Shuttle have demonstrated that the orbital velocity impact of ambient oxygen atoms on various Shuttle surfaces can lead to material degradation and mass loss. This has lead to the development of new materials which are more impervious to energetic oxygen atom attack, as well as to the development of laboratory facilities which can provide high flux beams of ~8 km/s oxygen atoms for material degradation studies. In this paper we will describe a novel technique for generation of a high flux of energetic (nominal ~5 eV) oxygen atoms. The generation technique involves laser-induced breakdown of molecular oxygen followed by a rapid expansion of the recombining plasma, resulting in the production of a flux of nearly mono-energetic oxygen atoms. We have consistently developed high velocity streams of oxygen atoms in an evacuated hypersonic nozzle and have measured average oxygen atom velocities of ~5 to 13 km/s with an estimated total production of 10^{18} atoms per pulse over pulse durations of several μs. The device is now being expanded to allow operation at 20 Hz corresponding to O-atom flows in excess of 2×10^{19} s^{-1}, and with more sophisticated diagnostics including laser induced fluorescence and mass spectrometry. The operating characteristics of the O-atom device and the properties of the pulsed beam itself will be described. Our observations of material degradation by energetic oxygen atom impact will be reviewed.

Introduction

The on-orbit environment around the Space Shuttle is very dynamic. Shuttle surface outgassing, exacerbated by solar heating and enhanced by thruster firings, provide for a contaminant "cloud" around Shuttle exhibiting local densities one to three orders of magnitude above ambient.[1] The interactions of the ambient species, dominantly neutral oxygen atoms and nitrogen molecules, and, at much lower concentrations, oxygen ions, with the contaminants, produces new species including a tenuous plasma which travels with Shuttle. This plasma, which can be effected by the earth's magnetic field, is not yet well diagnosed, but appears to exhibit instabilities which provide electron/ion heating.[1]

This contaminant "cloud" is not sufficiently dense to screen Shuttle surfaces from direct collision with ambient species. These interactions, which occur at orbital velocities of 8 km/s, produce several interesting phenomena including: selective charging of spacecraft surfaces; a ram-direction surface glow which is observed to extend more than 20 cm from the Shuttle surface; and, most important from a system design point of view, material degradation and mass loss.

46

This observed material degradation appears to result from surface interaction with ambient oxygen atoms although the Shuttle-based measurements are insufficiently exact to rule out contributions due to other species. Furthermore, any synergistic effect due to the Shuttle environment (i.e., solar UV, plasma, surface charging) discussed above remains to be determined.

Shuttle-based measurements of mass loss for a variety of materials have been converted to O-atom removal rate constants using model estimates of the ambient O-atom concentrations. Typical results, as reported by Leger et al.,[2] are presented in Table 1. The reaction rates are quite high for hydrocarbon materials, corresponding to O-atom collisional removal efficiencies of ~ 10 percent. These measurements correspond to data taken over about 1 week on orbit and do not address aging effects. Indeed laboratory tests[3] on teflon suggest aging effects are important for this material.

Oxygen atom induced material degradation will be important for any space structure operating in low-earth orbit. Leger et al.[2] have shown that for the case of space station, unacceptable surface recession would occur with selected structural materials over a station life of 30 years. Such observations have spurred the development of new structural materials or coatings which will provide hardening against oxygen atom attack. Further concern has developed over oxygen atom-induced surface modification resulting in the change of optical, thermal, or conductive properties of key spacecraft materials.

Such considerations have led NASA to develop a relatively detailed Shuttle material degradation study, designated EOIM-3, which will be manifested shortly after resumption of Space Shuttle flights. There has also, naturally, been significant activity in developing ground-based energetic oxygen atom facilities for material testing. Indeed there are over 15 such facilities presently in development in the United States. These oxygen atom sources may be broken up into three basic types. The first of these are asher sources, where oxygen atoms are formed by a variety of discharge techniques. For the most part these are thermal sources, although hypersonic expansion of such excited flows have produced oxygen atom beams having energies < 1 eV. The second type of source exploits ion beam neutralization. A beam of positive or negative oxygen ions is field accelerated to the desired energy and then neutralized by such techniques as gas phase charge exchange, solid interface neutralization or photo-detachment to produce the desired oxygen atom beam. These sources are straightforward and can produce the desired energy of 5 eV, but are limited in ultimate flux by Coulumbic repulsion of the ion beam. The third type of O-atom source utilizes laser heating to produce a high temperature gas which is subsequently expanded, thus converting the thermal energy to directed velocity. This can be achieved using either pulsed or CW lasers.

This paper is concerned with Physical Sciences Inc.'s (PSI) pulsed laser technique for generating a beam of energetic oxygen atoms. The next section provides a brief overview of the device and its current status. This is followed by a review of some preliminary material degradation studies.

2

Facility Description

The O-atom source has been described in detail previously[4] and will only be overviewed here. The basic concept of the device is shown schematically in Figure 1. First a pulse of molecular oxygen is introduced into an evacuated expansion nozzle. The duration of the gas pulse is chosen to just fill the nozzle. A pulsed CO_2 laser is then used to break down the gas creating a high temperature plasma in the throat region of the nozzle. The plasma expands down the nozzle as a blast wave, ingesting and dissociating the gas in front of it, with ultimate conversion of the thermal energy to directed velocity. The expansion is so tailored as to allow for electron-ion neutralization without atomic recombination. Thus each laser pulse produces a temporally narrow, high flux pulse of nearly mono-energetic oxygen atoms at the nozzle exhaust which can then be directed on materials of interest.

A general schematic of the device is shown in Figure 2. As presently configured the device is composed of three key sections: 1) a vacuum chamber which provides an operating background pressure of $< 10^{-4}$ torr, sufficiently low to ensure collision-free passage of the energetic oxygen atom beam; 2) a Newport Research pulsed molecular beam valve which allows rapid pulsed introduction of molecular oxygen into the nozzle; and 3) a Laser Applications Limited pulsed CO_2 laser which provides 18J of energy per pulse at 10 Hz. The device presently provides $\sim 3 \times 10^{18}$ 5 eV oxygen atoms per pulse at a 2 Hz pulse rate and has been standardly operated for several hours at a time producing average on target irradiances of 5×10^{20} oxygen atoms per square centimeter. A larger device is presently being assembled which will allow operation at 10 to 20 Hz and provide for irradiation of material areas as large as a few hundred square centimeters. This device will have both mass spectrometric and laser-induced fluorescence diagnostics for characterizing both beam properties and irradiated material effluents.

Beam Diagnostics

Optical measurements have been conducted to characterize the laser initiated O-atom beam. Beam velocities from 5 to 13 km/s were obtained by varying both the stagnation pressure and the laser energy. The velocities were deduced by monitoring the time history of the 777.3 nm atomic oxygen line emission with two filtered radiometers mounted on the top flange of the vacuum chamber. Additional measurements were performed with a mass flow meter to monitor the input oxygen flow rate, a dynamic pressure transducer to determine the temporal flow history of both cold and hot flows, a ballistic pendulum to measure the total impulse of the hot and cold flows. A pressure transducer was positioned at the same distance down stream from the nozzle throat as one of the radiometers. The peak in the pressure trace coincides with the peak in the radiometer signal demonstrating that the optical signal is indicative of the gas behavior during the hot flow.

A mass flow meter calibrated for oxygen, argon, hydrogen, neon, and helium was placed upstream of the pulsed valve to measure the average flow

through the system. The pulse rate was adjusted for 0.25, 0.5, 1.0, 2.0, and 4.0 Hz, and the mass flow rate was observed to track linearly with rep rate. Establishing that the mass per pulse is independent of repetition rate, the mass flow per pulse was changed by a factor of 2.4 by increasing the pulse duration, and the total measured impulse was observed to change by the same amount. These two measurements confirmed that the valve operation is reproducible and independent of repetition rate.

A ballistic pendulum was installed to measure the cold flow velocity of the gas exiting the nozzle. The configuration for this procedure is shown in Figure 3. The pendulum is simple consisting of a plastic drinking cup with a Handi-wrap[8] window to allow transmission of the laser beam into the nozzle. The motion of the pendulum was recorded on video tape and later analyzed for deflection using the standard ballistic pendulum equation. This requires a determination as to whether the gas surface collisions are elastic or inelastic inasmuch as the momentum transfer differs by a factor of two in these limits.

Ordinary collisions between inert gas molecules and a wall were expected to be elastic. In the extreme degree of expansion performed in the nozzle, the gas velocity should be close to the maximum achievable velocity, V_{max}:

$$V_{max} = \left[\left(2 \times \left(\gamma/\gamma - 1 \right) R T / M \right) \right]^{1/2} .$$

In helium, the velocity was observed to be 95 percent of V_{max}. However, in the other gases, the ratio was between 65 and 80 percent. The expansion is extreme, $P_o/P > 10^7$, and therefore the gas is extremely cold. For all gases except helium, the isentropic expansion pressure exceeds the vapor pressure at the expansion temperature by at least several orders of magnitude, implying that homogeneous or heterogeneous dimerization may occur changing both γ and molecular weight as well as collision elasticity.

This cold flow analysis was used in evaluating the mass flux of the oxygen atom beam. The situation is slightly more complicated here in that the laser breakdown causes acoustic valving , essentially shutting down the inlet gas flow in mid-pulse. The fractional mass flow which could be processed by laser heating was estimated by a transducer recording the dynamic pressure within the nozzle during cold flow. The mass of gas which is processed by the laser can be estimated, by using the ratio of the areas under the pressure trace until the laser fired to the total area under the trace, and normalizing the result with the measured mass flow rate. The ballistic pendulum measurements, after correcting for the difference in mass flow, yield a mass averaged velocity approximately equal to that obtained from the time of arrival of the pressure pulse at the transducer location and as determined by radiometric measurements. This analysis again assumes primarily elastic collisions and provides flux evaluations which are accurate to ± 20 percent. Further beam characterization utilizing laser-induced fluorescence is now in process.

4

Preliminary Material Degradation Studies

Preliminary material degradation studies have been conducted with the small test facility. Materials irradiated have included polyethylene, Teflon®, Kapton® (untreated and oxidation resistant treated samples), Mylar®, PEEK, PBT and Carbon Epoxy composites, as well as selected metals. Several of these measurements are described in Ref. 4.

Ground-based testing facilities must produce a surface morphology and mass removal rate similar to that produced on orbit to provide meaningful erosion data. Typical erosion morphology of a polymeric sample is shown in Figure 4 (graciously provided by J.T. Visentine),[5] for exposure levels of 5 to 9×10^{20} O-atom/cm^2, corresponding to ~1 week on orbit. Kapton samples irradiated in our facility to an exposure level of ~3.3×10^{20} O-atom/cm^2 show a remarkably similar surface morphology, Figure 5, and measurable mass loss (~1.3 mg). (Figure 6 shows a sample of Kapton 500H prior to exposure for comparison.) This morphology is not due to kinetic energy alone since another sample of Kapton was bombarded with ~5 eV Ar (Figure 7) and showed no mass loss. Similar results were obtained with low and high density polyethylene samples.

Current capabilities provide for exposure rates of ~1.5×10^{20} atom/cm^2-hr at ~5 eV (~1.6 Hz); and provide an exposure acceleration factor of 50 compared to LEO and 5000 for space station altitudes for ~6 cm^2 samples. The larger facility presently being assembled will allow for further accelerated testing over larger sample areas (~ 100 cm^2).

Acknowledgement

5

## References

1. Green, B.D., Caledonia, G.E., and Wilkerson, T.D., "The Shuttle Environment: Gases, Particulates, and Glow," J. Spacecraft Rock. $\underline{22}$, 5, September-October 1985, 500-511.

2. Leger, L.J., Visentine, J.T., and Schliesing, J.A., "A Consideration of Atomic Oxygen Interactions with Space Station," AIAA-85-0476 presented at AIAA 23rd Aerospace Sciences Meeting, January 1985, Reno, NV.

3. Gerde, H.B., Chun, T.R., and Low, S.J., "Degradation and Aging Effects on Teflon Exposed to an Oxidizing Plasma," in Proceedings of 18th International SAMPE Technical Conference, Vol. 18, eds. J.T. Hoggatt, S.G. Hill, and J.C. Johnson.

4. Caledonia, G.E., Krech, R.H., and Green, B.D., "Development of a High Flux Source of Energetic Oxygen Atoms for Material Degradation Studies," AIAA J. $\underline{25}$, 1, January 1987, 59-63.

5. Visentine, J.T., Leger, L.J., Kuminecz, J.F., and Spiker I.K., "STS-8 Atomic Oxygen Effects Experiment," AIAA-85-0415, presented at AIAA 23rd Aerpspace Sciences Meeting, January 1985, Reno, NV.

6

Table 1. Shuttle Observed Oxygen Atom Reaction Efficiencies for Composites, Polymers, and Organic Films (from Leger, Visentine, and Schliesing, 1985)

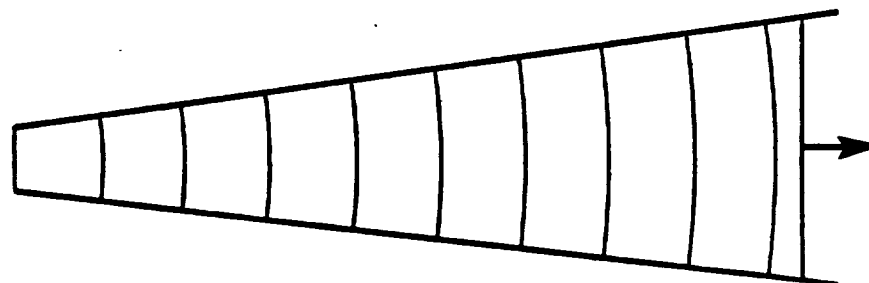| Material	Reaction Efficience (cm^3/atom)
Kapton	3.0×10^{-24}
Mylar	3.4
Tedlar	3.2
Polyethylene	3.7
PMMA[a]	3.1
Polyimide	3.3
Polysulfone	2.4
1034C Epoxy	2.1
5208/T300 Epoxy	2.6
Teflon, TFE	<0.05
Teflon, FEP	<0.05
[a]PMMA = Polymethylmethacrylate	
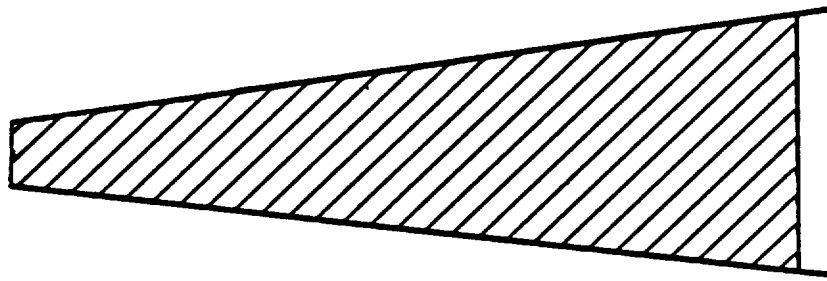
7

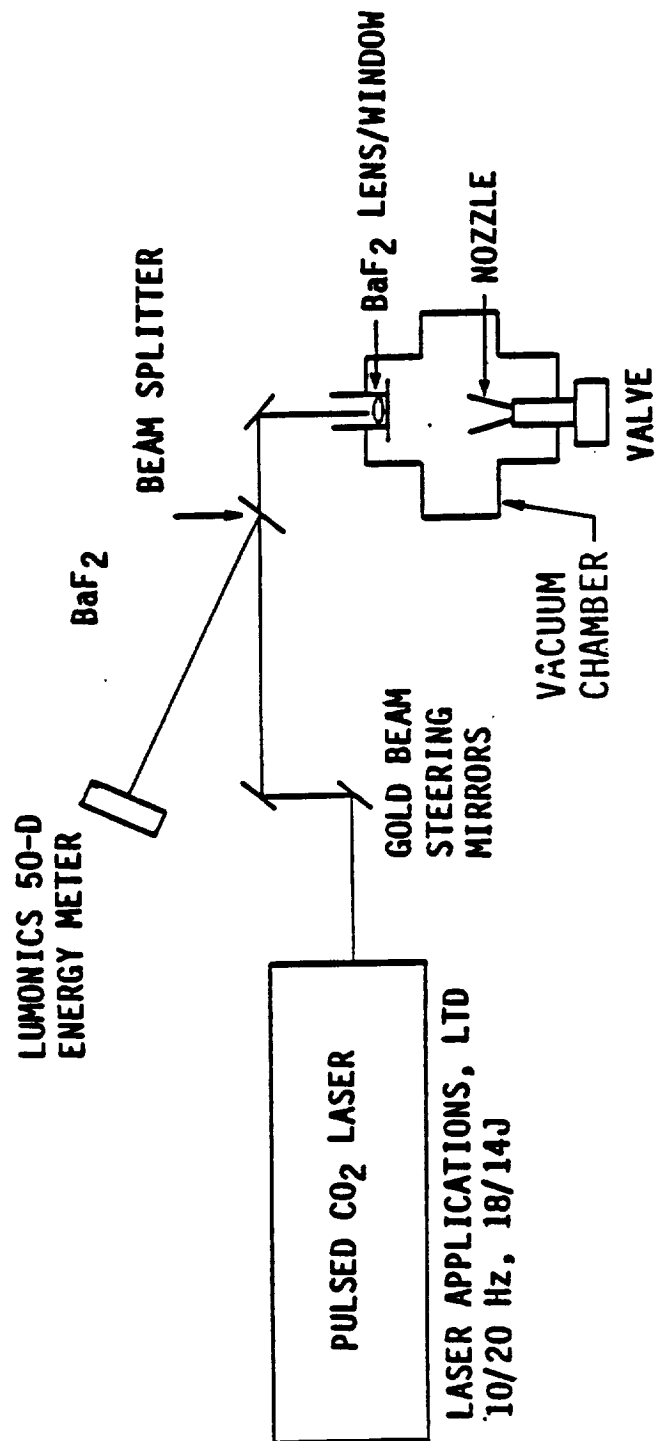GAS DYNAMIC MODEL

- INITIAL PULSED NOZZLE FILL
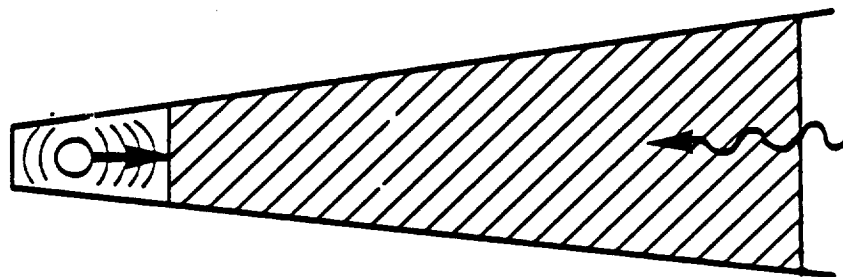
- BREAKDOWN
- RAPID LSD WAVE HEATING

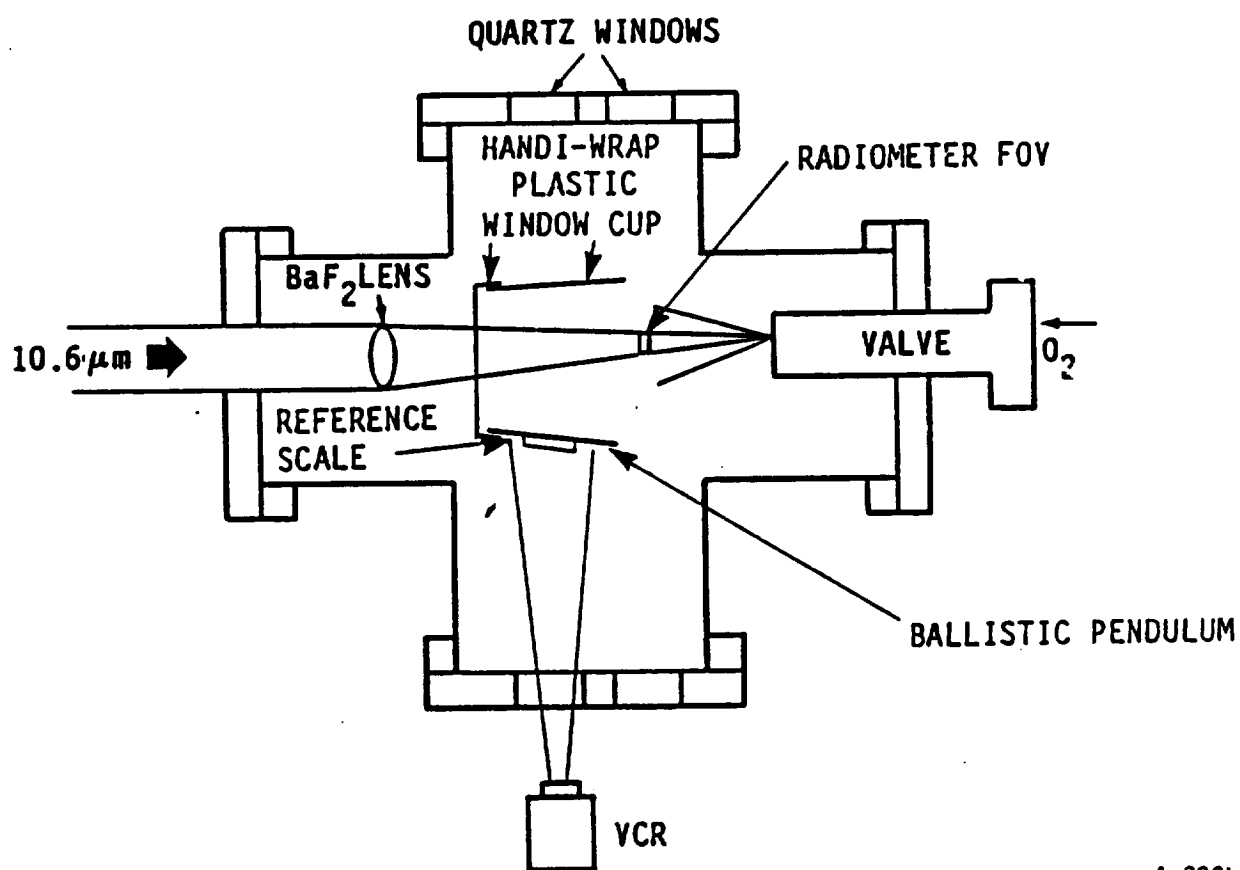- LASER ENERGY ABSORBED
- BLAST WAVE PROCESSING NOZZLE FILL

A-2060 a

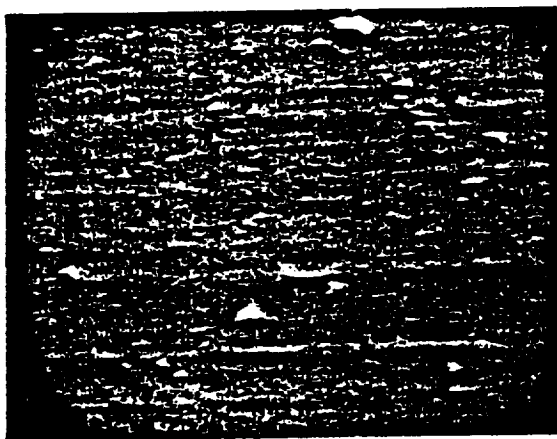Figure 1.   Schematic of Blast Wave Development

8

9

LUMONICS 50-D
ENERGY METER

BaF$_2$

BEAM SPLITTER

BaF$_2$ LENS/WINDOW

NOZZLE

GOLD BEAM
STEERING
MIRRORS

VACUUM
CHAMBER

VALVE

PULSED CO$_2$ LASER

LASER APPLICATIONS, LTD
10/20 Hz, 18/14J

A-888a

Figure 2. General O-Atom Facility Schematic

QUARTZ WINDOWS

HANDI-WRAP
PLASTIC
WINDOW CUP

RADIOMETER FOV

BaF$_2$LENS

10.6μm

REFERENCE
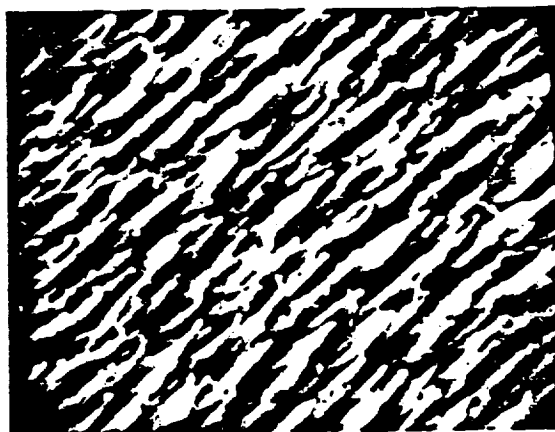SCALE

VALVE

O$_2$

BALLISTIC PENDULUM

VCR
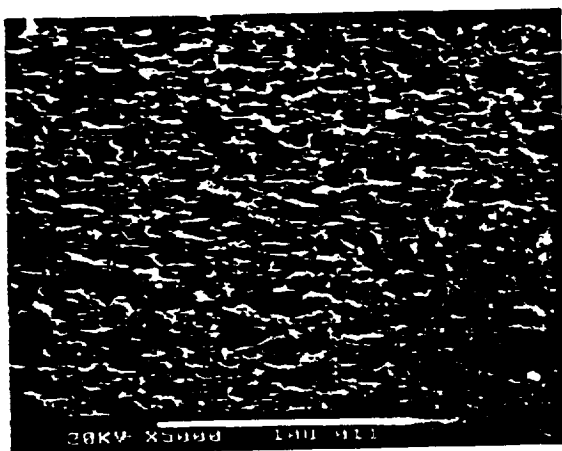
A-889b

Figure 3. Ballistic Pendulum Experimental Setup

10

PRIOR TO EXPOSURE
(10,000x)
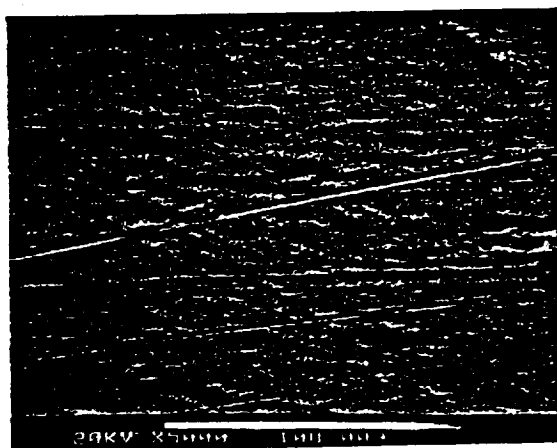
AFTER ATOMIC OXYGEN EXPOSURE
(10,000x)

Fig. 4.   SEM photograms of STS-8 Kapton specimens

AFTER 12000 PULSES (~3x10^{20}/cm^2)

BEFORE EXPOSURE

Fig. 5.   Kapton 500H after 12,000
          pulses (~3 x 10^{20}/cm^2)

Fig. 6.   Kapton 500H before
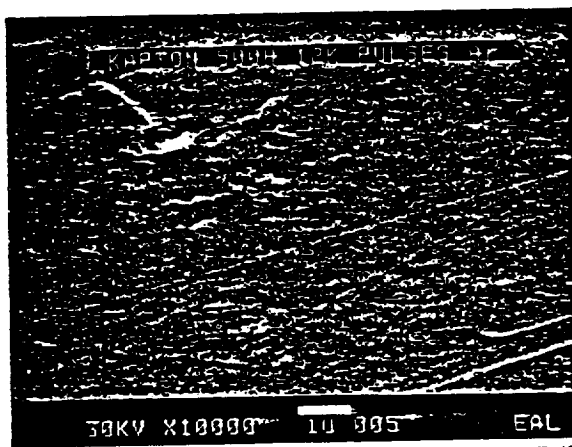   exposure

Fig. 7.   Kapton 500H irradiated by
          5 eV Ar for 12,000 pulses

APPENDIX B

A High Flux Source of Energetic Oxygen Atoms for
Material Degradation Studies

(PSI-1001/SR-270, copy attached in its entirety)

PULSED SOURCE OF ENERGETIC ATOMIC OXYGEN

George E. Caledonia and Robert H. Krech
Physical Sciences Inc.
Research Park, P.O. Box 3100
Andover, MA 01810

ABSTRACT

A pulsed high flux source of nearly monoenergetic atomic oxygen has been designed, built, and successfully demonstrated. Molecular oxygen at several atmospheres pressure is introduced into an evacuated supersonic expansion nozzle through a pulsed molecular beam valve. An 18J pulsed CO_2 TEA laser is focused to intensities $> 10^9$ W/cm^2 in the nozzle throat to generate a laser-induced breakdown. The resulting plasma is heated in excess of 20,000 K by a laser-supported detonation wave, and then rapidly expands and cools. Nozzle geometry confines the expansion to promote rapid electron-ion recombination into atomic oxygen. We have measured average O-atom beam velocities from 5 to 13 km/s at estimated fluxes to 10^{18} atoms per pulse. Preliminary materials testing has produced the same surface oxygen enrichment in polyethylene samples as obtained on the STS-8 mission. Scanning Electron Microscope examinations of irradiated polymer surfaces reveal an erosion morphology similar to that obtained in low earth orbit, with an estimated mass removal rate of $\sim 10^{-24}$ cm^3/atom. The characteristics of the O-atom source and the results of some preliminary materials testing studies will be reviewed.

INTRODUCTION

Satellites in low-earth orbit sweep at velocities of ~8 km/s through a rarefied atmosphere which consists primarily of atomic oxygen. Experimental pallets flown on Shuttle missions STS-5 and STS-8 clearly demonstrated a dependence of material degradation and mass loss on the ram direction atomic oxygen exposure.(1-4) These experiments indicate that most hydrocarbons and active metals are highly reactive, whereas material containing silicones, fluorides, oxides and noble metals are moderately inert. For Kapton,® an important aerospace polymer, it was observed that about one in ten atomic oxygen interactions lead to mass loss due to chemical reaction.(2,3)

The need for continued material degradation studies has been emphasized in a study by Leger et al.(5) where it was demonstrated that atomic oxygen induced material degradation could have a severe impact on the performance of Space Station. The EOIM-3 material pallet, with sophisticated instrumentation to detect atomic oxygen reaction products and to study reaction mechanisms, is scheduled to be deployed on a future Shuttle mis-sion, and NASA is actively pursuing the development of various hardening techniques to make materials more impervious to the effects of energetic atomic oxygen interactons.

The recent setbacks in launch capability have reemphasized the need for a high flux atomic oxygen source which can be used to study material degradation. Although in-flight experiments provide valuable test data, the large

matrix of materials and test parameters, and uncertain flight scheduling now mandate that most of these studies be performed in a ground test facility.

A high flux source of atomic oxygen has been developed at Physical Sciences Inc. (PSI) based on years of research in the area of pulsed laser propulsion.(6-8) The basic concept is to rapidly introduce a burst of gas into an evacuated nozzle and then to focus the output of a pulsed laser to cause a breakdown at the nozzle throat. The subsequent laser-initiated detonation wave will heat the major portion of the gas during the laser pulse creating a high temperature plasma. This plasma will then expand through a nozzle tailored to allow electron-ion recombination but not atomic recombination. As the gas expands its temperature and density will drop, however, its directed velocity increases correspondingly, producing a thermally "cold," high energy beam of oxygen atoms at the nozzle exit. This technique has been utilized to produce a high velocity O-atom source for material degradation studies. For example with 10^{-4}g of gas and a 5J laser pulse we predict formation of $>10^{18}$ oxygen atoms with a characteristic energy of 5 eV. For comparison with other sources, if the source is pulsed at 10 Hz, an average flux of $>10^{17}$ O-atoms/cm^2-s can be maintained on a 100 cm^2 target.

In our research effort at PSI we have constructed a small test facility to demonstrate that high velocity oxygen atoms can be produced. A series of measurements have been performed to demonstrate the presence of atomic oxygen and the measured velocities agreed with theoretical predictions. Measurements of the material degradation of O-atom irradiated targets are being performed, and these experimental observations are described. The design of a larger O-atom test facility presently under construction is also presented.

FACILITY DESCRIPTION

The present test facility consists of a stainless steel high vacuum chamber in which oxygen gas is rapidly pulsed through a conical expansion nozzle and laser heated by a pulsed CO_2 laser to temperatures above 20,000 K.

A schematic diagram of the apparatus is shown in Fig. 1. The vacuum chamber is a standard 20 cm diameter five-way stainless steel high vacuum cross with Con-Flat flanges. Each sidearm extends 20 cm from the center of the chamber. A sixth 10.0 cm diameter port was welded to the bottom of the chamber for evacuation. The top flange of the vacuum chamber has two radiometers for time-of-flight velocity measurements into the chamber. The pulsed valve/nozzle assembly is mounted on the end flange which also contains vacuum feed-throughs for electrical connections. The opposing flange holds the laser focusing lens. Each side

NOTES:
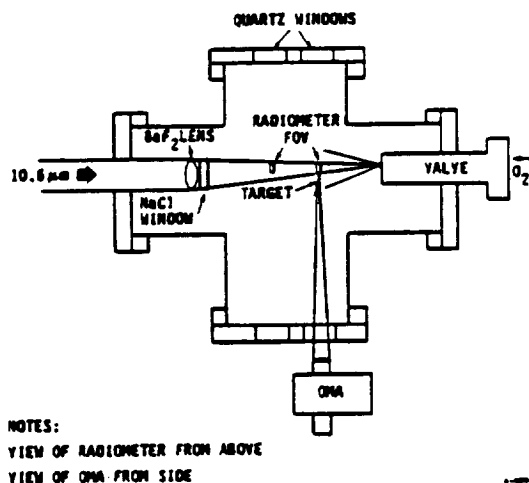VIEW OF RADIOMETER FROM ABOVE
VIEW OF OMA FROM SIDE

Fig. 1. Schematic diagram of O-atom apparatus

flange has two 5 cm diameter quartz view-ports for visual and spectroscopic observations.

The bottom flange is connected to a 10 cm diffusion pump stack equipped with an ionization gauge readout. The ultimate pressure in the chamber is 3×10^{-5} torr. In operation the chamber pressure is kept below 1×10^{-4} torr, to prevent beam interaction with the background gas. (Mean free path at 10^{-4} torr is 50 cm which is greater than the chamber length and is sufficient to provide a "collision free" environment.) The pumping speed of the vacuum chamber is sufficient to allow introduction of a pulse of 10^{-4}g of oxygen at 1 Hz into a background pressure below 1×10^{-4} torr.

The pulsed valve/nozzle assembly is shown schematically in Fig. 2. The valve is a modified Model BV-100V pulsed molecular beam valve from Newport Research, Inc. This valve allows the generation of short duration pulses of gas at high flowrates which cannot be continuously maintained under high vacuum conditions due to pumping speed limitations. The valve is operated with a 1 mm i.d. orifice plate, and is bolted directly to a 100 mm long, 20 deg full angle aluminum expansion nozzle with a 1 mm i.d. throat. The choked flowrate of the valve/nozzle assembly is 0.19g of oxygen per second per atmosphere stagnation pressure.
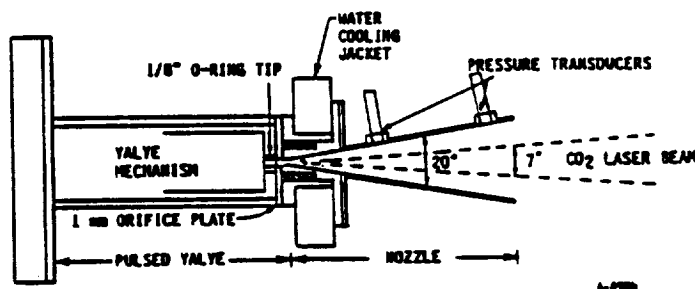

Fig. 2. O-atom osurce pulsed valve/ nozzle assembly

The nozzle has two flush mounted pressure transducers located 43 and 93 mm from the throat with 1 µs response time and 20 mV/psia sensitivity.

A Laser Applications Limited TEA CO_2 laser is used to generate 18J pulses of 10.6µ radiation. The energy is delivered in a 2.5 µs pulse, with approximately one-third of the energy delivered in the first 200 ns. The radiation in the gain switched spike generates a laser induced breakdown in the high pressure oxygen at the nozzle throat forming a plasma which continues to absorb the radiation as long as the laser is on.

The laser beam is directed to the test chamber by three gold turning mirrors (Fig. 3). A barium fluoride flat between the second and third mirror reflects eight percent of the beam to a calorimeter to monitor the laser energy. A 300 mm focal length barium fluoride lens is used to focus the laser beam to ~1 mm diameter spot size at the nozzle throat.
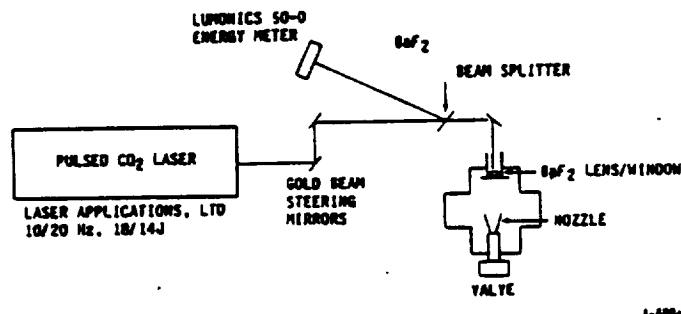

Fig. 3. Laser/optics assembly

60

BEAM DIAGNOSTICS

Optical measurements have been conducted to characterize the laser initiated O-atom beam. Beam velocities from 5 to 13 km/s were obtained by varying both the stagnation pressure and the laser energy. The velocities were deduced by monitoring the time history of the 777.3 nm atomic oxygen line emission with two filtered radiometers mounted on the top flange of the vacuum chamber.

The spectral measurements of the O-atom beam, and target interactions have been obtained using a Princeton Instruments Optical Multichannel Analyzer (OMA). The OMA head consists of a 1024 photodiode array with a gated S-20R intensifier. The spectrograph is a Jarrel Ash 0.275m MARK X with interchangeable grating, and a maximum resolution of 3Å. The optical field of view in the chamber was restricted to a 0.090 x 0.90 cm rectangle by a collecting telescope matched to the f number of the spectrograph. Glass cut-on filters were used to prevent second and higher order spectra from being recorded.

Spectra are recorded using the OMA in the gated mode. The diode array was gated on 5 µs after the laser trigger to prevent detection of scattered breakdown radiation. A number of spectral scans of the radiation from the expanded oxygen plasma were performed over the wavelength range of 400 to 800 nm. Results were highly reproducible. The strongest signals arose from atomic oxygen emission at 777 nm. No evidence of O_2 emission was identified, however, some atomic hydrogen emission was observed due to laser ablation of the valve tip elastomers, and H_2O impurities in the oxygen feed gas.

Characterization of the beam has been also performed by ballistic pendulum measurements of the cold and hot flows. This has allowed quantization of the atomic flow rate to within a factor of two. Refinements in the larger test facility, primarily a time-of-flight mass spectrometer probe, will further reduce this uncertainty.

PRELIMINARY MATERIAL DEGRADATION STUDIES

Preliminary material degradation studies have been conducted with the small test facility. Materials irradiated have included polyethylene, Teflon®, Kapton® (untreated and oxidation resistant treated samples), Mylar®, PEEK, PBT and Carbon Epoxy composites.

Ground-based testing facilities must produce a surface morphology and mass removal rate similar to that produced on orbit to provide meaningful erosion data. Typical erosion morphology of a polymeric sample is shown in Fig. 4 (graciously provided by J.T. Visentine), for exposure levels of 5 to 9 x 10^{20} O-atom/cm^2, corresponding to ~1 week on orbit. Kapton samples irradiated in our facility to an exposure level of ~3.3 x 10^{20} O-atom/cm^2 show a remarkably similar surface morphology Fig. 5, and measurable mass loss (~1.3 mg). (Fig. 6 shows a sample of Kapton 500H prior to exposure for comparison.) This morphology is not due to kinetic energy alone since another sample of Kapton was bombarded with ~5 eV Ar (Fig. 7) and showed no mass loss. Similar results were obtained with low and high density polyethylene samples.
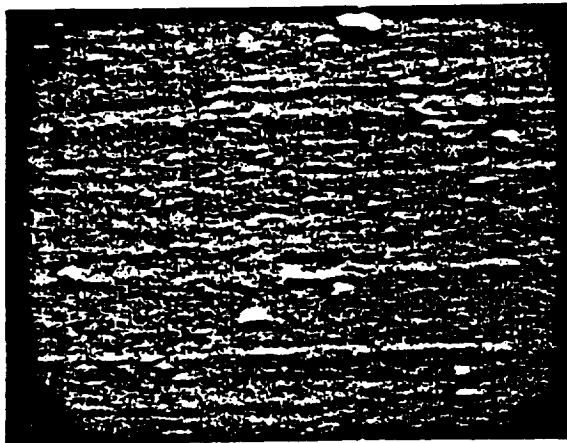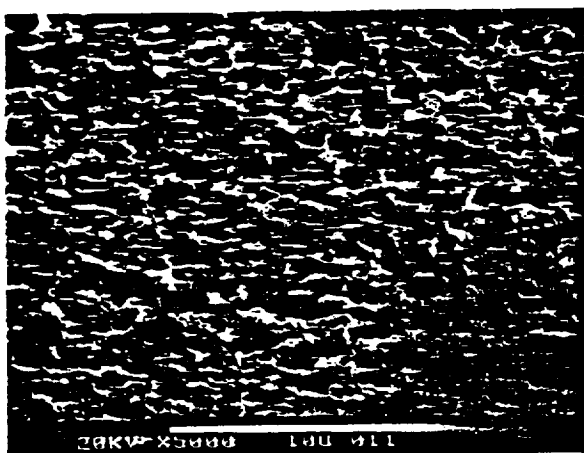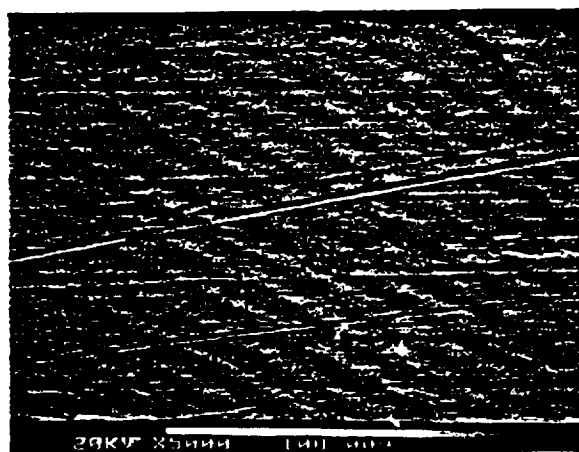
PRIOR TO EXPOSURE
(10,000x)
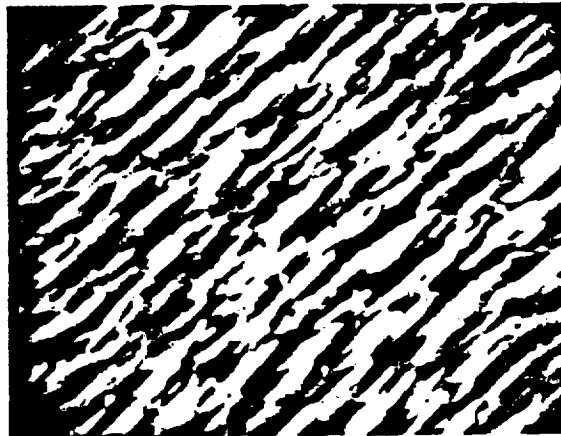
AFTER ATOMIC OXYGEN EXPOSURE
(10,000x)

Fig. 4. SEM photograms of STS-8 Kapton specimens

AFTER 12000 PULSES ($\sim 3 \times 10^{20}/cm^2$)

BEFORE EXPOSURE

Fig. 5. Kapton 500H after 12,000 pulses ($\sim 3 \times 10^{20}/cm^2$)

Fig. 6. Kapton 500H before exposure

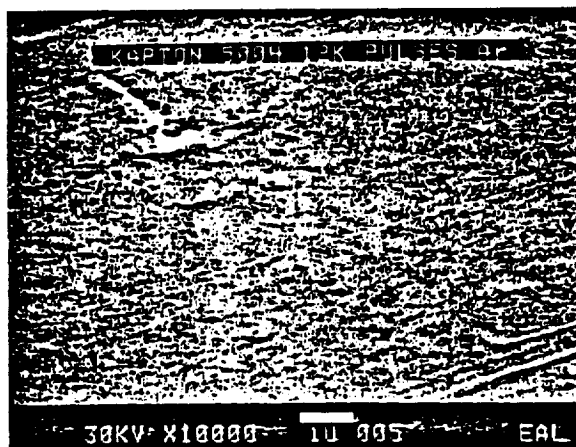Fig. 7. Kapton 500H irradiated by 5 eV Ar for 12,000 pulses

Current capabilities provide for exposure rates of ~1.5 x 10^{20} atom/ cm^2-hr at ~5 eV (~1.6 Hz); and provide an exposure acceleration factor of 50 compared to LEO and 5000 for space station altitudes for ~6 cm^2 samples. A larger facility described below will allow for further accelerated testing.

DESIGN OF LARGE-SCALE TEST FACILITY

The small test facility produces high density O-atom beams, but cannot irradiate large sample areas. Using the same techniques, we are constructing a large chamber to allow the testing of larger samples (~15 cm diameter) at a 10 to 20 Hz pulse rate.

In order to accommodate larger samples, or many smaller ones, the new chamber will be 40 cm o.d. six-way cross assembly. A chamber this size allows for convenient sample access, mass spectrometer probes for beam and target product analysis, in situ mass loss measurement, velocity dependent measurements and target irradiation by a UV solar simulator. A schematic of the chamber is shown in Fig. 8.
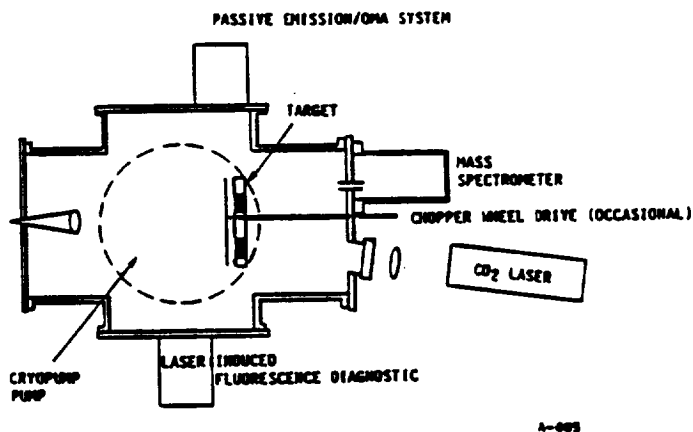

Fig. 8. Schematic of new O-atom facility

A Varian cryopump with a speed of ~3000 ℓ/s will maintain 10^{-4} torr in the chamber with a gas load of 10^{-3} g/s. A cryopump was chosen to eliminate any possible contamination of test samples by back diffusion of pump oil.

Two quadrupole mass spectrometer systems will be coupled to the main chamber. A Balzers QMS 311 will be used to monitor the atomic beam. It will sit in a differentially pumped chamber, separated from the main chamber by a sampling orifice. This QMS will monitor the pulse to pulse reproducibility of the O-atom beam, and when cross calibrated with the laser induced fluorescence diagnostic, will provide a real time quantitative O-atom detector. A second QMS will be suspended from the top flange of the chamber to monitor the reaction products of the atomic oxygen/interaction and will be mounted to allow for rotation with respect to the target for angular product dependence studies.

The pulsed CO_2 laser system was manufactured by Laser Applications Limited and provides 18J per pulse at 10 Hz. This allows a sufficient margin for transmission and reflection losses to process ~10^{-4}g bursts of gas into 5 eV O-atoms. Furthermore an option for 20 Hz operation is available to provide a higher throughput.

A Quantel 10 Hz YAG pump dye laser system will be used for multiphoton laser induced fluorescence detection of atomic oxygen. Approximately 1 mJ at 226 mm can be obtained for the excitation of ground state atomic oxygen

$(2p^4 {}^3P \rightarrow 2p^3 3p {}^3P)$ with subsequent fluorescence around 845 nm from the $3_p {}^3P \rightarrow 3_s {}^3S$ transitions in atomic oxygen, and the same technique can be used to detect the 1_D and 1_S metastables.

SUMMARY

Our goal is to build a reliable ground based energetic O-atom test facility which will be able to meet the NASA material testing requirements.

The concepts of the design have been demonstrated both experimentally and theoretically, and the technique exploits the characteristics of existing commercially available high power laser technology. At present repetitively pulsed CO_2 lasers provide the most convenient source of laser radiation in terms of reliability, cost and delivered energy.

With a 10 Hz pulse rate, the device will conservatively irradiate a 100 cm^2 area with $>10^{17}$ atoms/cm^2-s. In less than 2 hr of operation under these conditions, energetic oxygen atom fluences of 7×10^{20}/cm^2 will be possible over the exposed area. For comparison this O-atom fluence is equivalent to that seen by a ram direction shuttle surface for an entire week-long mission in low earth orbit (250 km) and is equivalent to the fluence seen by a ram surface of the Space Station at 500 km altitude during the course of an entire year (during a year of average solar activity). Although questions can be raised by accelerated testing, this new facility will provide the ability to identify materials most affected by O-atoms (which can then be tested further on-orbit), to systematically separate effects of UV irradiation, temperature, and O-atom energy, to study the rate of change of recession/material loss as surfaces change character, and to identify failure points (most susceptible to erosion) in assemblies such as solar cells. The importance of such effects has been clearly demonstrated in recent Space Shuttle flights.(5, 9-11).

With this new test facility we can perform quantitative erosion testing of materials, components, and even small assemblies (such as a solar cell array) in order to determine components or interfaces which are most vulnerable to O-atom erosion. This ground-based facility will allow accelerated testing to identify structures or materials which are in most critical need of protection so that remedial strategies or protective coatings can be developed and even tested in this ground test facility at a fraction of the cost and in a much more timely manner than on-orbit.

REFERENCES

1. Leger, L.J., Spiker, I.K., Kuminecz, J.F., and Visentine, J.T., "STS Flight 5 LEO Effects Experiments--Background Description and Thin Film Results," AIAA Paper 83-2631-CP, October 1983.

2. Leger, L.J., Visentine, J.F., and Kuminecz, J.F., "Low Earth Orbit Atomic Oxygen Effects on Surfaces," AIAA Paper 84-0548, January 1984.

3. Visentine, J.T., Leger, L.J., Kuminecz, J.F., and Spiker, I.K., "STS-8 Atomic Oxygen Effects Experiments," Paper presented at AIAA 23rd Aerospace Sciences Meeting, Reno, NV, January 1985.

4. Green, B.D., Caledonia, G.E., and Wilkerson, T.D., "The Shuttle Environment: Gases, Particulates and Glow," J. Spacecraft and Rockets 22, 5 Sept-Oct 1985, 500-511.

5. Leger, L.J., Visentine, J.T., and Schliesing, J.A., "A Consideration of the Atomic Oxygen Interactions with Space Stations," AIAA 85-0476, January 1985.

6. Simons, G.A. and Pirri, A.N. "The Fluid Mechanics of Pulsed Laser Propulsion," AIAA J. 15, 835 (1977).

7. Rosen, D.I., Pirri, A.N. Weiss, R.F., and Kemp, N.H., "Repetitively Pulsed Laser Propulsion: Needed Research," In progress in Astronautics and Aeronautics Vol. 89 (1985), ed. L.H. Caveny, pp. 95-108.

8. Rosen, D.I. Kemp, N.H., Weyl, G., Nebolsine, P.E., and Kothandaraman, G., "Pulsed Laser Propulsions Studies," Physical Sciences Inc. Technical Report TR-184, 1981.

9. Hall D.F. and Stewart, T.B., "Photo-Enhanced Spacecraft Contamination Deposition," AIAA 85-0953, June 1985.

10. Peterson, R.V. Hanna, W.D., and Mertz, L.O., "Results of Oxygen Atom Interaction with Kevlar and Fiberglass Fabrics on STS-8," AIAA 85-0990, June 1985.

11. Knopf, P.W. Martin, R.J., McCargo, M., and Dammann, R.E., "Correlation of Laboratory and Flight Data for the Effects of the LEO Atomic Oxygen on Polymeric Materials," AIAA 85-1066, June 1985.

ACKNOWLEDGMENT

A HIGH FLUX PULSED SOURCE OF ENERGETIC ATOMIC OXYGEN

Robert H. Krech and George E. Caledonia
Physical Sciences Inc.
Research Park, P.O. Box 3100
Andover, MA 01810

Abstract

A pulsed high flux source of nearly monoenergetic atomic oxygen has been designed, built, and successfully demonstrated. Molecular oxygen at several atmospheres pressure is introduced into an evacuated supersonic expansion nozzle through a pulsed molecular beam valve. The output of a 10J CO_2 TEA laser is focused to intensities $> 10^9$ W/cm^2 in the nozzle throat generating a laser-induced breakdown. The resulting plasma, heated in excess of 20,000 K, rapidly expands and cools. Nozzle geometry confines the expansion to promote rapid electron-ion recombination. We have measured average O-atom beam velocities from 5 to 13 km/s at estimated fluxes to 10^{18} atoms per pulse. Limited materials testing has produced the same surface oxygen enrichment in polyethylene samples as obtained on the STS-8 mission. The characteristics of the O-atom source and selected materials studies will be reviewed.

INTRODUCTION

Satellites in low-earth orbit sweep at velocities of ~8 km/s through a rarefied atmosphere which consists primarily of atomic oxygen. Experimental pallets flown on Shuttle missions STS-5 and STS-8 clearly demonstrated a dependence of material degradation and mass loss on the ram direction atomic oxygen exposure.(1-4) These experiments indicate that most hydrocarbons and active metals are highly reactive, whereas material containing silicones, fluorides, oxides and noble metals are moderately inert. For Kapton,® an important aerospace polymer, it was observed that about one in ten atomic oxygen interactions lead to mass loss due to chemical reactions.(2,3)

The need for continued material degradation studies has been emphasized in a study by Leger et al.(5) where it was demonstrated that atomic oxygen induced material degradation could have a severe impact on the performance of Space Station. The EOIM-3 material pallet, with sophisticated instrumentation to detect atomic oxygen reaction products and to study reaction mechanisms, is scheduled to be deployed on a future Shuttle mission, and NASA is actively pursuing the development of various hardening techniques to make materials more impervious to the effects of energetic atomic oxygen interactons.

The recent setbacks in launch capability have reemphasized the need for a high flux atomic oxygen source which can be used to study material degradation. Although inflight experiments provide valuable test data, the large matrix of materials and test parameters, and uncertain flight scheduling now mandate that most of these studies be performed in a ground test facility.

A high flux source of atomic oxygen has been developed at PSI, based on years of research in the area of pulsed laser propulsion.(6-8) The basic concept is to rapidly introduce a burst of gas into an evacuated nozzle and then to focus the output of a pulsed laser to cause a

breakdown at the nozzle throat. The subsequent laser-initiated detonation wave will heat the major portion of the gas during the laser pulse creating a high temperature plasma. This plasma will then expand through a nozzle tailored to allow electron-ion recombination but not atomic recombination. As the gas expands its temperature and density will drop, however, its directed velocity increases correspondingly, producing a thermally "cold," high energy beam of oxygen atoms at the nozzle exit. This technique has been utilized to produce a high velocity O-atom source for material degradation studies. For example with 10^{-4}g of gas and a 5J laser pulse we predict formation of $>10^{18}$ oxygen atoms with a characteristic energy of 5 eV. For comparison with other sources, if the source is pulsed at 10 Hz, an average flux of $>10^{17}$ O-atoms/cm^2-s can be maintained on a 100 cm^2 target.

In our research effort at PSI we have constructed a small test facility to demonstrate that high velocity oxygen atoms can be produced. A series of measurements were performed to demonstrate the presence of atomic oxygen and the measured velocities agreed with theoretical predictions. A few measurements of the material degradation of O-atom irradiated targets were performed, and these experimental observations are

described. The design of a larger O-atom test facility presently under construction is also presented.

FACILITY DESCRIPTION

The present test facility consists of a stainless steel high vacuum chamber in which oxygen gas is rapidly pulsed through a conical expansion nozzle and laser heated by a pulsed CO_2 laser to temperatures above 20,000 K.
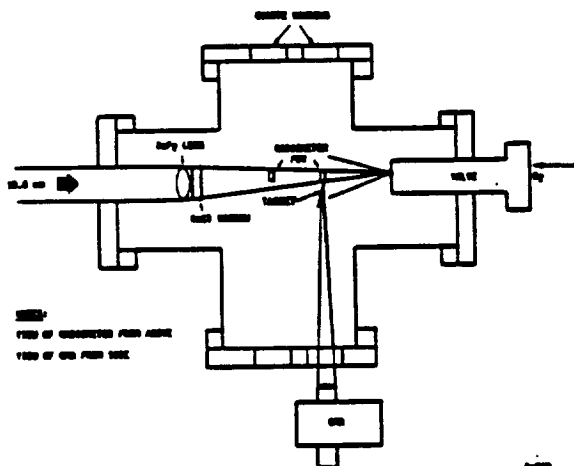
A schematic diagram of the apparatus is shown in Figure 1.

Figure 1.   Schematic diagram of
            O-atom apparatus

The vacuum chamber is a standard 20 cm diameter 5-way stainless steel high vacuum cross with Con-Flat flanges. Each sidearm extends 20 cm from the center of the chamber. A sixth 3.8 cm diameter port was welded to the bottom of the chamber for evacuation. The top flange of the vacuum chamber has two radiometers for time-of-flight velocity measurements into the

chamber. The pulsed valve/nozzle assembly is mounted on the end flange which also contains vacuum feed-throughs for electrical connections. The opposing flange holds the laser focusing lens. Each side flange has two 5 cm diameter quartz view-ports for visual and spectroscopic observations.

The bottom flange is connected to a 5 cm diffusion pump stack equipped with an ionization gauge readout. The ultimate pressure in the chamber is 3×10^{-5} torr, restricted by a slight leakage through the pulsed valve/nozzle assembly. In operation the chamber pressure is kept below $\times 10^{-4}$ torr, to prevent beam interaction with the background gas. (Mean free path at 10^{-4} torr is 50 cm which is greater than the chamber length and is sufficient to provide a "collision free" environment.) The pumping speed of the vacuum chamber is sufficient to allow introduction of ~1 pulse of 10^{-4}g of oxygen every 5s into a background pressure below 1×10^{-4} torr.

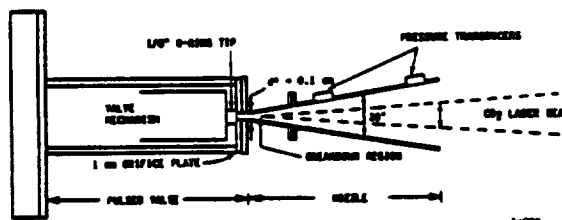The pulsed valve/nozzle assembly is shown schematically in Figure 2.

Figure 2.   Diagram of pulsed valve-

The valve is a modified Model BV-100V pulsed molecular beam valve from Newport Research, Inc. This valve allows the generation of short duration pulses of gas at high flowrates which cannot be continuously maintained under high vacuum conditions due to pumping speed limitations. The valve is operated with a 1 mm i.d. orifice plate, and is bolted directly to a 100 mm long, 20 degree full angle aluminum expansion nozzle with a 1 mm i.d. throat. The choked flowrate of the valve/nozzle assembly is 0.19g of oxygen per second per atmosphere stagnation pressure.

The nozzle has two flush mounted pressure transducers located 43 and 93 mm from the throat with 1 μs response time and 20 mV/psia sensitivity.

A Lumonics K-103 TEA laser was used to generate 10J pulses of 10.6μ radiation. The energy is delivered in a 2.5 μs pulse, with approximately one-third of the energy delivered in the first 200 ns. The radiation in the gain switched spike generates a laser induced breakdown in the high pressure oxygen at the nozzle throat forming a plasma which continues to absorb the radiation as long as the laser is on.

The laser beam is directed to the test chamber by three gold turning

ride flat between the second and third mirror reflects eight percent of the beam to a calorimeter to monitor the laser energy. A 300 mm focal length barium fluoride lens is used to focus the laser beam to ~1 mm diameter spot size at the nozzle throat.
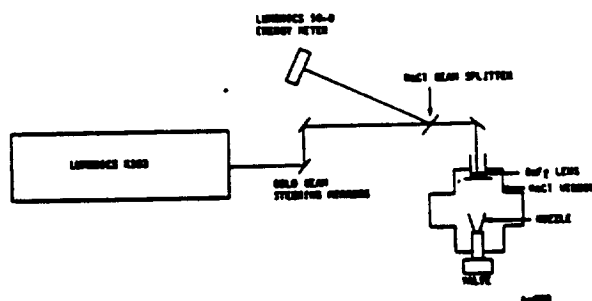

Figure 3. Laser/optics assembly

Losses in the optical train result in ~50 percent reduction of the laser energy, and thus ~5J of laser energy is typically delivered to the focal spot. Peak spike intensity of ~2 x 10^9 W/cm^2 is sufficient to cause a rapid breakdown in the gas.

BEAM DIAGNOSTICS

Optical measurements were conducted to probe the laser initiated O-atom beam. Beam velocities from 5 to 13 km/s were obtained by varying both the stagnation pressure and the laser energy. The velocities were deduced by monitoring the time history of the 777.3 nm atomic oxygen line emission with two filtered radiometers mounted on the top flange of the vacuum chamber.

The spectral measurements of the O-atom beam, and target interactions are obtained using a Princeton Instruments Optical Multichannel Analyzer (OMA). The OMA head consists of a 1024 photodiode array with a gated S-20R intensifier. The spectrograph is a Jarrel Ash 0.275m MARK X with interchangeable grating, and a maximum resolution of 3Å. The optical field of view in the chamber was restricted to a 0.090 x 0.90 cm rectangle by a collecting telescope matched to the f number of the spectrograph. Glass cut-on filters were used to prevent second and higher order spectra from being recorded.

Spectra are recorded using the OMA in the gated mode. The diode array was gated on 5 µs after the laser trigger to prevent detection of scattered breakdown radiation. A number of spectral scans of the radiation from the expanded oxygen plasma were performed over the wavelength range of 400 to 800 nm. Results were highly reproducible. The strongest signals arose from atomic oxygen emission at 777 nm. No evidence of O_2 emission was identified, however, some atomic hydrogen emission was observed due to laser ablation of the valve tip elastomers, and H_2O impurities in the oxygen feed gas.

PRELIMINARY MATERIAL DEGRADATION STUDIES

Some preliminary material degradation studies have been conducted with the small test facility, which was designed primarily for beam characterization studies and does not require high repetition rates or high pumping speeds. Materials irradiated have included polyethylene, Teflon,® Kapton® (untreated and oxidation resistant treated samples), Mylar,® PEEK, PBT and Carbon Epoxy composites.

The polyethylene sample was supplied by the Jet Propulsion Laboratory (JPL) and was from the same lot of material that flew on the STS-8 pallet. After irradiation and ESCA analysis of this sample, the measured oxygen surface enrichment was found to be very similar to that observed in postflight analysis of the STS-8 samples. Portions of the sample in the chamber not exposed to the beam showed no enhancement.

The remaining samples were provided by several sources including JPL, Tekmat Corporation (Ashland, MA), and Foster-Miller, Inc. (Waltham, MA). The complete analysis of these materials is not available at press time, but will be available for the presentation. A very preliminary survey of some of the samples indicates possible surface

roughening and oxygen enrichment of directly exposed surfaces.

DESIGN OF LARGE-SCALE
TEST FACILITY

The small test facility produces high density O-atom beams, but cannot irradiate large sample areas. Using the same techniques, we are constructing a large chamber to allow the testing of larger samples ($\sim$15 cm diameter) at a 10-20 Hz pulse rate.

In order to accommodate larger samples, or many smaller ones, the new chamber will be 40 cm o.d. six-way cross assembly. A chamber this size allows for convenient sample access, mass spectrometer probes for beam and target product analysis, in situ mass loss measurement, velocity dependent measurements and target irradiation by a UV solar simulator. A schematic of the chamber is shown in Figure. 4.
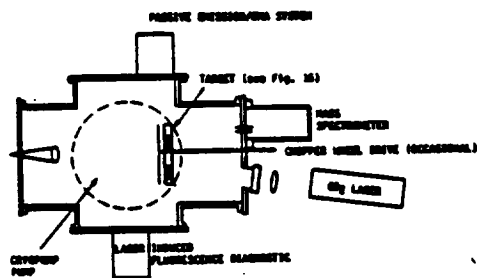
Figure 4. Schematic of enlarged O-atom facility

A cryopump with a speed of $\sim$3000 ℓ/s will maintain 10^{-4} torr

10^{-3} g/s. A cryopump was chosen to eliminate any possible contamination of test samples by back diffusion of pump oil.

Two quadrupole mass spectrometer systems will be coupled to the main chamber. A Balzers QMS 311 will be used to monitor the atomic beam. It will sit in a differentially pumped chamber, separated from the main chamber by a sampling orifice. This QMS will monitor the pulse to pulse reproducibility of the O-atom beam, and when cross calibrated with the laser induced fluorescence diagnostic, will provide a real time quantitative O-atom detector. A second QMS will be suspended from the top flange of the chamber to monitor the reaction products of the atomic oxygen and the targets, and will be mounted to allow for rotation with respect to the target for angular product dependence studies.

A pulsed CO_2 laser system has been delivered by Laser Applications Limited (England) and provides 18J per pulse at 10 Hz. This allows a sufficient margin for transmission and reflection losses to process $\sim 10^{-4}$g bursts of gas into 5 eV O-atoms. Furthermore an option for 20 Hz operation is available to provide a higher throughput.

A Cahn Microbalance will be mounted on the top flange of the chamber to measure target mass loss. Samples

71

would be suspended from the balance in the chamber and the mass loss versus time recorded in situ. The sensitivity of the balance is 100 ng, so microgram-scale mass losses should be readily observed.

A Quantel 10 Hz YAG pump dye laser system will be used for multiphoton laser induced fluorescence detection of atomic oxygen. Approximately 1 mJ at 226 mm can be obtained for the excitation of ground state atomic oxygen ($2p^4 {}^3P \rightarrow 2p^3 3p\,^3P$) with subsequent fluorescence around 845 nm from the $3_p\,^3P \rightarrow 3_s\,^3S$ transitions in atomic oxygen, and the same technique can be used to detect the ^1D and ^1S metastables.

SUMMARY

Our goal is to build a reliable ground based energetic O-atom test facility which will be able to meet the NASA material testing requirements.

The concepts of the design have been demonstrated both experimentally and theoretically, and the technique exploits the characteristics of existing commercially available high power laser technology. At present repetitively pulsed CO_2 lasers provide the most convenient source of laser radiation in terms of reliability, cost and delivered energy. With a 10 Hz pulse rate, the device will conser-

vatively irradiate a 100 cm^2 area with $>10^{17}$ atoms/cm^2-s. In less than 2 hours of operation under these conditions, energetic oxygen atom fluences of $7 \times 10^{20}/\,cm^2$ will be possible over the exposed area. For comparison this O-atom fluence is equivalent to that seen by a ram direction shuttle surface for an entire week-long mission in low earth orbit (250 km) and is equivalent to the fluence seen by a ram surface of the Space Station at 500 km altitude during the course of an entire year (during a year of average solar activity). Although questions can be raised by accelerated testing, this new facility will provide the ability to identify materials most affected by O-atoms (which can then be tested further on-orbit), to systematically separate effects of UV irradiation, temperature, and O-atom energy, to study the rate of change of recession/material loss as surfaces change character, and to identify failure points (most susceptible to erosion) in assemblies such as solar cells. The importance of such effects has been clearly demonstrated in recent Space Shuttle flights.(5, 9-11).

With this test facility we intend to perform quantitative erosion testing of materials, components, and even small assemblies (such as a solar cell array) in order to determine components or interfaces which are most vulnerable to O-atom

erosion. This ground-based facility will allow accelerated testing to identify structures or materials which are in most critical need of protection so that remedial strategies or protective coatings can be developed and even tested in this ground test facility at a fraction of the cost and in a much more timely manner than on-orbit.

REFERENCES

1. Leger, L.J., Spiker, I.K., Kuminecz, J.F., and Visentine, J.T., "STS Flight 5 LEO Effects Experiments--Background Description and Thin Film Results," AIAA Paper 83-2631-CP, October 1983.

2. Leger, L.J., Visentine, J.F., and Kuminecz, J.F., "Low Earth Orbit Atomic Oxygen Effects on Surfaces," AIAA Paper 84-0548, January 1984.

3. Visentine, J.T., Leger, L.J., Kuminecz, J.F., and Spiker, I.K., "STS-8 Atomic Oxygen Effects Experiments," Paper presented at AIAA 23rd Aerospace Sciences Meeting, Reno, NV, January 1985.

4. Green, B.D., Caledonia, G.E., and Wilkerson, T.D., "The Shuttle Environment: Gases, Particulates and Glow," J. Spacecraft and Rockets 22, 5 Sept-Oct 1985. 500-511.

5. Leger, L.J.; Visentine, J.T., and Schliesing, J.A., "A Consideration of the Atomic Oxygen Interactions with Space Stations," AIAA 85-0476, January 1985.

6. Simons, G.A. and Pirri, A.N. "The Fluid Mechanics of Pulsed Laser Propulsion," AIAA J. 15, 835 (1977).

7. Rosen, D.I., Pirri, A.N. Weiss, R.F., and Kemp, N.H., "Repetitively Pulsed Laser Propulsion: Needed Research," In progress in Astronautics and Aeronautics Vol. 89 (1985), ed. L.H. Caveny, pp. 95-108.

8. Rosen, D.I. Kemp, N.H., Weyl, G., Nebolsine, P.E., and Kothandaraman, G., "Pulsed Laser Propulsions Studies," Physical Sciences Inc. Technical Report TR-184, 1981.

9. Hall D.F. and Stewart, T.B., "Photo-Enhanced Spacecraft Contamination Deposition," AIAA 85-0953, June 1985.

10. Peterson, R.V. Hanna, W.D., and Mertz, L.O., "Results of Oxygen Atom Interaction with Kevlar and Fiberglass Fabrics on STS-8," AIAA 85-0990, June 1985.

11. Knopf, P.W. Martin, R.J., McCargo, M., and Dammann, R.E.,

73

"Correlation of Laboratory and Flight Data for the Effects of the LEO Atomic Oxygen on Polymeric Materials," AIAA 85-1066, June 1985.

BIBLIOGRAPHIES

ROBERT H. KRECH

During the last 10 years at Physical Sciences Inc., Mr. Krech has conducted a number of shock tube measurements to determine the radiation properties of hot gases in laser heated sorbent thrusters, stellar atmospheres, and chemical laser systems.

Mr. Krech, a Principal Scientist at Physical Sciences Inc. received his B.S. and M.S. in Chemistry from Boston College. During the last 10 years at PSI, Mr. Krech has performed a number of shock tube measurements to determine the radiation properties of hot gases in laser-heated sorbent thrusters, stellar atmospheres and chemical lasers. He has also studied the interaction of high power lasers with liquid films, induced unimolecular decomposition of azides for chemical laser applications and designed optical diagnostics for gas electron-beam interaction studies.

GEORGE E. CALEDONIA

George E. Caledonia is Vice President for Corporate Research at Physical Sciences Inc. His interests include upper atmospheric physics, neutral and ionic chemistry and radiation physics, with emphasis on the radiative and chemical behavior of heated gases. His current activities include investigation of the interaction between space and re-entry vehicles and the environment.

LABORATORY SIMULATIONS OF ENERGETIC ATOM INTERACTIONS

OCCURRING IN LOW EARTH ORBIT

G.E. Caledonia

Physical Sciences Inc.

Andover, MA, USA

ABSTRACT

The Space Shuttle flights provided the first significant data base on the
environment experienced by a large space structure operating in low earth
orbit (LEO). A number of interesting and unanticipated effects were observed.
These include: material erosion induced by ambient oxygen atoms; the visible
shuttle glow occurring above surfaces exposed to the ram flow; and large near-
field perturbations and variability in the gaseous neutral and plasma environ-
ment about the shuttle. These latter observations are coupled to the con-
taminants introduced by the shuttle and their interaction with the ambient
gases. The understanding of these phenomena is critical to the proper design
and specification of future large LEO space structures such as space station.
This paper provides a brief overview of these observations and their
phenomenological interpretation, and then discusses laboratory approaches for
their investigation. The emphasis of the paper will be on the state-of-the-
art in the development of energetic (v ~ 8 km/s) oxygen atom sources and the
variety of experiments presently being performed with such devices.

INTRODUCTION

The Space Shuttle flights provided the first opportunity to quantita-
tively examine the local environment found about a large space structure in

1

low-earth orbit (LEO), 250 to 350 km. In essence, it was found that con-
taminants on Shuttle surfaces continually outgassed forming a contaminant
cloud about the Shuttle. The interaction between the ambient environment and
the Space Shuttle with its contaminant cloud occurs at the orbital velocity of
8 km/s and can produce deterious effects for Shuttle performance (see Ref. 1
for an overview). These include material erosion, Shuttle glows, and plasma
enhancements.

This interaction can provide for structural disfunction by material
erosion as well as operational disfunction through oxidation or coating
phenomena. Furthermore, the contaminant cloud can provide a more difficult
environment for external probes to operate in because of increased radiative
backgrounds due to surface and "cloud" glows, enhanced plasmas and surface
charging, and also direct deterioration of diagnostic equipment.

In the next section we will provide a brief overview of the phenomenology
occurring in this ambient environment/contaminant cloud Shuttle interaction
and review the physical data required to characterize it. This discussion
will be followed by a description of laboratory beam techniques presently
being developed to provide the required data and brief examples of typical
measurements made on the Physical Sciences Inc. (PSI) energetic oxygen atom
facility.

The Contaminant Cloud

Of course the dominant source of the contaminant cloud is the Space
structure itself. Contaminant species are naturally introduced around the
structure and on its surfaces during operational events such as thruster
firings, water dumps and other vents. Furthermore, particles will shake off

of surfaces and outgassing will occur. The ambient hard UV flux will also act to enhance desorption and outgassing, and indeed may interact with some species to provide polymerization on surfaces. Thus, the specification of the chemical form of these outgassed species is itself critical to determining their ultimate impact on Space structure performance.

Ambient species, primarily O and N_2, but also lesser species such as N, O_2, and H, will impact Station surfaces at orbital velocities of 8 km s^{-1}. It has been found that in many materials this interaction produces material erosion. It is generally assumed that this erosion is the result of oxygen atom attack and for many hydrocarbon materials mass loss is estimated to occur in one out of ten impacts.[2] The reaction products of these interactions have not been measured, but in many cases can be estimated from mechanistic arguments. Erosion species identification is, of course, critical for specification of subsequent reaction, evaluation of deposition tendency, and understanding of erosion induced glows. It has been suggested in the past that limited key components could be protected from oxygen atom attack by the application of sacrificial coatings. The ultimate impact of these eroded materials on the local environment must be carefully evaluated prior to such applications.

Oxygen atom attack can also provide for functional deterioration in more insidious ways. For example, Leger and Visentine[3] have recently pointed out that moly-disulfide, a common lubricant, can oxidize under oxygen atom attack, becoming abrasive. Such a transformation would provide increased particle loading and decreased mobility for moving parts. Other materials, while not eroding, will oxidize, resulting in changing thermal and radiative properties. Furthermore, possible synergistic effects on material erosion resulting from UV loading or surface charging remain to be evaluated.

3

The catalytic properties of various materials in high velocity inter-
actions must also be evaluated. For example, knowledge of the surface
accommodation coefficient for momentum is critical to specifying the local
cloud density. Specifically if the ambient species accommodate their momentum
on the surface they will then effuse away thermally, resulting in a higher
local gas density than if they had scattered elastically from the surface.
The momentum accommodation coefficient is a key parameter in contaminant cloud
models. As another example, catalytic reactions of ambient species on
surfaces have long been suggested[4] as possible sources for excited states
which could then either further interact or themselves produce a surface glow.
No data are presently available on such catalytic effects at orbital
velocities for the various materials of importance to Space Station.

The ambient gasses will also interact with outgassed species around the
Space structure. This interaction, initially occurring at orbital velocities
but also of importance at lower velocities, will produce a scattering pattern
which plays a role in defining the density profile and extent of the con-
taminant cloud. To the author's knowledge there are no measurements of the
angular differential cross sections or momentum transfer resulting from such
heavy body collisions. Furthermore, inelastic collisions will also occur
producing radiation from direct excitation or chemi-excitation, as well as
species transformation. The data base for such interactions is very sparse in
the energy range of interest.

Lastly, the importance of positive ion reactions must be evaluated.
Although ambient ion concentrations are typically small compared to neutral
concentrations there can be charge buildup around the Space structure. One
way this can occur is through reactions between ambient ions and contaminant

4

neutrals. Many reactions of this type will move charge between species without significant momentum transfer. Thus, charge initially at rest in the Earth frame may be swept along with Shuttle.[5] Such reactions can also produce excited species which can radiate and new ionic species which are more likely to provide surface deposition. The efficiencies for ion neutralization on various Space Station materials remain to be evaluated. We note that enhanced ionization levels have been proposed as a source of Shuttle glow.[6]

The various data requirements discussed above have been summarized in Table 1. Potential laboratory techniques for developing this data base are examined below.

Laboratory Studies

Development of the data base requires the use of state-of-the-art neutral and ionic beams exhibiting characteristic velocities of 8 km s^{-1}. A number of neutral oxygen atom beams have been under development in response to the Shuttle observations of significant material erosion (for example, Refs. 7-14). These devices have recently been reviewed by Visentine and Leger[15] and the discussion below is an expansion of their effort.

Presently extant oxygen atom sources may be broken into five types: thermal, high temperature electrical discharges; ion beams, beam-surface interaction, and laser breakdown.

Thermal sources employ a variety of techniques to partially dissociate oxygen molecules without significantly altering the thermal content of the gas. Such techniques include plasma ashers, microwave discharges, etc. These sources tend to have low atomic fluxes in that the atoms have only thermal velocities, and can be plagued by significant concentrations of other reactive

5

species, particularly metastable states. These devices are frequently used for material testing because of their wide availability and simplicity of operation. Nevertheless, their value as a simulation of the higher velocity space interaction remains to be demonstrated.

Higher velocity beams can be achieved by strongly heating gases as in a plasma torch. Here the concept is to highly excite a gas by RF, DC, or microwave sources and subsequently expand the gas through a free jet or hypersonic nozzle converting the sensible heat to velocity. The characteristics of several such sources are listed in Table 2. In order to maximize the expanded velocity helium is the gas of choice for excitation with a few percent of oxygen added downstream. The expanded beam is then composed of a mix of oxygen atoms and molecules dilute in helium. These are high flux devices, allowing oxygen atom brightnesses of 10^{18} to 10^{19} atoms/s-sr but are limited to 0-atom energies below 3 eV, primarily by material limitations.

Perhaps the most popular type of beam under development is the ion source. Here positive or negative ions are created by either electron-bombardment or RF excitation and then are electrostatically accelerated and focussed to achieve the proper velocity, at which point the charge is stripped by various techniques such as charge exchange or grazing incidence surface neutralization. Such beams can readily achieve the appropriate velocity, however, are typically limited to low fluxes because of Coulombic repulsion effects. For standard ion sources achievable neutral fluxes as high as 10^{15} cm^{-2} s^{-1} have been predicted but not yet demonstrated.

An overview of existing ion sources is provided in Table 3. Note that focusing limitations caused by Coulombic repulsion can be eliminated by modifying the beam to be a neutral plasma, i.e., electron injection. Singh et

al.[12] and Langer et al.[10] have adopted the technique and report higher fluxes; the beam of Singh et al. has not been neutralized after focusing, however, and remains a beam of O^+,e pairs rather than oxygen atoms. Indeed, ultimate beam neutralization appears to present a major complication for positive ion sources. Gaseous charge exchange is inefficient because of low cross sections, and surface neutralization produces dispersed beams. Indeed, the majority of positive ion sources are presently being operated as ion rather than neutral beam sources. The negative ion sources show more promise inasmuch as laser photodetachment can be utilized for the neutralization process. Furthermore, variable beam $O(^1D)$ to $O(^3P)$ concentrations can be achieved by adjusting the photodetaching laser wavelength appropriately.

As outlined in Table 4, several groups have utilized beamed energy/ surface interactions to provide energetic oxygen atoms. The approach is to use beamed energy in various forms (electrons, ions, lasers) to promote oxygen atom removal from surfaces. Ferrieri et al.[13] have examined ion sputtering off of metal pentoxides and Brinza[13] has utilized laser/surface breakdown as a sputter source. Of course, other elements present in the solid can track the resulting oxygen atoms. Brinza's approach of breaking down cryogenically deposited thin films of ozone is appealing in this respect. Outlaw's[11] technique can provide a high purity oxygen atom beam. In his approach high pressure and vacuum chambers are connected by a silver membrane. Oxygen molecules introduced into the high pressure chamber interact with the silver, dissociate, diffuse through the membrane and ultimately are adsorbed on the vacuum-side silver surface. Electron-stimulated desorption is then used to free and energize the oxygen atoms. The predicted ultimate oxygen atom flux

7

achievable by this technique is 10^{15} cm^{-2} s^{-1}. These devices are all operational, their disadvantages are wide energy spread and diverging beams.

Perhaps the most mature technology for materials testing applications are the laser-sustained discharge sources,[8,9] e.g., where lasers are used to produce a high temperature plasma which is subsequently expanded in a free jet or supersonic nozzle to produce a high velocity neutral beam. Such sources have been demonstrated to produce beams of the desired velocity of 8 km s^{-1} at flux levels of 10^{17} to 10^{18} cm^{-2} s^{-1}. To date they are the only O-atom devices which exhibit both the appropriate energy for orbital simulation and high flux. The characteristics of the two extant devices are listed in Table 5. Both devices have been operated for long periods of time and are useful for aging studies.

Example Beam Experiments

In principle, many of the devices described above can be used to develop a data base for the phenomenology listed in Table 1. For purposes of illustrations, several such measurements performed with the PSI pulsed laser oxygen atom source will be briefly described below.

The PSI source has been described in some detail elsewhere[8,16] and will only be briefly reviewed here. In operation a fast acting valve is used to introduce a pulse of oxygen molecules into a previously evacuated supersonic nozzle. A pulsed CO_2 laser focused near the nozzle throat is used to break down this gas and form a high temperature plasma. The plasma subsequently expands producing a high velocity beam made up primarily of oxygen atoms. A schematic of the PSI system, as it is used for material erosion studies, is provided in Figure 1. The laser beam enters from the left and the atomic beam

8

propagates to the right striking material targets as shown. The large expansion ratio allows samples as large as several hundred square centimeters to be irradiated. A mass spectrometer is available for beam characterization and radiative diagnostics are available to monitor both beam properties and radiation from the beam target interaction. A second mass spectrometer head will soon be installed to allow monitoring of erosion products.

A number of materials have already been studied with this device with total 8 km s^{-1} O-atom irradiation levels typical of those encountered during a few weeks operation at Shuttle altitudes, $\leq 10^{21}$ O-atoms cm^{-2}. In general mass removal rates and surface properties have been found to be similar to those observed during Shuttle operation.[16]

A typical SEM sequence of an irradiated material, carbon fiber reinforced phenolic (CFRP), is shown in Figure 2. Irradiation level was $\sim 3 \times 10^{20}$ oxygen atoms/cm^2. The top left panel of the figure contrasts virgin and irradiated portions of the material and then, with increasing magnification the remaining panels highlight the differing erosion patterns of the fiber and phenolic portions of the composite. These rug-like erosion patterns are similar to those observed on materials irradiated on Space Shuttle flights.

As soon as the second mass spectrometer head is operational this system will be capable of addressing many of the issues discussed in the previous sections. These include mass loss rates, erosion species identification, and surface property changes. Synergistic effects resulting from UV loading, heating cycles, stress, and flexing can also be investigated with modest system improvements.

Although the system was not developed specifically to study glows, such observations can readily be performed above irradiated surfaces using standard

9

radiative diagnostic techniques. We have seen numerous material specific radiative signatures above surfaces both visually and using an optical multi-channel analyzer (OMA). We are presently examining erosion-induced infrared signatures above surfaces. We have observed radiation from species such as CO, CO_2, and OH when we irradiate materials such as carbon, polyethylene, and kapton. We find that the temporal pulse shape of erosive gases mirrors that of our oxygen atom beam. Possible catalytic surface glows can be studied in a similar manner. PSI has developed an 8 km s^{-1} beam of a mix of nitrogen atoms and molecules using similar phenomenology and anticipates no problem in incorporating oxygen in the mix as well. The neutral species mix in such beams will be evaluated using the mass spectrometer.

PSI has also developed a crossed beam experiment to study infrared excitation resulting from energetic oxygen atom collisions with species such as CO, CO_2, and CH_4. A schematic of the device is shown in Figure 3. Here a skimmed beam of fast oxygen atoms is crossed at right angles with a skimmed pulse (again using a fast pulsing valve) of thermal target molecules. The IR radiation produced by the interaction is monitored by a wide field of view, variable-filtered detector. This experiment design is challenging in that the measurement must be made under single collision conditions; i.e., both the target molecules and the oxygen atoms are required to experience only one collision in the interaction zone to ensure that the radiation is character-istic of fast atom impact. These measurements are in process and sufficient signal is available to evaluate excitation cross sections. Similar techniques can be used to study visible excitation and chemical reaction in such systems.

10

Summary

A number of important quantities which must be evaluated in order to both understand and predict the contamination field about large LEO space structure have been enumerated. It has been shown that the recent development of energetic oxygen atom sources enables the laboratory evaluation of the majority of these quantities. A number of potential measurement techniques have been briefly reviewed.

Acknowledgment

References

[1] Green, B.D., Caledonia, G.E., and Wilkerson, D.T., "The Shuttle Environment: Gases, Particulates, and Glow," J. Spacecraft & Roc., 22, 1985, pp. 500-511.

[2] Leger, L.J. and Visentine, J.T., "A Consideration of Atomic Oxygen Interactions with the Space Station," J. Spacecraft & Roc,, 23, 1986, pp. 50-56.

[3] Leger, L.J. and Visentine, J.T., unpublished results (1987).

[4] Green, B.D., Rawlins, W.T., and Marinelli, W.J., "Chemiluminescent Processes Occurring Above Shuttle Surfaces," Planet. Space Sci., 34, 1986, pp. 879-887.

[5] Caledonia, G.E., Person, J.C., and Hastings, D.E., "The Interpretation of Space Shuttle Measurements of Ionic Species," J. Geophys. Res., 92, 1987, pp. 273-281.

[6] Papadopoulos, K., "On the Shuttle Glow (The Plasma Alternative)," Radio Sci., 19, 1974, pp. 571-577.

11

[7]Arnold, G.S. and Peplinski, D.R., "Reaction of Atomic Oxygen with Vitreous Carbon Laboratory and STS-5 Comparisons," AIAA J., 23, June 1985, pp. 976-977.

[8]Caledonia, G.E., R.H. Krech, and B.D. Green, "A High Flux Source of Energetic Oxygen Atoms for Material Degradation Studies," AIAA J., 25, 1987, pp. 59-63.

[9]Cross, J.B. and Cremers, D.A., "High Kinetic Energy (1 to 10 eV) Laser Sustained Neutral Atom Beam Source," Nuc. Instr. Methds., 813, 1986, p. 658.

[10]Langer, W.D., Coben, S.A., Manus, D.M., Motley, P.W., Oro, M., Paul, S.F., Roberts, D., and Selberg, H., "Detection of Surface Glow Related to Spacecraft Glow Phenomena," Geophys. Res. Lett., 13, 1986, pp. 377-386.

[11]Outlaw, R.A., Hoflund, G.B., and Corallo, G.R., "Electron-Stimulated Desorption of Atom: Oxygen From Polycrystalline Ag," Appl. Surf. Res., 28, 1987, pp. 235-246.

[12]Singh, B., Amore, L.J., Saylor, W., and Racette, G., "Laboratory Simulation of Low-Earth Orbital Atomic Oxygen Interaction with Spacecraft Surfaces," AIAA-85-0477, AIAA 23rd Aerospace Sciences Meeting, Jan. 14-17, 1985, Reno, NV.

[13]Brinza, D., ed, Proceedings of the NASA Workshop on Atomic Oxygen Effects, JPL Publication 67-14, 1987.

[14]Hoggatt, J.T., Hill, S.G., and Johnson, J.C., eds., "Materials for Space - The Gathering Momentun," 18th International SAMPE Technical Conf., Vol. 18, Oct. 7-9, 1986, Society for the Advancement of Material and Process Engineering.

[15]Visentine, J.T. and L.J. Leger, Atomic Oxygen effects Experiments: Current Status and Future Directions, NASA TM, JSC, to be published.

[16]Caledonia, G.E. and R.H. Krech, "Energetic Oxygen Atom Material Degradation Studies," AIAA-87-0105, 25th Aerospace Sciences Meeting, January 1987, Reno, Nevada.

12

Table 1. Required Data For Space Station Contamination Level Specification

Data Required		

· Material behavior under UV loading
    – Outgassing rates
    – Products
    – Surface effects
    – Particle formation
 	
 · Material "erosion" studies under energetic species impact
    – Erosion rates
    – Passivation effects – nonlinear behavior
    – Species produced
      * state changes
      * deposition
    – Surface property changes
    – Erosion induced glows
    – Synergistic effects
      * UV loading
      * charged surfaces
	· Ambient/surface inter- actions
	    – Momentum transfer/ accommodation
	    – Surface reactions
	      e.g., fast $N_2 \rightarrow$
	      $N + N \rightarrow N_2(A)$
	    – Surface collision induced glows
	    – Material dependence of all above
	
	 · Ambient/contaminant cloud interactions
	    – Differential scattering cross sections
	    – Inelastic collisions
	      * chemical reaction
	      * radiative inducing
	      e.g., $0 + M \rightarrow 0 + M^*$;
	      $0 + AB \rightarrow OA^* + B$
		· Ionic interactions
		    – Surface neutraliza- tion efficiencies
		    – Ambient ion/ contaminant reactions
		      * ion velocity separation
		      * quasi-neutrality
		    – Non-linear effects

13

Table 2. Discharge Created Neutral Beams

Type	Technique	Source	Species	Energy	Status
Surfatron (microwave)	Free Jet	UTIAS, Tennyson et al.	$0,0_2,98\%$ He	<3 eV	Operational
Plasma torch (DC arc)	Sueprsonic nozzle	Aerospace, Arnold and Peplinski	$0,0_2,98\%$ He	1-2 eV	Operational
Plasma torch (DC arc)	Supersonic nozzle	ARI, Freeman	$0(He,0_2)$	1.3 eV	Operational

Table 3. Ion Beam Techniques

Type	Technique	Source	Species	Energy (eV)	Status
Electron Bombardment	Charge	Martin Marrieta; Sjoiander; MSFC Carruth	O^+, O_2^+	5	Ions only at present
Electron Bombardment	X^+ surface neutralization	Vanderbilt U., Tolk and Albridge*	0	5-10	Low flux device
Electron Bombardment	Charge exchange	Lerc, Banks and Rutledge	O^+, O, O_2	40-200	Ions only at present, adding UV
Electron Bombardment	Neutral plasma	G.E., Singh	O^+, O_2^+, e	3-10	No neutralization plans
RF Discharge	Neutral plasma surface neutralization	Princeton U., Langer	O, O_2	~5	In construction
Hollow Anode Discharge	Charge exchange	USCLA, Munz	O^+, O_2^+		Ions only at present
Electron Bombardment/ N_2O	O^- Photo-detachment	Boeing, REMPF	0	5	Proof of principle
Electron Bombardment/ N_2O	O^- Photo-detachment	JPL, Chutjian	0	5	Proof of principle

*Also examining negative ion beams

15

Table 4. Beam-Surface Interaction Devices

Type	Technique	Source	Species	Energy (eV)	Status
Ion blowoff	Sputtering on thin films, e.g., VaO_5, TaO_5	Brookhaven, Ferrieri	O	2-18	Operational
Laser blowoff	Breakdown on thin films, e.g., O_3, ITO	JPL, Brinza	O	2-7	Operational
Electron stimulated desorption	Surface dissociation/ diffusion through Ag membrane	LARC, Outlaw	O	5	Proof of principle, 10^{12} cm^{-2} s^{-1}

16

Table 5. Laser Sustained Discharge Neutral Beams

Type	Technique	Source	Species	Energy (ev)	Status
Laser discharge	CW breakdown	Los Alamos, Cross	O, O_2, He	<4	Operational
Laser discharge	Pulsed breakdown	PSI, Caledonia and Krech	O, O_2	2-14	Operational

17
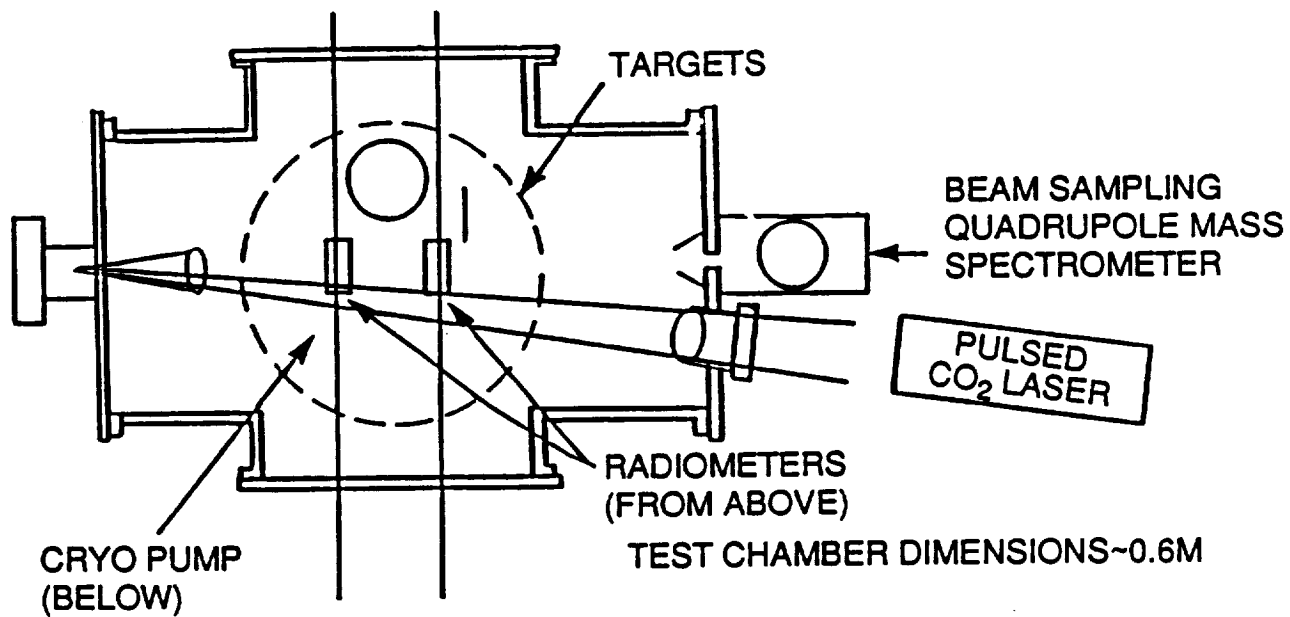
Figure 1. PSI Oxygen Atom Test Facility Under Development

FIBER   **MATRIX**

80092 20KV 500U   80098 20KV 5U

80099 20KV 0.5U   80000 20KV 0.5U
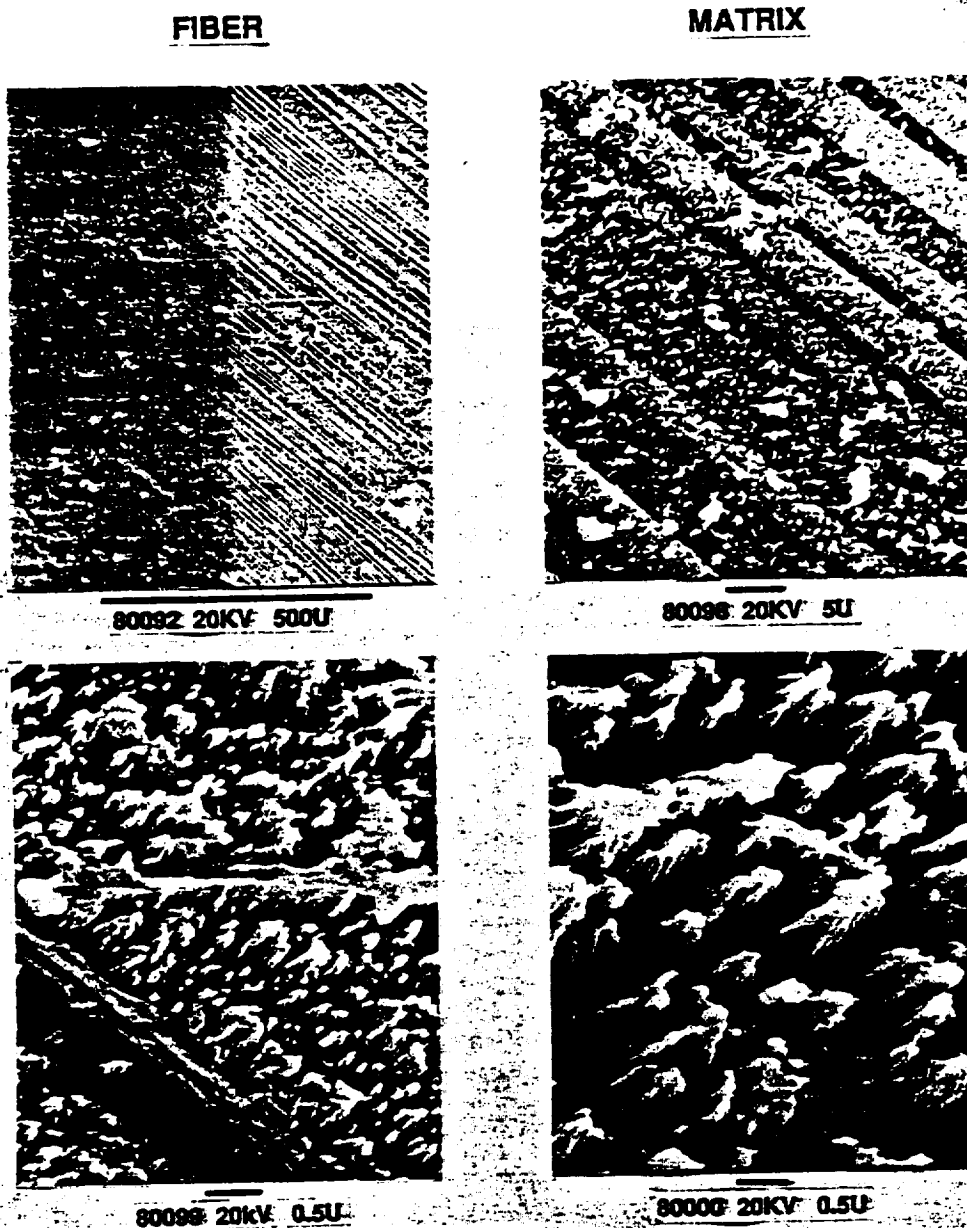
Figure 2. Scanning electron micrograph analysis of carbon fiber
reinforced phenolic. Irradiated by ~ 3 x 10^{20}/cm^2
5 eV oxygen atoms. Top left contrasts virgin and
irradiated materials. Remaining views emphasize
erosion patterns at increased magnification as shown.

19

O-ATOM BEAM
FORMATION CHAMBER

MOLECULAR
BEAM VALUE

O_2 BEAM
VALVE

O-ATOMS

MASS
SPECTROMETER

CO$_2$ LASER

DIFFUSION
PUMP

SKIMMER

CRYOPUMP
PUMP

InSb DETECTOR

TELESCOPE

INTERACTION/DETECTION
CHAMBER
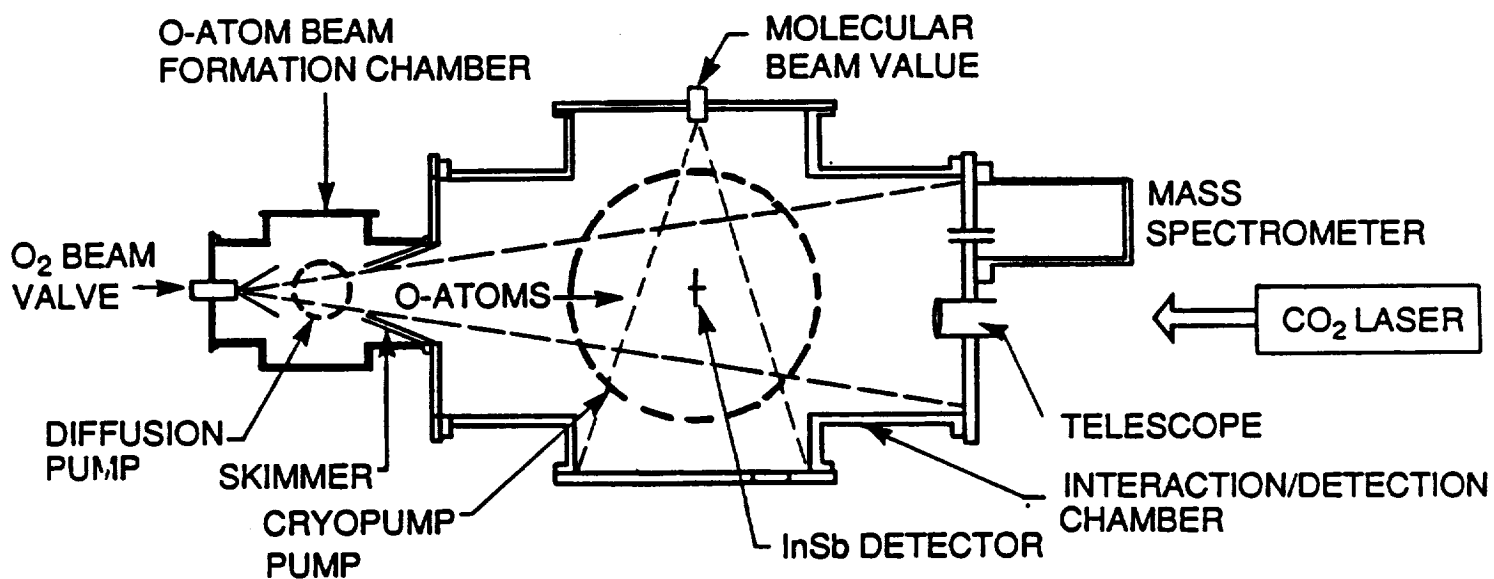
A-885dd

Figure 3.   Crossed Beam Facility

20

SR-381

PULSED SOURCE OF ENERGETIC ATOMIC OXYGEN

George E. Caledonia and Robert H. Krech

Physical Sciences Inc.
Research Park, P.O. Box 3100
Andover, MA 01810, USA

PULSED SOURCE OF ENERGETIC ATOMIC OXYGEN

GEORGE E. CALEDONIA AND ROBERT H. KRECH

Physical Sciences Inc.
Andover, MA, USA

ABSTRACT

A large area, high flux beam of energetic oxygen atoms, E ~5 eV, has been developed to study the interaction of atomic oxygen with materials appropriate for space craft in low earth orbit. A description of the operating conditions and characteristics of the beam along with typical sample irradiation results are provided.

1. INTRODUCTION

Satellites in low-earth orbit sweep at velocities of ~8 km/s through a rarefied atmosphere which consists primarily of atomic oxygen. Experimental pallets flow on early Space Shuttle missions clearly demonstrated a dependence of material degradation and mass loss on the ram direction atomic oxygen exposure.[1,2] These observations have provided the impetus to space engineers to develop and use materials more impervious to oxygen atom attack for LEO applications, and emphasized the need for a high flux atomic oxygen source which can be used to study material degradation under simulated flight conditions.

A pulsed high flux source of nearly monoenergetic atomic oxygen has been designed, built, and successfully demonstrated at Physical Sciences Inc.[3,4] Molecular oxygen at several atmospheres pressure is introduced into an evacuated supersonic expansion nozzle through a pulsed molecular beam valve. An 18J pulsed CO_2 TEA laser is focused to intensities $> 10^9$ W/cm^2 in the nozzle throat to generate a laser-induced breakdown. The resulting plasma is heated in excess of 20,000 K by a laser-supported detonation wave, and then rapidly expands and cools. Nozzle geometry confines the expansion to promote rapid electron-ion recombination into atomic oxygen. We can vary the average O-atom beam velocity from 5 to 13 km/s, with an estimated flux of 2 x 10^{18} atoms per pulse at 8 km/s.

At present, there are two devices incorporating this technique in our laboratory: FAST-1 (Fast Atom Sample Tester), an 2 PPS version of the prototype chamber used to demonstrate the concept; and FAST-2, a larger, higher throughput 10 PPS device currently under development which uses the original prototype chamber as the beam formation chamber prior to the sample test chamber. The FAST-2device will allow uniform irradiation of samples larger than 100 cm^2 in area.

The details and operating characteristics of these devices are described in Section 2 while typical results from selected material studies are provided in Section 3. Summary and conclusions are presented in Section 4.

2. OXYGEN ATOM BEAM OPERATING CONDITIONS AND CHARACTERISTICS

The details of the oxygen atom beam have been provided previously[3,4] and will only be touched upon here. In brief, a fast acting valve is used to nearly fill a evacuated hypersonic nozzle with molecular oxygen at which point a high energy pulsed CO_2 laser focused on the nozzle throat is used to break down and heat the oxygen gas. The resulting flow behavior may be broken down into three regions as is shown schematically in Figure 1. The laser pulse has a short duration (200 ns) gain switched spike which contains ~1/3 of the pulse energy and creates the initial breakdown. The remainder of the pulse is then absorbed in a laser supported detonation wave which can propagate several cm down the nozzle during the 2 μs laser pulse time. After the laser pulse termination the high temperature plasma continues to expand down the nozzle as a blast wave ingesting and processing the cold gas before it. As the blast wave expands, the plasma cools, and the electrons and ions recombine to form neutral oxygen atoms, which have insufficient time to recombine back to molecular oxygen. The inertia of the ingested gas has a snow-plow effect on the wave resulting in a high velocity, temporally narrow pulse of gas exiting the nozzle with a Maxwellian velocity distribution about the mean characterized by the local gas temperature of a few thousand degrees K.

$C\text{-}2$

2
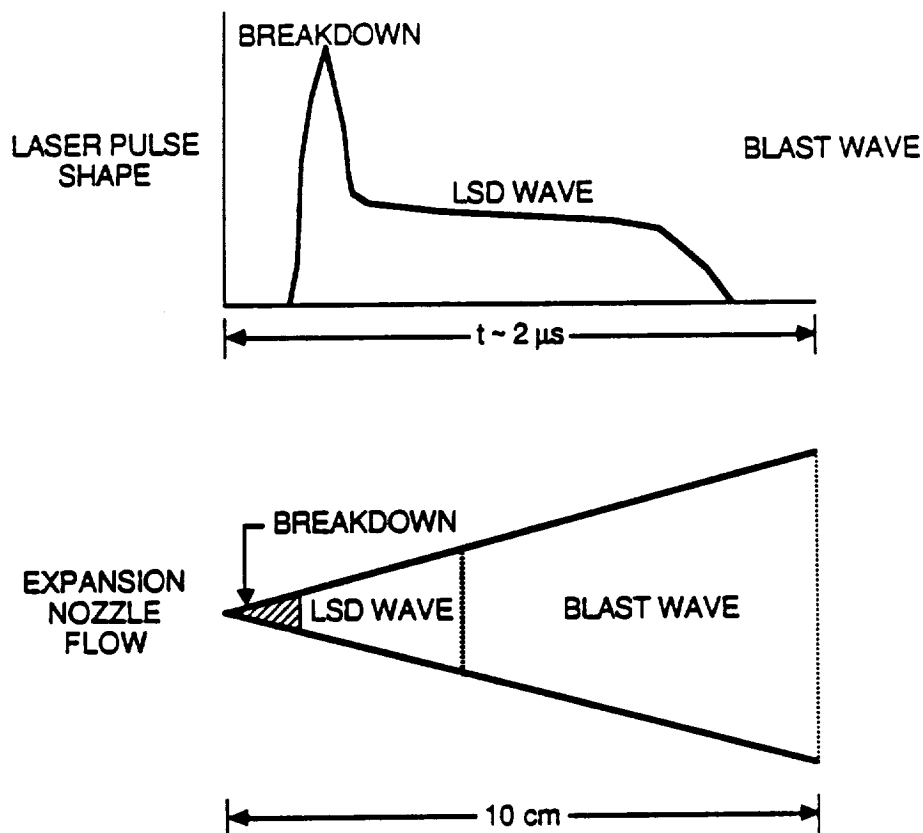
Figure 1. Time/space domains of the pulsed O-atom beam.

A schematic of the FAST-2 facility is shown in Figure 2. FAST-2 is a three chamber device incorporating the equivalent of the FAST-1 source chamber close coupled to a 40 cm o.d. six-way cross exposure chamber, and a separately pumped quadrupole mass spectrometer beam sampling chamber. The exposure chamber is pumped by a 3000 1/s cryo-pump and maintained at pressures below 10^{-5} torr between pulses. In the separately pumped 20 cm o.d. six-way cross source chamber oxygen gas at a pressure of approximately 8 atmospheres is introduced into a 12.5 cm long 20 deg conical nozzle through a fast acting valve. The laser light (10+ J pulsed 10.6 μm CO_2 TEA laser) is provided opposite to the flow either axially, or off axis at 7 degrees to normal, and focused to produce break-down at the nozzle throat. Radiometers positioned in the source chamber are used to monitor beam velocity.

The temporal pulse width at nozzle exit is about 10 μs for 8 km/s operation. A comparison of the oxygen atom pulse shape at this point as measured both by the radiometer and by a pressure transducer is shown in Figure 3. It can be seen that the radiometer provides a good measure of the gas flow. As the O-atom pulse traverses the chamber it broadens temporally due to the Maxwellian velocity spread and also grows spatially as distance squared from the source. A typical pulse will have ~2 x 10^{18} O-atoms and be 30 cm^2 in area near the nozzle exhaust, growing to over 1000 cm^2 by the end of the FAST-2 exposure chamber. This corresponds to a fluence per pulse varying from 7 x 10^{16} to 2 x 10^{15} atom/cm^2. Maximum repetition rates are presently 2 Hz for FAST-1 and 10 Hz for FAST-2. The estimated velocity spread is ± 1.6 km/s and Maxwellian.
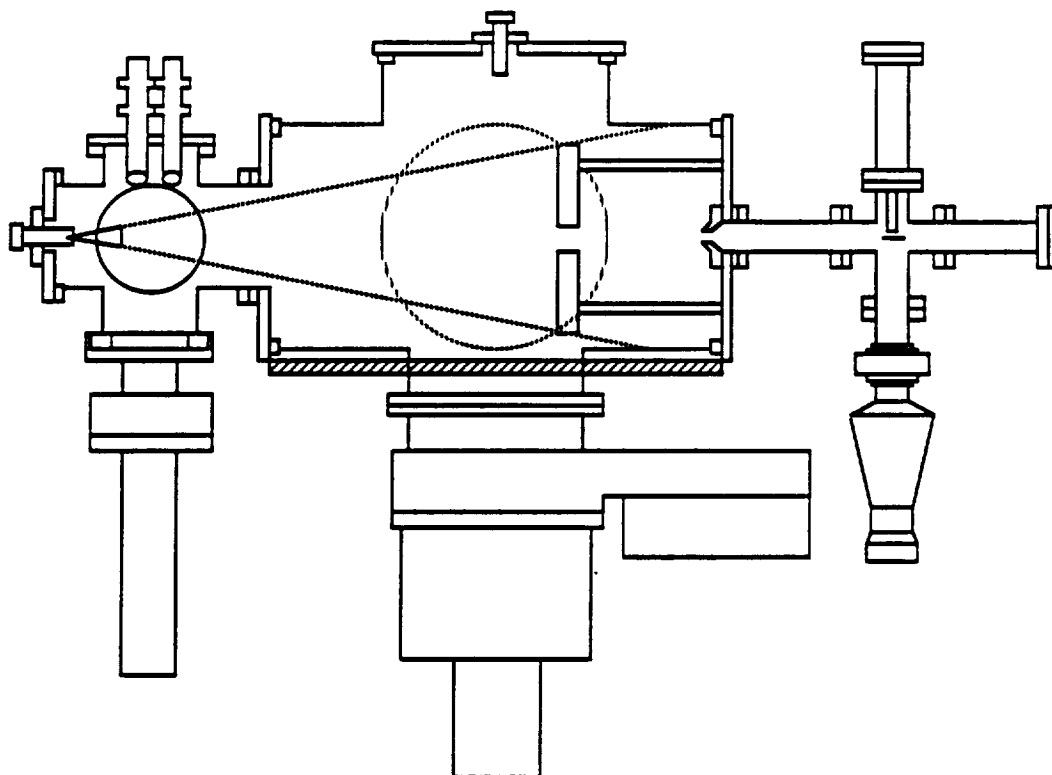
- 10 HZ OPERATION
- LARGER BEAM EXPANSION

A-7410a

Figure 2.   Expanded PSI oxygen atom test facility (FAST-2).
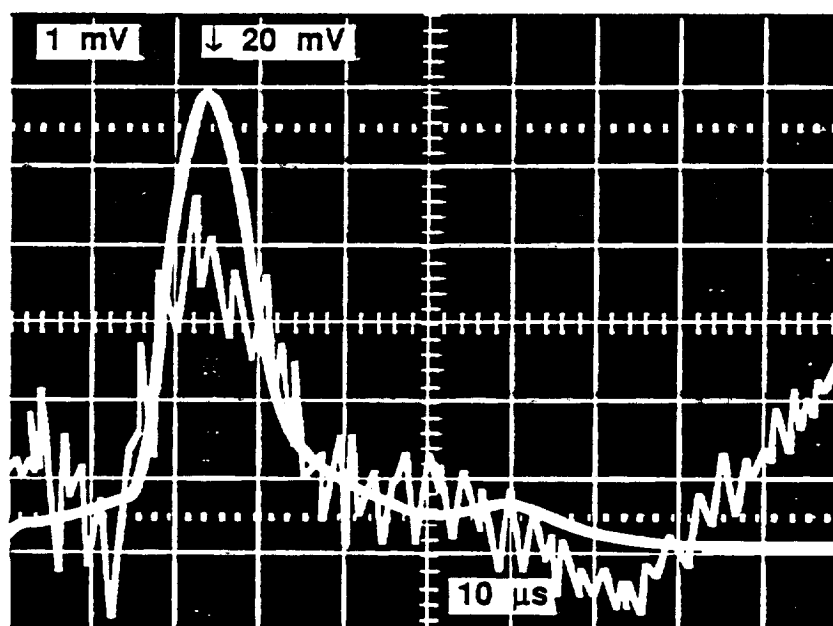
V-49

Figure 3.   Pressure history - optical signatures of 0-atom beam.
Top trace 777 nm radiometer
Lower trace dynamic pressure transducer
Both 21 cm from nozzle throat

4

The spatial extent of the beam has been mapped by monitoring the mass loss on small samples placed at different radial positions in the beam. The measured mass loss is assumed to correlate with total fluence on the sample. As an example, measurements of relative mass loss on two different materials, kapton in the FAST-1 device, and polyethylene in the FAST-2 device, as measured at a distance of 41.5 cm from the nozzle throat are shown in Figure 4. The comparison between the two beams is quite good with the fluence apparently varying homogeneously by a factor of 1.5 from center to edge. Geometric limitations precluded measurement at further distances however it is expected that the beam fluence will drop precipitously at ~10 cm radius. Note that measurements can be performed on beam center in FAST-2 because the laser beam is introduced at an angle to the beam axis.

Similar measurements made at 75 cm downstream from the nozzle throat show a beam extent about twice as large, with accordingly lower fluences. It should be noted that the beam grows both because of the flow angle and the natural Maxwellian spread of the hot oxygen atoms.

Measurements made with the mass spectrometer exhibits temporal beam widths of ~120 to 150 µs in line with expectations based on the velocity spread. The spectrometer introduces a response non-linearity with velocity because of the changing atom residence time within the ionizer. Beam species measurements to date are only preliminary, however, beam ion concentrations are well below 1 percent and the beam is 50 to 80 percent oxygen atoms with the remainder O_2. The possible role of atom recombination on surfaces within the mass spectrometer is presently being investigated.
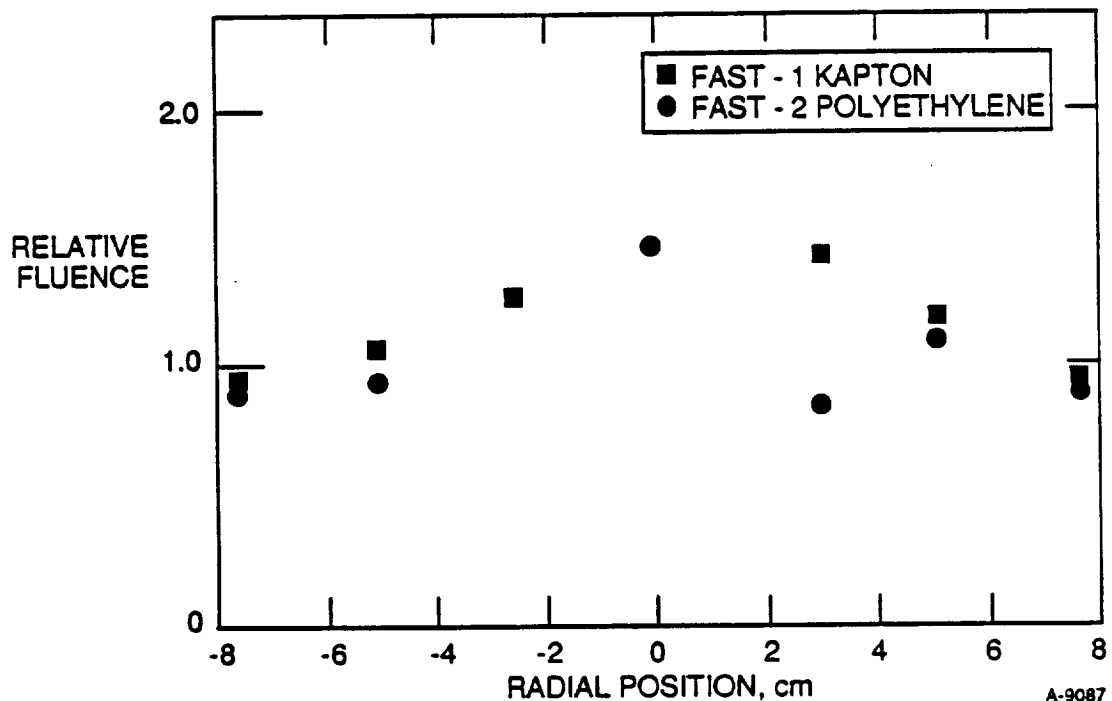
Figure 4. Radial beam profile from mass erosion data - 42 cm from nozzle throat.

3. MATERIAL STUDIES

We have examined a number of materials in our FAST-1 device, including many polymers such as polyethylene, kapton and teflon. Our observed surface morphologies are similar to those of samples exposed on Space Shuttle experiments. One such example, an SEM of carbon fiber re-inforced plastic is shown in Figure 5. The irradiation level for this case was approximately 3 x 10^{20} 0-atoms/cm^2. The top left scan contrasts the virgin and irradiated materials and the following scans show magnifications of the irradiated materials clearly delineating the different erosion structures in the fiber and filled regions of the material. A similar shag-rug like behavior is observed for many of the polymers irradiated.

FIBER   **MATRIX**

80092 20KV 500U

80098 20KV 5U

80099 20kV 0.5U

80000 20KV 0.5U
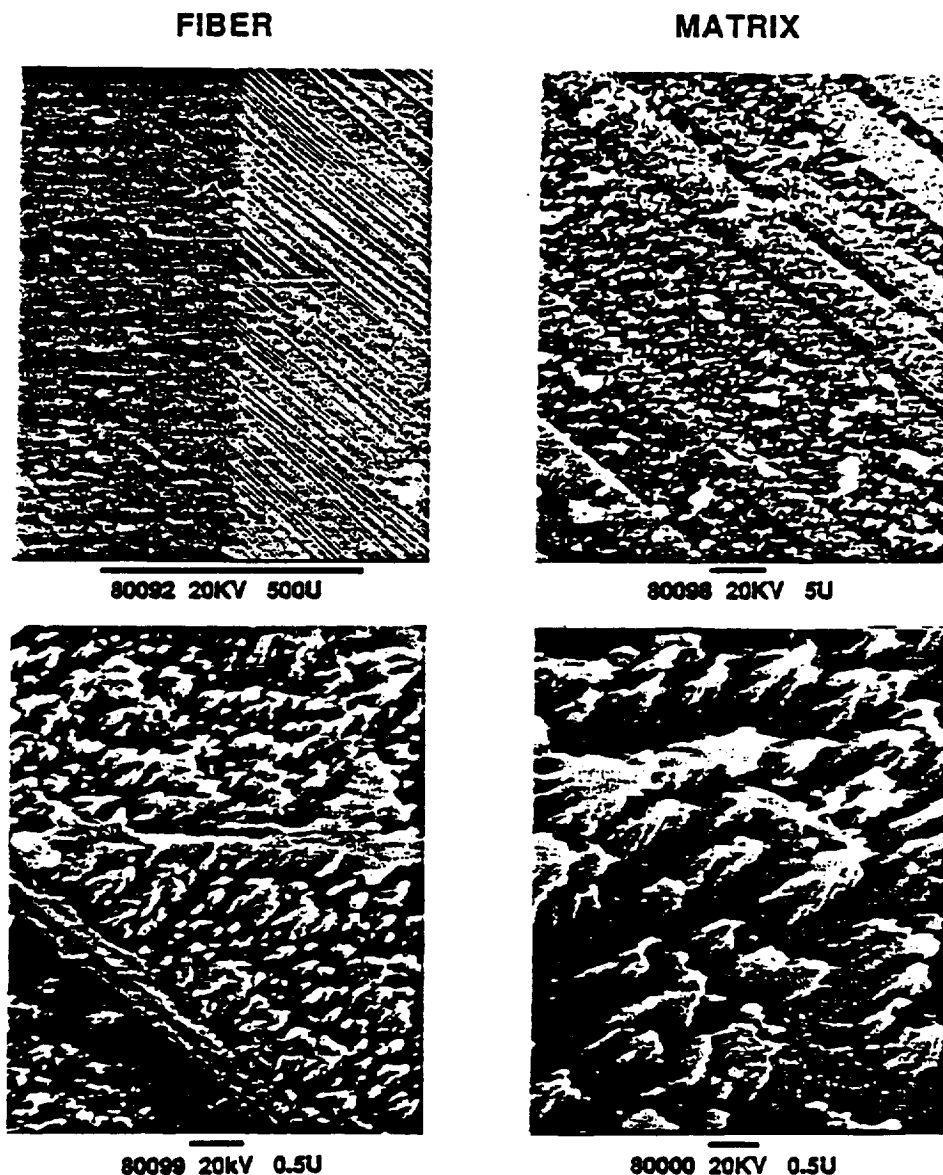
Figure 5. Scanning electron micrograph analysis of carbon fiber reinforced plastic irradiated by ~3 x 10^{20}/cm^2 5 eV oxygen atoms. Top left contrasts virgin and irradiated materials. Remaining views emphasize erosion patterns at increased magnification as shown.

At present we do not yet have the capability to monitor erosion products with a mass spectrometer, however we have found that infrared radiometers can provide useful information on the erosion behavior of the irradiated sample. We have used filtered infrared radiometers to study radiation between 1.5 to 5.5 μm from erosion products of an irradiated polyethylene target, and have observed radiation in bands characteristic of OH, H_2O, CO and CO_2. These are the most elemental species one might expect to be formed in the interaction of oxygen atoms with ethylene.

We have also examined the temporal variation of the erosion product behavior in one of these bands during a single O-atom pulse with a narrow field-of-view radiometer. It was found that within a few centimeters of the target the shape of the erosion product pulse is very similar to that of the O-atom pulse (width of ~100 μs) with no significant induction time between O-atom arrival and erosion product removal. Looking further in front of the target it is found that the erosion product pulse has widened, due to the diffusion of the erosion products. A characteristic erosion product velocity can be deduced by measuring the time between erosion product pulse appearances at different points in front of the target. A velocity of 1.3 km/s, independent of O-atom velocity (between 6 to 12 km/s) was deduced in this manner.

Absolute radiometric measurements of this type coupled with mass spectrometric evolutions should be invaluable in analyzing reaction mechanisms for different materials. For example, in one experiment a series of polyethylene samples were irradiated to different fluence levels and then ESCA was used to evaluate the surface oxygen atom content. It was found that the oxide concentration initally increased rapidly with fluence and then asymptoted to a constant value at a fluence level of several x 10^{17} atoms/cm^2. A radiometric measurement of the time history of the erosion products exhibited identical behavior, clearly coupling the erosion rate to the surface oxide content.

We have recently completed relative mass loss measurements for several standard materials provided by Banks[6]. Here we irradiated several 1 x 1 in. samples of three different materials simultaneously in two different entries. The irradiation level was ~1.7 x 10^{20} O-atoms/cm^2 for each entry. The results are tabulated in Table 1 and as can be seen the data scatter was quite small. Absolute volume removal cross sections are listed under the assumptions that the beam is ether 80 or 50 percent oxygen atoms. Since our fluence monitor is total mass flow the difference between these two assumptions is a factor of two. We plan to remove this uncertainty in the near future.

In terms of the relative cross sections, it is clear that our teflon mass removal efficiency is much larger than that observed in Shuttle experiments.[1] One possible cause of this difference could be the UV loading produced by our source. The high temperature plasma produced in our initial breakdown may produce UV radiation with a significantly different spectral content than that of the sun. One advantage of a pulsed device is that there is a sufficient time lag between plasma decay and O-beam arrival so that plasma produced radiation can be shutter-screened from the sample. This should be investigated. Potential temperature dependent erosion effects should also be reviewed.

TABLE 1. FAST-1 Erosion studies (fluence 1.7 x 10^{20}/cm^2)

Material (# Samples)	Relative σ	$\sigma(20\% \; O_2)$ x 10^{24} cm^3/Atom	$\sigma(50\% \; O_2)$ x 10^{24} cm^3/Atom
Kapton HN(5)	1($\pm$ 20%)	1.3	2.6
Polyethylene (6)	0.9($\pm$ 7%)	1.1	2.2
FEP Teflon (6)	0.6($\pm$ 11%)	0.8	1.6

The infrared radiometer has been used to monitor the dependence of erosion produced intensity on 0-atom fluence. In the case of kapton it was found that the magnitude of the signal varied only by 20 percent from the very first pulse. On the other hand, the teflon signal rose by more than a factor of three as the 0-atom fluence increased from 10^{15}/cm^2 to 10^{18}/cm^2. This observation may suggest that in the case of teflon a surface activation occurred prior to the development of a significant erosion rate. As mentioned earlier, polyethylene is observed to behave similarly to teflon.

4. SUMMARY

The FAST-1 and FAST-2 3 km/s oxygen atom facilities are reliably operational and have been successfully used relatively trouble free to study material erosion at typical fluence levels of 10^{21} atoms/cm^2. The beam velocity, velocity spread, growth and spatial homogeneity are now reasonably well characterized although species content remains to be fully specified. Beam areas greater than 1000 cm^2 are now standardly produced. Average beam fluences per pulse may now be varied between 2 x 10^{15} atoms/cm^2 and 7 x 10^{16} atoms/cm^2, and a peak flux of 7 x 10^{17} atoms/cm^2-5 is achievable.

For the most part irradiated materials are found to behave similarly in terms of mass loss and surface morphology to those exposed on shuttle. Teflon provides a glaring discrepancy, however, and must be investigated further.

REFERENCES

1. Visentine, J.T., Leger, L.J., Kuminecz, J.F., and Spiker, I.K., "STS-8 Atomic Oxygen Effects Experiment," AIAA-85-0415, presented at AIAA 23rd Aerospace Sciences Meeting, January 14-17, 1985 Reno, Nevada.

2. Green, B.D., Caledonia, G.E., and Wilkerson, D.T., "The Shuttle Environment: Gases, Particulates, and Glow," J. Spacecraft & Rock., 22, 1985, pp. 500-511.

3. Caledonia, G.E., Krech, R.H., and Green, B.D., "A High Flux Source of Energetic Oxygen Atoms for Material Degradation Studies," AIAA J., 25, 1987, pp. 59-63.

4. Caledonia, G.E. and Krech, R.H., "Energetic Oxygen Atom Material Degradation Studies," AIAA-87-0105, 25th Aerospace Sciences Meeting, January 1987, Reno Nevada.

5. Zimcik, D. and Maag, C.R., "Results of Apparent Atomic Oxygen Reactions with Spacecraft Materials During Shuttle Flight STS-41G," J. Spacecraft, 25, 1988, pp. 162-168.

6. Banks, B., Private Communication, 1988.

```
4.  STIMS 3X ACC#  9336030        IPS-FILE ADABAS # =  186507
FICHE AVAIL    = AD            HARD COPY AVL = OK        COPYRIGHT      = N
ORIG AGENCY    = NASA          RECEIPT TYPE  = REG       ACCTS TYPE     = REG
DOCUMENT CLASS= TRP            ACCESS LEVEL  = O         ACCESS RESTR   = UNRES
LIMITATION CAT= NONE           DOCUMENT SEC  = NC        TITLE SECURITY= NC
SUBJECT CATGRY= 25             SPECIAL HANDL =           PAGE COUNT     = 00104
INC AUTHOR LST= N              INC CNTRCT LST= N         LANGUAGE       = EN
COUNTRY ORIGIN= US             COUNTRY FINANC= US        ABSTRACT PREP  = NON
PUB DATE       = 19881000       CORP SOURCE   = PQ626284

TITLE          = Novel oxygen atom source for material degradation
TITLE          = studies
TITLE SUPP     = Final Report, 1 Mar. 1986 - 1 Sep. 1988
AUTHOR         = KRECH, R. H.
AUTHOR         = CALEDONIA, G. E.
CONTRACT NUM   = NAS7-963
CONTRACT NUM   = SBIR-04.14-9030
REPORT NUM     = NASA-CR-191323
REPORT NUM     = NAS 1.26:191323
REPORT NUM     = PSI-1001/TR-871
SALES AGY PRIC= Contact the JPL SBIR Field Center Manager for furt
SALES AGY PRIC= her information
MAJOR TERMS    = ATOMIC BEAMS
MAJOR TERMS    = ION SOURCES
MAJOR TERMS    = IRRADIATION
MAJOR TERMS    = OXYGEN ATOMS
MAJOR TERMS    = SPACE ENVIRONMENT SIMULATION
MINOR TERMS    = CALIBRATING
MINOR TERMS    = EARTH ORBITAL ENVIRONMENTS
MINOR TERMS    = EROSION
MINOR TERMS    = FLUENCE
FORM OF INPUT  = HC

****************         END OF ADABAS RECORD #   186507        ****************
```